

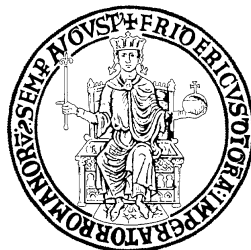
UNIVERSITY OF NAPOLI FEDERICO II

Doctorate School in Molecular Medicine

**Doctorate Program in
Genetics and Molecular Medicine
Coordinator: Prof. Lucio Nitsch
XXVI Cycle**

**“The role of Fe65 in the response to DNA
damage”**

ANNA GARGIULO



Napoli 2014

The role of Fe65 in the response to DNA damage

Table of contents

Abstract	1
Background	2
1 Alzheimer's disease	2
2 The Adaptor Protein Fe65	3
2.1 Fe65 functions	5
2.2 Cytosolic Fe65	6
2.3 Nuclear Fe65	8
3 DNA damage response (DDR)	9
3.1 AKT kinase	10
3.2 PTEN phosphatase	11
3.3 JNK kinase	12
3.4 Fe65 in the cellular response to DNA damage.....	14
Aims of the study	17
Materials and Methods	18
1 Mouse embryo fibroblasts (MEFs) isolation and cell culture	18
2 Cell cycle analysis.....	18
3 Retroviral infections.....	19
4 PCR and Quantitative RT-PCR.....	19
5 Co-immunoprecipitation and Western Blot	20
6 Anchorage-independent growth assay	20
7 Bisulfite genomic sequencing (BGS).....	21
Results and discussion	22
1 Fe65 suppression affect the apoptotic response to DNA damaging agents ...	22
1.1 The oncogene-induced apoptosis is hampered in Fe65 KO MEFs	24
2 Altered proliferative behavior of Fe65 ^{-/-} MEFs	25
2.1 Fe65 knock down (KD) cells have the same phenotype of KO MEFs	26
2.2 Fe65 suppression affects the cell cycle control.....	27
3 Fe65 deficiency favors oncogenic transformation <i>in vitro</i>	29
3.1 Fe65 expression levels are decreased in various human lymphoma and ovary cancers.....	31
4 The apoptotic response of the cells to genotoxic stress is altered in Fe65 ^{-/-} MEFs	31
5 Discussion	37
Conclusions	39
References	40

List of publications

1 de Candia P., Minopoli G., Verga V., **Gargiulo A.**, Vanoni M., Alberghina L. (2011) “Nutritional limitation sensitizes mammalian cells to GSK-3 β inhibitors and leads to growth impairment” Am J Pathol. 2011 pr;178(4):1814-23.

2 Minopoli G., **Gargiulo A.**, Parisi S., Russo T. (2012) “ Fe65 matters: new light on an old molecule” IUBMB Life. 2012 Dec;64(12):936-42.

Abstract

Fe65 is an adaptor protein able to interact with many different partners. Several results supposed the possible involvement of Fe65 in the cell response to DNA damage (DDR). Indeed, Fe65 null mice are more sensitive to genotoxic stress and this increased sensitivity appears to be dependent, at least in part, on defects of DNA repair. Many results indicate that the suppression of DDR plays an important role in tumor development and progression. Mutations of various members of the DDR pathway often result in an increased tumorigenesis. To investigate the involvement of Fe65 in tumor development I analyzed the phenotype of primary embryonic fibroblasts (MEFs) derived from Fe65^{-/-} mice. I found that the apoptosis induced by ionizing radiations, UV rays or Myc ectopic expression is lower in Fe65^{-/-} primary MEFs. This effect is accompanied by an increase in proliferation rate with an altered cell cycle kinetics. Despite a normal phosphorylation of p53, Fe65^{-/-} MEFs failed to accumulate BAX and PUMA mRNAs upon DNA damage. Furthermore, Fe65^{-/-} MEFs showed an increase of the basal levels of the phosphorylated form of AKT, which was accompanied by a slight decrease of the amount of PTEN. It was previously demonstrated that Fe65 interacts with JNK1 and γ -H2A.X. Fe65 suppression prevents the co-immunoprecipitation of these two proteins, thus suggesting that the resistance to apoptosis in Fe65^{-/-} MEFs could be, at least in part, a consequence of the reduced activation of JNK-dependent pro-apoptotic pathway. While, as expected, early passage wild type primary MEFs are poorly sensitive to Myc-induced transformation, Myc overexpression induced the growth of a significant number of colonies of Fe65^{-/-} cells. Similarly, the silencing of Fe65 in NIH3T3 cells significantly enhanced the transforming efficiency of oncogenic Ras. Furthermore, I found that Fe65 expression is reduced both in a transformed cell line and in human tumors and this effect doesn't depend on gene deletion or promoter methylation. These results suggest the possibility that Fe65 is a tumor suppressor gene.

Background

1 Alzheimer's disease

Alzheimer's disease (AD) is a slowly progressive neurodegenerative disorder that represents the most common form of dementia. This disorder is characterized by two pathological features that are observed post mortem: amyloid plaques and neurofibrillary tangles in the cerebral cortex and limbic system, which are unanimously recognized as the hallmarks of the disease. Alzheimer's disease is a heterogeneous syndrome with both familial and sporadic forms. Familial AD is an autosomal dominant disorder with onset before 65 years. Four genes have been unequivocally implicated in inherited forms of AD and mutations or polymorphisms in these genes cause excessive cerebral accumulation of amyloid β -peptides and subsequent neuronal and glial pathology in brain regions important for memory and cognition. The first mutation causing the familial form of the disease was identified in the amyloid precursor protein (APP) gene on chromosome 21 (St George-Hyslop et al., 1990), however mutations of this gene explain only a few familial cases. Indeed in 1995 mutations in the highly homologous presenilin 1 (PSEN1) and presenilin 2 (PSEN2) genes were also linked to early-onset familial AD (Levy-Lahad et al., 1995) (Rogaev et al., 1995) and they account for most cases of familial disease.

At microscopic level, the characteristic lesions in Alzheimer's disease are senile or neuritic plaques and neurofibrillary tangles (Figure 1) in the medial temporal lobe structures and cortical areas of the brain, together with a degeneration of the neurons and synapses. The plaques are composed primarily of the 39–43-residue amyloid β -peptide ($A\beta$) (Wolfe, 2006). $A\beta$ is released from the amyloid precursor protein (APP) by the sequential action of β - and γ -secretases, with the latter cutting relatively heterogeneously (Esler and Wolfe, 2001). Most of the $A\beta$ produced by γ -secretase is the 40-residue form ($A\beta_{40}$); however, the major $A\beta$ species deposited in the plaques is the 42-residue variant ($A\beta_{42}$), although this peptide represents only 5–10% of all $A\beta$ produced.

Neurofibrillary tangles are large, non membrane bound bundles of abnormal fibers that accumulate in the perinuclear region of cytoplasm. Electron microscopy reveals that most of these fibers consist of pairs of 10-nm filaments wound into helices (paired helical filaments or PHF), composed of the microtubule-associated protein Tau (Wood et al., 1986) which is present in a hyperphosphorylated form. A variety of kinases have been shown to be able of phosphorylating Tau *in vitro* at various sites (Martin et al., 2011) that leads to its apparent dissociation from microtubules and aggregation into insoluble paired helical filaments.

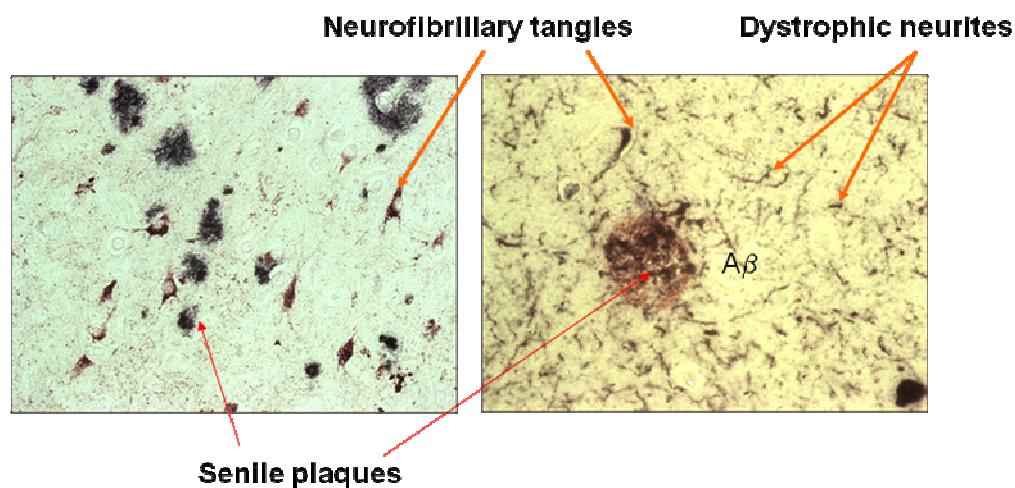


Figure 1: Plaques and tangles in the cerebral cortex in Alzheimer's disease

Plaques are extracellular deposits of A β surrounded by dystrophic neurites, reactive astrocytes, and microglia, whereas tangles are intracellular aggregates composed of a hyperphosphorylated form of the microtubule-associated protein Tau.

Genetic and pathological evidence strongly supports the amyloid cascade hypothesis of AD, which states that A β 42 has an early and vital role in all cases of AD. Indeed APP mutations associated with early-onset dominant AD are located in and around the A β region of APP or of the presenilin genes, which encode the catalytic activity of γ -secretase (Bertram et al., 2010). These mutations were soon determined to alter the amount of A β produced, the ratio of A β 42 to A β 40 or the amino-acid sequence of A β (Selkoe and Kopan, 2003).

Experimental evidence supports the possibility that APP and/or γ -secretase dysfunction could lead to neurodegeneration (Robakis, 2011). Obviously, the understanding of the functions of APP and of its processing is crucial to explore loss of function hypotheses in the pathogenesis of AD.

In 1995, we observed that the NPXY motif present in the small cytodomain of APP interacts with a PTB/PI domain of a protein of unknown function, named Fe65 (Fiore et al., 1995) (Simeone et al., 1994).

2 The Adaptor Protein Fe65

Fe65, together Fe65L1 and Fe65L2 (its paralogs in mammals), is a member of a multigene family of adaptor proteins which share three highly conserved protein-protein interaction domains (Minopoli et al., 2012). Although ubiquitous, Fe65 is expressed at high levels in neurons (Bressler et

al., 1996), and its expression is developmentally regulated, with levels declining after embryonic day 15 and increasing again progressively from postnatal day 10 to adulthood (Simeone et al., 1994) (Kesavapany et al., 2002).

The *Apbb1* gene encoding Fe65 was identified by a screen as a mRNA expressed at high levels in the brain (Esposito et al., 1990), and subsequently it was found evolutionary conserved from nematode to human (Zambrano et al., 2002). Fe65 mRNA encodes a protein of 711 amino acids with molecular adapter features; indeed it has three different protein-protein interaction domains, a WW domain and two consecutive PTB domains (Zambrano et al., 1997a) (Figure 2).

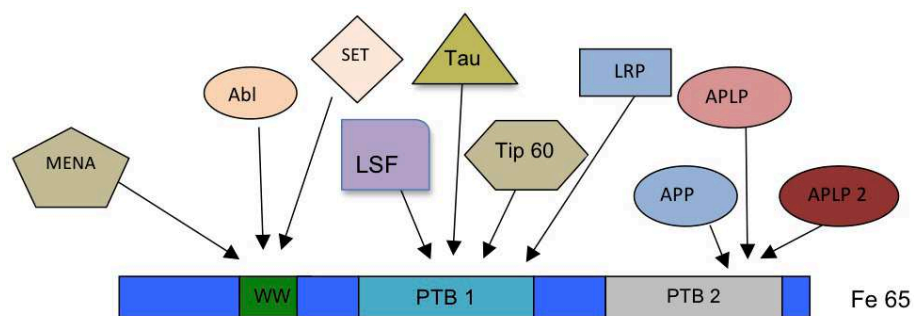


Figure 2: Schematic representation of Fe65 protein.

The regions corresponding to the three protein-protein interaction domains, the WW domain (green) with its interactors (Mena - Abl - Set) and the two domains PTB1 and PTB2 (blue and grey) and their cognate ligands (LSF - Tip60 - LRP for PTB1 and APP - APLP1 - APLP2 for PTB2).

Through screenings for Fe65 binding partners, many proteins that interact with Fe65 were identified. One of these is APP and its related protein APLP1 and APLP2 that interact with Fe65 PTB2 domain. In particular Fe65 binds the NPTY-containing region of all APP and APP-like proteins. Furthermore, it was identified the small G-protein Dexas1 as a novel interacting partner of Fe65 PTB2 domain. This interaction is regulated by the phosphorylation of Fe65 on Y547. Dexas1 inhibited FE65-mediated transcription without an apparent effect on binding of FE65 to APP, so defective FE65 phosphorylation could lead to transcription of potential FE65-APP-regulated genes such as *BACE*, *GSK3 β* , and *APP*, which are linked to the pathogenesis of Alzheimer disease (Lau et al., 2008). PTB1 domain of Fe65 binds the transcription factor CP2/LSF/LBP1 (Zambrano et al., 1998) and this interaction is implicated in the regulation of transcription of GS3K β (glycogen synthase kinase-3 β) (Kim et al., 2003) and timidilate synthase (Bruni et al., 2002). Another strong interactor of Fe65 PTB1 is the histone acetyltransferase Tip60 (Cao and Sudhof, 2001). In addition to CP2/LSF and Tip60 the PTB1 has also been found to interact with LRP (Waldron et al., 2006), which is a

receptor for ApoE and α -2 macroglobulin, also involved in the scavenging secreted A β (Trommsdorff et al., 1998). Fe65 also binds, through its PTB1 domain, another member of the LRP family, the ApoER2 (Hoe et al., 2006). The complex between Fe65 and the members of the LDL-related proteins might affect the APP processing. Furthermore, Fe65 PTB1 domain interacts with the other protein involved in Alzheimer's disease, Tau protein, and their interaction is regulated by Tau phosphorylation (Barbato et al., 2005). The WW domain is the most N-terminal domain of the three protein interacting domains. It has been demonstrated to interact with Mena, a member of ENA/WASP family, which is involved in actin remodelling (Ermekova et al., 1997); c-Abl, a tyrosine kinase, which phosphorylates APP on Y682 (Zambrano et al., 2001) and Fe65 on Y547 (Perkinton et al., 2004) and finally, SET, a member of INHAT complex, and Teashirt3 (Kajiwara et al., 2009) involved in the chromatin remodeling (Telese et al., 2005).

2.1 Fe65 functions

The function of Fe65 is still not understood. Relevant information about the possible functions of Fe65 comes from the analysis of knock-out animals. In *Caenorhabditis elegans* there is a single gene coding for a protein very similar to mammalian Fe65. This ortholog, called *feh-1*, has the same multimodular structure of mammalian Fe65s; indeed, it interacts with the nematode ortholog of APP, *aph* (Zambrano et al., 2002). The *feh-1*-null worms are not compatible with proper development of *C. elegans*: due to a block at the embryonic stage. Embryonic arrest phenotype results in severe developmental defects, leading to disorganized embryos, with cells that either detach or degenerate. Heterozygous worms, instead, presented an elevated rhythm of pharyngeal contractions and hyperactive head movements. (Bimonte et al., 2004). The phenotype of *feh-1*-null worms is very similar to that caused by the suppression of the nematode ortholog of APP. The ablation of Fe65 by gene targeting in mice didn't show any macroscopic phenotypes, likely due to gene redundancy. Indeed, the double knock-out of Fe65 and Fe65L1 genes shows significant defects in the development of the central nervous system (Guenette et al., 2006) that resemble those observed in the APP;APLP1;APLP2 gene knock-out mice (Herms et al., 2004). This observation suggests that Fe65 and APP are involved in common mechanisms. Mice lacking Fe65 look like normal but they may have some not evident phenotypes. First of all, the absence of Fe65 enhances neurogenesis (Ma et al., 2008), like APP knock-out mice, and suppresses the GnRH-1 neurogenic program (Forni et al., 2011); then, it is involved also in impairment in the memory and learning (Wang et al., 2004). Recently, it was demonstrated that Fe65 null mice are more sensitive to DNA-damaging agents (Minopoli et al., 2007). More information about possible functions of Fe65 came from study on cellular system. Among the identified binding partners of Fe65 there are both

cytosolic and nuclear proteins thus suggesting that Fe65 could have function in both cellular compartments.

2.2 Cytosolic Fe65

All three Fe65 proteins form complexes *in vivo* with APP, APLP1 and APLP2, suggesting that Fe65 could be involved in the proteolytic processing of these proteins.

APP is a type I membrane protein with a large glycosylated extracellular/intraluminal (EC/IL) domain, a single transmembrane tract, and a short cytosolic domain (Figure 3). APP undergoes a complex proteolytic processing by three different enzymatic activities called α , β and γ -secretases. The first event involves the release of the large extracellular domain. This can be generated by two different enzymes, the α - or β -secretase. The α -secretase interrupts the sequence of the peptide A β , preventing its production, and releases the soluble fragment sAPP α . Alternatively, the cut can be catalyzed by the aspartil protease BACE (β -APP cleaving enzyme), which releases large soluble fragment sAPP β and cleaves APP at the N-terminus of the A β peptide, initiating the amyloidogenic pathway. The fragments C83 and C99, anchored to the membrane after the cleavage of APP by α - or β -secretase, become substrates of γ -secretase, which catalyzes the intramembrane cutting. This event releases the non-neurotoxic fragment P3, after the α -secretase action, and the A β peptide, when APP is cleaved by β -secretase. A β peptide is very hydrophobic and its aggregation causes the formation of soluble oligomers. The accumulation of such oligomers gives rise to large insoluble aggregates that form the senile plaques. In both proteolytic pathways, the action of γ -secretase releases the cytosolic domain AICD (APP Intra Cellular Domain).



Figure 3: APP and its interactors.

The cytosolic tail of APP is reported with the GYENPTY motif in red. Some of the PTB-containing proteins that interact with AICD are shown. It is represented the Tyr residue phosphorylated by Abl and involved in the binding to activated Abl and Src tyrosine kinases.

The dominant signal for APP endocytosis resides in the motif YENPTY but also other signals in the C-terminus of APP could be involved in the APP trafficking, which determines APP processing and so, A β production (Perez et al., 1999). The YENPTY motif is the binding site of Fe65, this suggested that the binding of Fe65 to APP could influence the endocytosis and in turn the processing. Data addressing this point showed discordant results; indeed, there are reports indicating that A β production is increased by Fe65 overexpression (Sabo et al., 1999) and reduced by Fe65 knockdown (Xie et al., 2007); on the other hand, other studies reported that Fe65 overexpression increased sAPP α and decreased A β production (Ando et al., 2001). This problem is difficult to understand for the complexity protein–protein interaction network centered at the YENPTY motif of the cytodomain of APP and for the variable abundance of secretases in the different cellular type.

Fe65 is involved, in the cytosol, also in cytoskeleton remodeling and in cell movement. Indeed, it interacts with Mena by the WW domain. Mena is a cytoskeleton regulatory protein involved in the regulation of cell motility and adhesion (Kwiatkowski et al., 2003). Mena binds actin and thus links Fe65 and APP to motility and cell morphology and to cytoskeletal dynamics (Sabo et al., 2001). Indeed, it was well demonstrated that the *Fe65/Fe65L1* DKO mice (Guenette et al., 2006) and those of the triple KO of *APP/APLP1/APLP2* (Herms et al., 2004) or *Mena/VASP/EVL* (Santiard-Baron et al., 2005) have the same phenotypic abnormalities, suggesting a functional interaction between these three protein families during neuronal development *in vivo*. Furthermore, it is known that Dab1, the mammalian ortholog of *Drosophila* disabled, binds APP and together Abl (Fe65 ligand) antagonizes the effects of Mena on cytoskeleton remodeling and cell movement. All these proteins compete to regulate the motility and the morphology of the cytoskeleton. Indeed, Mena and c-Abl compete for the interaction to Fe65 WW domain whilst Dab1 and c-Abl compete for the binding to APP. It has been suggested that the Fe65 interactions could be regulated by conformational changes (Cao and Sudhof, 2001). A possible model that could explain the regulation of the Mena activity is focused on the mutually exclusive interaction of Dab1 and Fe65 to APP cytodomain. Whether Dab1 binds to APP, Mena can't interact with Fe65 because it is in a "closed" conformation due to the intramolecular interaction of the WW domain with the PTB2 domain. In these conditions Mena is unable to interact with Fe65 and it is available to regulate the cytoskeleton. The Fe65 PTB2 binding to APP led the transition of Fe65 to the "open" conformation that unmask the WW domain. In this way Mena is in its inactive form. When c-Abl was activated it can compete with Mena for the interaction with Fe65; allowing Mena to switch from inactive to active form. Clearly, in this context, there are other partners of Fe65 or APP that can play a role in remodeling of cytoskeleton.

2.3 Nuclear Fe65

Previous results suggested that Fe65 could have some nuclear functions, considering its presence in the nucleus and its interaction with several nuclear proteins. These results supported the hypothesis that Fe65 could be involved in nuclear functions and that APP could regulate these functions. Indeed, Fe65 overexpression results in its accumulation in the nucleus and APP functions as an extranuclear anchor that prevents Fe65 nuclear translocation (Minopoli et al., 2001). It was observed that the cotransfection of Fe65 and APP in cultured cells causes the complete exclusion of Fe65 from the nucleus. A mutant GFP-Fe65 protein lacking of PTB2 domain or with a point mutation in this domain, that affects the binding with APP, is always translocated into the nucleus even if the cell co-expresses APP. Furthermore, the C-terminal fragment of APP resulting from the cleavage catalyzed by γ -secretase was found in the nucleus associated with Fe65 (Kimberly et al., 2001). The localization in the nucleus of Fe65 by APP could be regulated by the cleavage of γ -secretase that releases the Fe65/AICD complex. So, Fe65 is not anchored to the membrane, then it translocate to the nucleus. On the other hand, Fe65 can translocate into the nucleus by competition with other ligand of the APP cytosolic domain. The last is a small structure and Fe65, X11 and mDab1 compete among themselves to this domain. This competition and the resulting displacement can be determined by the increase in concentration of one of the two competitors, or by an increase in APP affinity for one or for both. The increase in affinity may be due to a conformational change of X11 and / or mDab1, for example mediated by post-translational modification.

Finally, the phosphorylation of threonine 668 of APP cytodomain decreases the affinity of APP for Fe65. Therefore, another possible mechanism is that this phosphorylation induces a conformational change in APP cytodomain, which causes the release of Fe65 and its translocation into the nucleus (Ando et al., 2001).

Fe65 could have some roles in transcription activation; indeed, it interacts with CP2/LSF/LBP1 and Tip60. In this function, the nuclear localization of Fe65 could be dependent from the cytosolic fragment of APP, AICD. The potential importance of AICD in this mechanism was suggested by the recognition of similarities between APP and another type I transmembrane protein, Notch. Notch is a single transmembrane receptor consisting of the extracellular region, a heterodimerization domain and the membrane-tethered intracellular domains (Kimberly et al., 2001). Also Notch is cleaved by γ -secretase that, during its proteolytic processing, allows to release the Notch cytosolic domain (NCID). This domain binds to the CSL protein and goes to the nucleus, where activates the transcription of downstream genes. Similarly, after the proteolytic cleavage of APP, the AICD-Fe65-Tip60 complex goes to the nucleus where it could regulate gene transcription. Several genes have been suggested to be direct targets of AICD-Fe65, like *APP* itself, *BACE*, *Tip60*,

KAI1, *LRP*, *nephrilysin*, and *Stathmin1* (von Rotz et al., 2004) (Baek et al., 2002) (Pardossi-Piquard et al., 2005) (Muller et al., 2012). However, AICD overexpression or γ -secretase inhibition doesn't cause significant effects on protein levels of genes that were suggested to be regulated by AICD (Hass and Yankner, 2005) (Hebert et al., 2006). Therefore, the mechanism of the AICD-dependent gene regulation is still understood.

3 DNA damage response (DDR)

The integrity of genetic information is essential for species survival. All organisms are exposed to DNA damaging agents as part of everyday life. To counteract damages to DNA, the cells have evolved mechanisms – collectively termed the DNA-damage response (DDR) – to detect DNA lesions, signal their presence and promote their repair (Ciccia and Elledge, 2010). Cells defective in these mechanisms generally display increased sensitivity towards DNA-damaging agents and many such defects cause human diseases. The DDR is a hierarchical process which is involved in an intricate signal transduction pathway that has the ability to sense DNA damage and transduce this information to the cell to influence cellular responses to DNA damage. Indeed, this process can be divided into three steps. First, localization of DDR factors to sites of DNA damage is initiated by DDR-sensor proteins (DDRS) that directly recognize specific DNA lesions and activate the DDR. Following the recognition of the damage, other proteins, called DDR-transducer protein (DDRT), are recruited on the site of the lesion to transmit the signal to the last series of proteins involved, called DDR-effector protein (DDRE). The last conduct different functions, including: to repair material damage, to regulate the cell cycle during the repair, to modify gene transcription and, in the case of irreparable damage, to trigger a death program. This response culminates in the activation of cellular checkpoints and activation of the appropriate repair system, or alternatively, in the initiation of a program of death (Jackson and Bartek, 2009).

The DDR is primarily mediated by proteins of the phosphatidylinositol 3-kinase-like protein kinases (PIKKs) family — ATM, ATR and DNA-PK — and by members of the poly (ADP) ribose polymerase (PARP) family (Ciccia and Elledge, 2010). The DDR regulates physiological processes such as the decision to activate apoptosis program, differentiation, senescence, activation of enhanced immune surveillance, DNA repair (Cui et al., 2007) (Gasser and Raulet, 2006) (Zhou and Elledge, 2000). The assembly of the DDR cascade is dependent on a broad spectrum of post-translational modifications such as: phosphorylation, ubiquitination, sumoylation, poly ADPribosylation, acetylation, methylation that are induced by the activation of the DNA damage response (Bergink and Jentsch, 2009) (Harper and Elledge, 2007). These post-translational modifications regulate the recruitment of the DDR proteins to DNA damage sites. Phosphorylation acts as a molecular switch for many

regulatory events in signalling pathways that drive cell division, proliferation, differentiation, and apoptosis. Kinases and phosphatases proteins have a spatial distribution in the cells, to ensure an appropriate balance of protein phosphorylation. This spatial separation regulates protein phosphorylation that, in turn, regulates the activity of other proteins, enzymes, and the transfer of other post-translational modifications (Bononi et al., 2011).

3.1 AKT kinase

The serine/threonine kinase AKT represents an important connection in diverse signaling cascades downstream of growth factor receptor tyrosine kinases, and other cellular stimuli. AKT plays an essential role in cell survival, growth, proliferation, angiogenesis, metabolism, migration and self renewal of stem cells. Deregulation of AKT activity has been associated with cancer and other disease conditions, such as neurodegenerative diseases and muscle hypotrophy (Bononi et al., 2011). Among the downstream effectors of PI3Ks, AKT is the most important and best studied. The three AKT isoforms have extensive homology with protein kinases A, G, and C within their kinase domains and are, therefore, members of the AGC kinase family (Manning and Cantley, 2007). AKT possesses an N-terminal PH domain of approximately 100 amino acids, similar to PH domains found in other signalling molecules that bind 3-phosphoinositides. It binds, with its PH domain, to both PIP3 and phosphatidylinositol 4,5- bisphosphate (PIP2) with similar affinity (Frech et al., 1997). The kinase catalytic domain is located in the central region of the protein (Nicholson and Anderson, 2002). Finally, the C-terminal tail contains a second regulatory phosphorylation site. This region possesses the F-X-X-F/Y-S/T-Y/F hydrophobic motif that is characteristic of the AGC kinase family.

AKT is activated through receptor tyrosine kinase pathways. Full activation of AKT is a multistep process, and the final step is the phosphorylation of AKT on two sites, Thr308 and Ser473 via PDK1 and PDK2, respectively. (Alessi et al., 1996). The molecular interaction between the phosphorylated hydrophobic motif and the cavity, formed by the α B and C-helices, stabilizes the catalytic domain: this is very important for the complete activation of AKT. The activation of the PI3K signaling pathway by growth factor stimulation leads to recruitment of AKT to the plasma membrane through binding to PIP3, here, AKT can be activated by two different kinases, PDK1 (Stephens et al., 1998) and the mTORC2 (Sarbasov et al., 2005). Then, AKT is addressed to various subcellular compartments where it phosphorylates substrates or interacts with other molecules. Through phosphorylation, AKT may either positively or negatively affect the function of these substrates, alter their subcellular localization, or modify their protein stabilities. Depending on phosphorylated substrates AKT leads to uncontrolled cell proliferation, inhibited apoptotic pathways, and strong cell cycle dysregulation, typical hallmarks of many human cancers.

Nuclear AKT has a crucial role in apoptosis as a regulator of transcriptional factors for the expression of pro- or anti-apoptotic molecules, such as: YAP, CREB, FOXO proteins, or NF- κ B, and MDM2. The latter is a well known negative regulator of the p53. Phosphorylation of some transcription factors like: CREB and NF- κ B induces upregulation of antiapoptotic Bcl-2 family members, whereas phosphorylation of other proteins (FOXO family members) impairs the apoptotic response (Rena et al., 1999) (Biggs et al., 1999). Indeed, among the several target of AKT there is Bad, a pro-apoptotic member of Bcl2 family. Phosphorylation of Bad on S136 by AKT blocks its interaction with Bcl-2/Bcl-XL, sequestering Bad in the cytosol, and preventing the apoptotic response. In the same way, AKT phosphorylates also the pro-apoptotic Bax protein on S184, suppressing its translocation to mitochondria, and impairs the apoptotic response (Gardai et al., 2004).

The best known function of AKT is its role in promoting cell growth. In this function is involved mTORC1 complex, which is regulated by both nutrients and growth factor signalling. AKT has been suggested to directly phosphorylate mTOR on S2448 (Scott et al., 1998), but the role of this phosphorylation remains still unclear. In this context, this phosphorylation seems to be important for cell proliferation, controlling the translation of proteins important for cell-cycle progression.

3.2 PTEN phosphatase

In the 1990s, two groups independently found a locus that is frequently deleted in a variety of advanced cancers, identified a new phosphatase termed PTEN (Li et al., 1997). This locus appears to be the second most frequently mutated tumor-suppressor gene in human cancers after p53 (Chalhoub and Baker, 2009). Today, it is well documented that PTEN is involved in diverse cellular processes such as cell-cycle progression, cell proliferation, apoptosis, ageing, DNA damage response, angiogenesis, muscle contractility, chemotaxis, cell polarity, and stem cell maintenance.

The human PTEN gene is made up of 9 exons and codes for a 403-amino-acid protein. This protein is characterized by five functional domains: a short N-terminal PIP2-binding domain, a phosphatase domain, a C2 domain, a C-terminal tail containing PEST (proline, glutamic acid, serine, threonine) sequences, and a PDZ interaction motif (Chalhoub and Baker, 2009). As its name suggests, the PTEN is a dual-specific phosphatases and it is able to remove phosphates from protein and lipid substrates. PTEN has the Cys-X5-Arg-Thr/Ser (CX5RT/S) phosphatase catalytic signature and belongs to the protein tyrosine phosphatase superfamily. It has been suggested that cytosolic PTEN is found in an inactive conformation with the PIP2-binding domain masking its catalytic site, whereas binding to PIP2 at the plasma membrane could result in an open active conformation of the PTEN protein. PTEN acts as a negative regulator of the PI3K-AKT pathway by removing the phosphate

from the three-position of the inositol ring to generate PIP₂. (Haas-Kogan et al., 1998). So, the loss of PTEN leads to constitutively high levels of PIP₃, which promotes the recruitment of a subset of proteins to cellular membranes, including PDK1 and AKT kinase. As described above, AKT is the major downstream effector of PI3K signalling that can phosphorylate several substrates and, thus, stimulates cell growth, proliferation, and survival (Manning and Cantley, 2007) (Figure 4).

3.3 JNK kinase

The mitogen-activated protein kinase (MAPK) signaling pathway is one of the major signaling systems that transduce extracellular signals into cells. These pathways regulate several different cellular functions such as proliferation, differentiation and survival. There are three major groups of MAPKs: the extracellular signal-regulated kinase (ERK), the c-Jun N-terminal kinase (JNK) and the p38 MAPKs. All of these pathways are involved in cancer progression. They also have a high degree of interaction and cross-talk with the PI3K/AKT pathway (Rodriguez-Viciana et al., 1994). The second MAPK signaling transduction pathway (JNK pathway) is involved in cellular stress, apoptosis, survival, transformation and differentiation. MAPKKKs for the JNK pathway are stimulated by a variety of factors, primarily by cytokines and exposure to environmental stress. Upon stimulation, one of several MAPKKKs activates either one of JNK pathway's MAPKKs (MKK4 or MKK7). Following JNK activation, several substrates could be phosphorylated (ATF2, c-Myc, p53, Paxilin); however, a major target of the JNK signaling pathway is the activation of AP-1 transcription factor that is

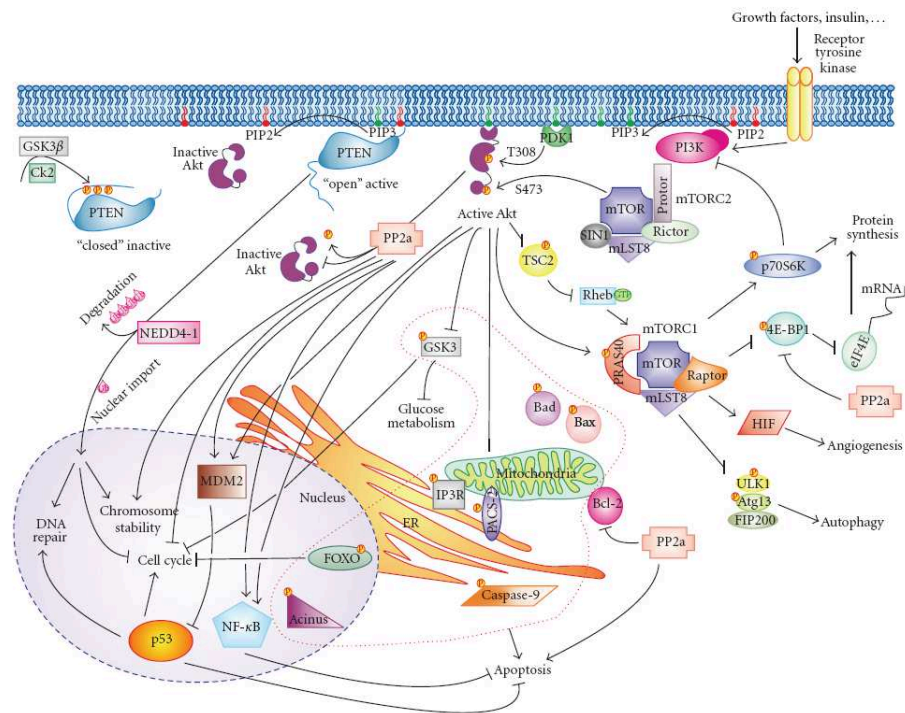


Figure 4: PI3K signalling pathway.

The phosphatidylinositol 3-kinase (PI3K) signaling pathway starts with the binding of growth factors to receptor tyrosine kinases. This binding activates PI3K. After, PI3K phosphorylates the lipid second messenger PIP2 (indicated by red phosphoinositide) in PIP3 (indicated by green phosphoinositide). This leads to the recruitment of AKT on the plasma membrane, where it is phosphorylated for its activation. Then, AKT favors cell proliferation and survival by regulation of several pro-apoptotic targets (hold by the red dotted line), or by activation of mTOR complex 1. AKT is inhibited by protein phosphatase 2a (PP2a) family, favoring apoptosis, or by the tumor suppressor phosphatase PTEN, which dephosphorylates PIP3, converting it back to PIP2. (Bononi et al., 2011).

mediated by the phosphorylation of c-Jun and related transcription factor that is mediated by the phosphorylation of c-Jun and related molecules (Weston and Davis, 2002). Finally, these transduction signals activated target genes controlling cell cycle, proliferation, differentiation as well as death. Like other pathways, JNK controls the apoptotic response by balancing the expression levels of proteins such as Bcl-2, Bad, Bax. There is the possibility of the existence of a feedback loop between the AKT and JNK pathways. In response to various proapoptotic stimuli, many pathways including AKT can inhibit JNK to promote cell survival. Indeed, AKT substrates and ASK1 have a similar

sequence, so ASK is an upstream regulator of the JNK pathway. This promotes apoptosis and activates the next component in the JNK pathway. One study has shown that AKT can phosphorylate ASK1 at Ser83 residue, thereby, inhibiting ASK1 and leading to blockade of apoptosis and promoting cell survival (Jazirehi et al., 2012). Furthermore, AKT and JNK share the same substrate, that is FOXO3A, which is involved in the activation of the apoptotic response.

3.4 Fe65 in the cellular response to DNA damage

Several experimental data have shown that chromatin remodeling, in the region surrounding the damaged DNA site, is a key event for the success of the cellular response to DNA damage. The chromatin remodeling involves a series of post-translational modifications on the amino-terminal tail of histones of the nucleosome, in particular H3 and H4. It has been shown that in the remodeling associated with DNA damage repair, the main changes involve the acetylation of histone H4 by the NuA4 complex containing the histone acetyltransferase Tip60 (interactor of Fe65) and its cofactor TRRAP, which are rapidly recruited to double strand breaks (DSBs) (Bird et al., 2002). Tip60 has a key role in the response to DNA damage and it can affect tumorigenesis in different ways. First, Tip60 is a co-regulator of transcription factors that either promote or suppress tumorigenesis, such as Myc and p53. Furthermore, it has an important role in response to DNA damage triggered by oncogenes. This leads to the conclusion that Tip60 is a tumor suppressor required in response to DNA damage induced by oncogene (Gorrini et al., 2007). The interaction between Fe65 and Tip60 has suggested that also Fe65 is involved in the DNA damage response. Indeed, the study of the phenotype of Fe65 null mice led to the observation that these mice are more sensitive to DNA-damaging agents (Minopoli et al., 2007) and, similarly, wild-type mouse embryo fibroblasts (MEFs), treated with low doses of etoposide or H₂O₂, have only marginal effects compared to knock-out MEFs that have high levels of DNA damage and accumulation of γ -H2AX. Same results were obtained in NIH3T3 and N2A cells where the Fe65 expression was silenced by RNA interference. This phenotype depends on the presence of Fe65 in the nucleus. Indeed, the phenotype of increased sensitivity to DNA damage cell knock-out is recovered by the expression of proteins wild-type but not by a protein Fe65 fused with a nuclear export signal, unable to remain in the nucleus (Minopoli et al., 2007). These observations have suggested the possibility that Fe65 is a protein that binds chromatin. Indeed, studies of chromatin immunoprecipitation with histone H3 at the genomic level and global analysis of the accessibility of chromatin to digestion by micrococcal nuclease in cells wild-type and knock-out or knock-down for Fe65, showed that in the chromatin is more relaxed than in wild-type.

The molecular basis of the phenotypes observed in cells knock-out/knock-down for Fe65, after DNA damage, is still not completely

understood. This increased sensitivity seems to be dependent, at least *in vitro*, on a defective DNA damage repair, due to a decreased recruitment of Tip60/TRAPP complex at DNA double strand breaks and in turn the acetylation of histone H4 in cells Fe65 knock-out and knock-down. This phenotype depends from Fe65 and Tip60 interaction although it is rescued by Fe65 full-length but not by Fe65 Δ -PTB1 mutant, unable to interact with Tip60. Furthermore, Fe65 is subjected to rapid phosphorylation upon DNA damage, suggesting that phosphorylation could be the triggering mechanism for the correct localization of the complex NuA4.

Several data suggest that the cleavage by the γ -secretase is necessary for the nuclear localization of Fe65-AICD. Indeed, in cells treated with etoposide APP maturation by the γ -secretase was observed, and that this maturation is dependent on the changes of Fe65 induced by genotoxic stress. So, the interaction APP / AICD is necessary to allow proper function of Fe65 during the repair, as it allows the association of Fe65 with chromatin. Indeed, the interaction of Fe65 with APP induces a conformational change leading Fe65 from a “closed” to an “open” conformation, allowing Fe65 to acquire the most appropriate form for the response to DNA damage. Another interesting possibility is that Fe65, bound to APP cytodomain and thus in its “open” active conformation, is released from APP as a consequence of APP phosphorylation at Thr668, possibly catalyzed by c-Jun N-terminal kinase JNK (Taru and Suzuki, 2004) (Figure 5). Nuclear Fe65 is then rapidly modified, likely phosphorylated, and it is necessary for Tip60 recruitment at the DNA breaks. Further results were obtained by studying of APP and APLP2 knock-down, in which there isn't the recruitment of Tip60 and, therefore, the acetylation of histone H4, as Fe65 is not bound to chromatin (Stante et al., 2009). In conclusion, in the native chromatin Fe65 favors the packing of chromatin, whereas DNA DSBs, stimulates the recruitment of Tip60, acetylation of histone H4 and the local relaxation of chromatin.

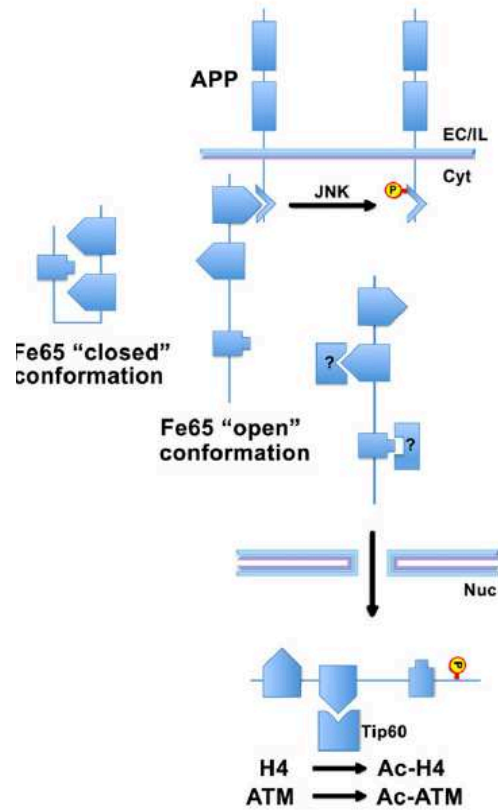


Figure 5: The Fe65–Tip60 complex in the DNA repair mechanisms.

Available results support the hypothesis that Fe65 exists in two conformations. The interaction with the cytodomain of APP induces Fe65 from a “close” to an “open” conformation. The cleavage of APP or its phosphorylation may cause the release of Fe65 from the membrane anchor thus allowing its association with chromatin. In basal conditions, chromatinized Fe65 appears to have a general role in favoring chromatin condensation. Chromatin associated Fe65 is necessary for the recruitment of Tip60-TRRAP-containing complex at DNA double strand breaks. Loss of function of the Fe65-APP machinery induces a significant decrease of DNA repair efficiency (Minopoli et al., 2012).

Aims of the study

The possible involvement of Fe65 in the DDR, suggested us to explore whether it has any role in transformation. To this aim I investigated the role of Fe65 in the apoptotic response of the cells to genotoxic stress and to oncogene activation. Furthermore, I observed that Fe65 behaves as a tumor suppressor gene, promoting oncogene-induced transformation *in vitro* and *in vivo*.

Materials and Methods

1 Mouse embryo fibroblasts (MEFs) isolation and cell culture

Primary MEFs were isolated from Fe65^{+/+}, Fe65^{+/-} and Fe65^{-/-} embryos, obtained by crossing Fe65^{+/+} x Fe65^{+/+}, Fe65^{+/+} x Fe65^{-/-}, and Fe65^{-/-} x Fe65^{-/-} mice, respectively. Embryos were collected at day 13.5 p.c. and, after removal of head and internal organs, minced and trypsinized. Cell suspension was centrifuged at 1100 rpm for 5 minutes and then plated in a 100 mm dish containing DMEM (Sigma-Aldrich, Saint-Louis, MO, USA), 10% fetal bovine serum (FBS; Hyclone, Watham, MA, USA), 2 mM glutamine (Lonza, Basel, Switzerland), 100 U/ml penicillin (Invitrogen, Carlsbad, CA, USA), 100 µg/ml streptomycin (Invitrogen) and incubated at 37°C in 5% CO₂. The cells were routinely passaged just before reaching confluence. Unless otherwise specified, experiments were performed on MEFs at passage 2. The samples Fe65^{+/+} represent one pool of three different wild-type embryos. The same is for Fe65^{+/-} and Fe65^{-/-} samples.

NIH 3T3 cells were cultured in DMEM supplemented with 10% FBS, 2 mM glutamine, 100 U/ml penicillin, 100 µg/ml streptomycin

Proliferation Fe65^{-/-} MEFs was assayed by doubling time experiments: 10 x 10⁴ cells were seeded in 60mm dish, and viable cells counted at various time points up to 7 days with trypan blue. MEFs were irradiated with 1 or 5 or 15 Gy of X rays, as indicated, by using RS2000 Biological Irradiator (Rad Source, Suwanee, GA, USA) or with 30 J/m² by using UV Stratalinker 1800 (Stratagene, La Jolla, CA, USA) and incubated for indicated times before analysis. Apoptotic cells were measured by TUNEL assays kit (Millipore, Billerica, MA, USA) following the manufacturer's instructions.

2 Cell cycle analysis

Cell cycle entry experiments were performed on asynchronous cells, starved cells and irradiated cells. They were plated in 100 mm dishes and grown up to passage 2. Confluence-arrested cells were starved in medium without serum for 72 h and then stimulated with medium containing 10% FBS. To monitor entry into the cell cycle, cells were harvested at specific time points, washed three times with PBS, resuspended in PBS containing 0.02 mg/ml propidium iodide (Sigma), 0.004% NP40 (Sigma) and 0.5 mg/ml DNase-free RNase (Applichem GmbH, Darmstadt, Germany) and analyzed by FACS using a FACScanto (BD Biosciences, San Jose, CA, USA) instrument. Exponentially growing cells were exposed to 1 Gy of X rays and analyzed after 24 hours.

3 Retroviral infections

Retroviruses were prepared by transfecting the Platinum-E ecotropic packaging cell line (Cell Biolabs Inc., San Diego, CA, USA) with pMXs-c-Myc (32, Addgene plasmid 13375) and/or pLZRS-RasV12 (33, Addgene Plasmid 21203) or pLZRS-EGFP vectors with Lipofectamine 2000 (Invitrogen) following the manufacturer's instructions. 24 hours after transfection, medium was replaced and virus-containing supernatants from transfected Plat E cells were collected after further 24 hours. MEFs (5 x10⁵ / 100 mm dish) were infected with control EGFP virus, c-Myc virus alone or c-Myc plus RasV12 in the presence of 4 mg/ml polybrene (Sigma) for 14-16 hours at 37°C. After replacement of viral supernatants with fresh culture medium, MEFs were incubated at 37°C for additional 48 hours. For c-Myc plus RasV12 infections, MEFs were infected sequentially with c-Myc virus first and 48 hours later with RasV12 virus. Parallel infections with EGFP expressing virus were used to determine the infection efficiency.

4 PCR and Quantitative RT-PCR

For genotyping, genomic DNA was extracted with Qiagen Genra Puregene Kit (Qiagen, Hilden, Germany) following the manufacturer's procedures. The oligonucleotide primers used for amplifications are reported in Table 1.

Table 1: Oligonucleotides used for mice genotyping

mFe65 Intr1 forward	5'-TGGTGTTTGCTGGCTTACTGA-3'
neo up forward	5'-TGCGGTGGGCTCTATGGCTTCTG-3'
mFe65 Ex2 reverse	5'-CTCCTCCTCCTCTTCGTCTTC-3'

Fe65 exons were amplified with oligonucleotide primers indicated in Table 2.

Table 2: Oligonucleotide primers for mouse and human Fe65 gene analysis

	Primer Forward
mFe65 ex 9 for	5'-GACTTTGCCTACGTAGCTCGAGA-3'
mFe65 ex 10 rev	5'-TGGAAGGGACATCCACGAGT-3'
hFe65 ex 2 for	5'-GAGCTGCCAAGCCATGT-3'
hFe65 ex 2 rev	5'-AGAGTACAGGTGTATCAGGCCTTT-3'
hFe65 ex 3 for	5'-TTCTGGAACCCCAACGCCT-3'
hFe65 ex 5 rev	5'-CTGAGGCTCTGAGCTGGGAA-3'
hFe65 ex 9 for	5'-GCCTACGTAGCTCGTGATAAGCT-3'
hFe65 ex 10 rev	5'-CTTGGAAGGGACATCCACAAGTTT-3'
hFe65 ex 12 for	5'-ATGTGATTAATGGGGCCCTCGA-3'
hFe65 ex 13 rev	5'-TCTGAGAGGCTGGCAGCATT-3'

Total RNA was purified from MEFs using the TRI reagent (Sigma) and the cDNA was prepared with M-MLV RT, following manufacturer's instructions (New England Biolabs, Ipswich, MA, USA). Real-time RT-PCR was carried out on an ABI PRISM 7900HT Sequence Detection System (Applied Biosystems, Foster City, CA, USA) using Power SYBR Green PCR Master mix (Applied Biosystems). The GAPDH mRNA was used to normalize the samples. Gene-specific primers are reported in Table 2.

Table 2: Oligonucleotides used for quantitative Real Time PCR experiments

	Primer Forward	Primer Reverse
mGapdh	5'-GTATGACTCCACTCACGGCAAA-3'	5'-TTCCATTCTCGGCCTTG-3'
mBax	5'-ACAGATCATGAAGACAGGGG-3'	5'-CAAAGTAGAAGAGGGCAACC-3'
mPuma	5'-ATGGCGGACGACCTCAAC-3'	5'-AGTCATGAAGAGATTGTACATGAC-3'
mFe65	5'-CCTCCTTCTGCTGTCACATGTTT-3'	5'-TTCTGGTAGCGGAGCATGC-3'
mp21	5'-TCAGAGTCTAGGGGAATTGGA-3'	5'-AATCACGGCGCAACTGCT-3'
hFe65	5'-GGAAGTCAAGCTGGGCTACCT-3'	5'-GTTGGGGTTCCAGAAGGAAT-3'
hGapdh	5'-GAAGATGGTGATGGGATTTC-3'	5'-GAAGGTGAAGGTCGGAGTC-3'

5 Co-immunoprecipitation and Western Blot

MEFs were irradiated with 15 Gy of X-rays and, after 30 min; nuclear proteins were purified from control and irradiated cells as previously described (Minopoli et al., 2007). 1 mg of each nuclear extract was precleared with Protein A/G plus agarose beads (Santa Cruz Biotechnology, Santa Cruz, CA, USA). Cleared supernatants were incubated with 3 µg of γ H2A.X antibody (Millipore) or with 3 µg of mouse IgG (Santa Cruz Biotechnology, Santa Cruz, CA, USA) overnight at 4°C. Immunoprecipitated proteins were analyzed by western blot with JNK antibody (Santa Cruz Biotechnology). The antibodies used for western blot experiments are: AKT, phospho-S473 AKT, phospho-S15 p53 and phospho-(T183, Y185) JNK (Cell Signaling, Danvers, MA, USA), PTEN (Abcam, Cambridge, UK), GAPDH (Santa Cruz Biotechnology), total H2A.X (Bethyl Laboratories Inc., Montgomery, TX, USA), β -actin (Sigma-Aldrich, Saint-Louis, MO, USA) rabbit polyclonal anti-Fe65 ((Zambrano et al., 1997a)).

6 Anchorage-independent growth assay

MEFs were mock infected or infected with c-Myc alone or with c-Myc plus RasV12 as described above. Twelve hours after infection 3×10^4 cells were suspended in DMEM containing 0,3% bacto-agar and seeded in 60 mm plates on a bottom layer containing 0.5% bacto-agar.

100000 NIH3T3 cells were seeded in 100-mm dishes, transfected by lipofectamine with Fe65 siRNAs pool or non-silencing siRNA (Dharmacon, Lafayette, CO, USA) and, 24 hours later, with pRCmv-K-Ras A59T (34) or pRCmv empty vector. 24h after transfection, 5×10^3 cells were harvested and seeded in 60 mm plates containing 2 ml of a 0.3% bacto-agar suspension in DMEM plus 10% FBS and incubated at 37°C with 5% CO₂ for 4 weeks. The transforming efficiency was expressed as number of colonies/plate, in triplicate in three independent experiments.

7 Bisulfite genomic sequencing (BGS)

Genomic DNA was extracted from frozen tissue of 3 ovary cancers and from a control ovary specimen with Purgene Core Kit A (Quiagen) following the manufacture's instruction. 2 µg the purified DNA for each sample were treated with sodium bisulfite and purified by using the EpiTect Bisulfite Kit (Quiagen) according with the instruction of the manufacture. 200 ng of each converted DNA were amplified by PCR with 2,5 U of HotStarTaq DNA polymerase (Quiagen). Amplified DNA fragments were extracted from agarose by using Wizard SV Gel and PCR Clean-Up System (Promega) and cloned in the pGEM- T Easy Vector (Promega). 5 clones of each sample were sequenced

Results and discussion

1 Fe65 suppression affects the apoptotic response to DNA damaging agents

Among the events induced by genotoxic stress, apoptosis plays a crucial role as a natural barrier against the possible dangerous consequences of DNA damages. It is known that Fe65 $-/-$ MEFs are more sensitive to genotoxic stress than wild-type counterparts so, I observed whether Fe65 suppression affects the apoptotic response of the cells to DNA damage. To this aim, Fe65 $-/-$ mouse embryo fibroblasts (MEFs) Fe65 $+/-$ and the wt counterpart were obtained from E13.5 embryos and used in all the experiments at passage 2. In the experiments reported in figure 1, I checked the expression of Fe65 in MEFs for both mRNA (panel A) and protein (panel B), and I observed a strong decrease of Fe65 expression in Fe 65 $-/-$ MEFs.

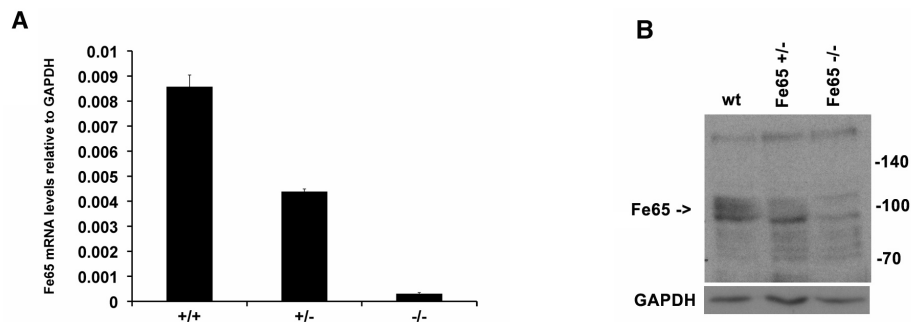


Figure 1: Fe65 mRNA and protein levels in wt and mutant MEFs

(A) Q-PCR analysis of RNA from wt, Fe65 $+/-$ and Fe65 $-/-$ MEFs. (B) Western blot analysis of extracts from wt, Fe65 $+/-$ and Fe65 $-/-$ MEFs with Fe65 polyclonal antibody.

The first experiment, that I performed on this cell, was the TUNEL Assay. This is a method for detecting DNA fragmentation that results from apoptotic signaling cascades by labeling the terminal end of nucleic acids. The assay relies on the presence of nicks in the DNA which can be identified by terminal deoxynucleotidyl transferase or TdT, an enzyme that will catalyze the addition of dUTPs that are secondarily labeled with a marker. For this purpose Fe65 $+/+$ and Fe65 $-/-$ MEFs were irradiated with 15 Gy of X-rays. As shown in Figure 2 Fe65 $-/-$ MEFs don't activate the apoptotic response because there are a little number of cells undergoing apoptosis, compared to

wt. Very similar results were obtained by exposing the cells to 30 J/sqm of UV rays.

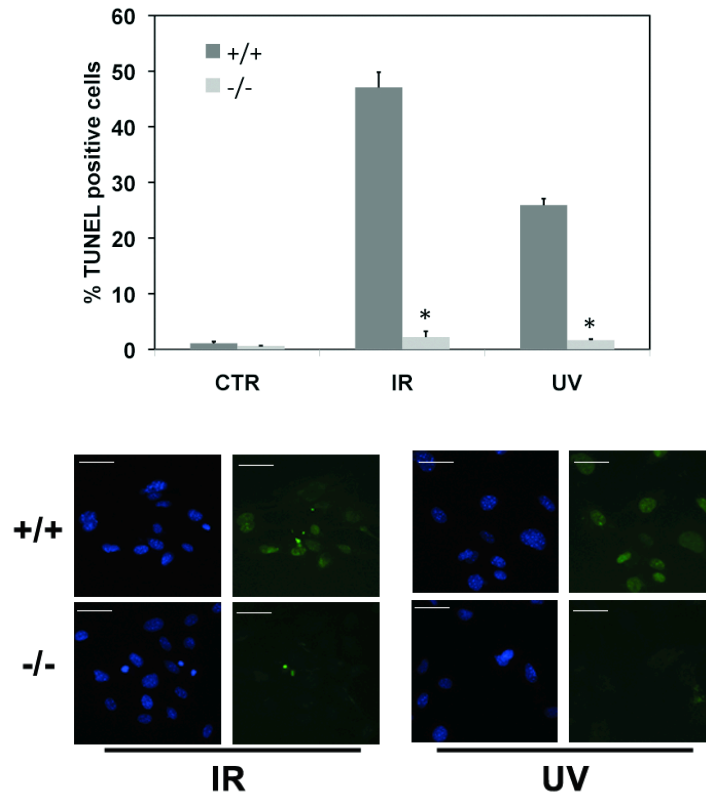


Figure 2: Fe65 suppression hampers apoptotic response to DNA damage

Fe65^{-/-} and wt MEFs were exposed to 15 Gy of X rays (IR) or to 30 J/sqm of UV rays (UV). 16 hours after the exposure, the cells were fixed and apoptotic cells analyzed by TUNEL assay. Apoptotic cells are reported as percentage of total cell. Histograms report the mean values of three independent experiments. Each MEF preparation consists in a pool of at least three distinct embryos. Representative examples of DAPI (blue) and TUNEL (green) staining are shown (scale bar= 50 mm).

1.1 The oncogene-induced apoptosis is hampered in Fe65 KO MEFs

The apoptotic response to genotoxic stress is also induced by oncogenes. Indeed, the constitutive expression of c-Myc induces MEFs to undergo apoptosis, thus failing to transform primary mouse fibroblasts, whereas the contemporary expression of c-Myc and oncogenic Ras is needed to induce transformation. Therefore, wt, Fe65 +/- and Fe65 -/- MEFs were infected with the virus driving the expression of c-Myc with or without the virus driving the expression of H-RasV12. As shown in Figure 3, the expression of c-Myc alone induced, as expected, the wt MEFs to undergo apoptosis, while no apoptosis was seen in these cells when infected with c-Myc plus oncogenic Ras. On the contrary, Fe65 -/- cells infected with c-Myc alone didn't show an induction of apoptosis, thus indicating that the absence of Fe65 affects the apoptotic response of MEFs to genotoxic stress induced by c-Myc.

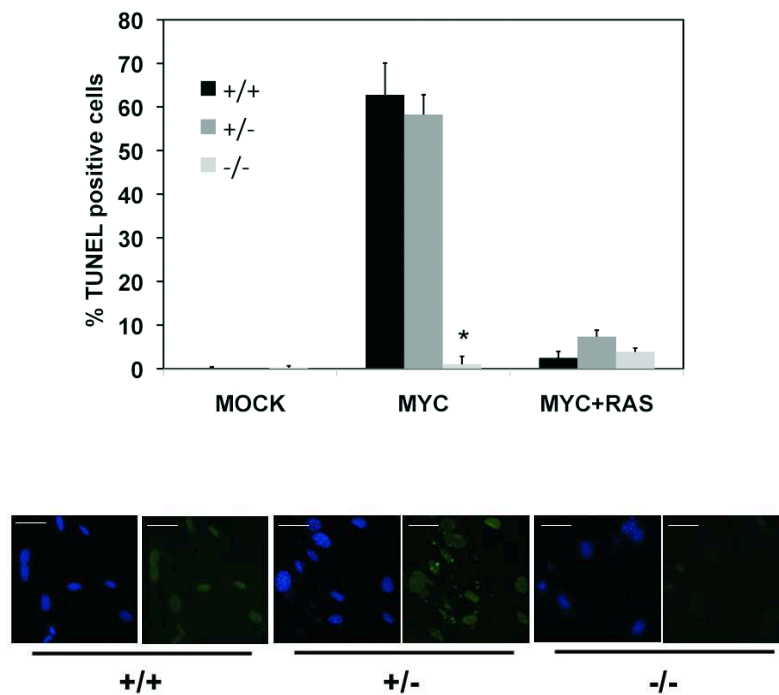


Figure 3: Apoptotic response induced by oncogene in Fe65 KO MEFs

Fe65^{-/-}, Fe65^{+/-} and wt MEFs were infected with Myc alone or with Myc and RasV12 vectors. 48 hours after the infection cells undergoing apoptosis were analyzed by TUNEL as in panel A. Error bars represent S.D.. The asterisks indicate a significant difference with a p < 0.001. Representative examples of DAPI (blue) and TUNEL (green) staining of Myc transfected cells are shown (scale bar = 50 nm).

2 Altered proliferative behavior of Fe65^{-/-} MEFs

Cellular Myc levels have profound consequences on cell proliferation; because I observed that the overexpression of Myc doesn't induce the apoptotic response in Fe65^{-/-} MEFs, I decided to investigate whether cell proliferation was affected by loss of Fe65 in MEFs. To this aim Fe65^{+/+}, Fe65^{+/-} and Fe65^{-/-} were plated at 10⁵ cells/60 mm dish at day 0 and counted every 24 hours for a week. As shown in figure 4 Fe65^{-/-} MEFs showed a growth rate higher than that observed in wt cells, whereas Fe65^{+/-} MEFs have a phenotype similar to that of Fe65^{+/+} MEFs. This observation was confirmed in three cell preparations from different embryos of each genotype.

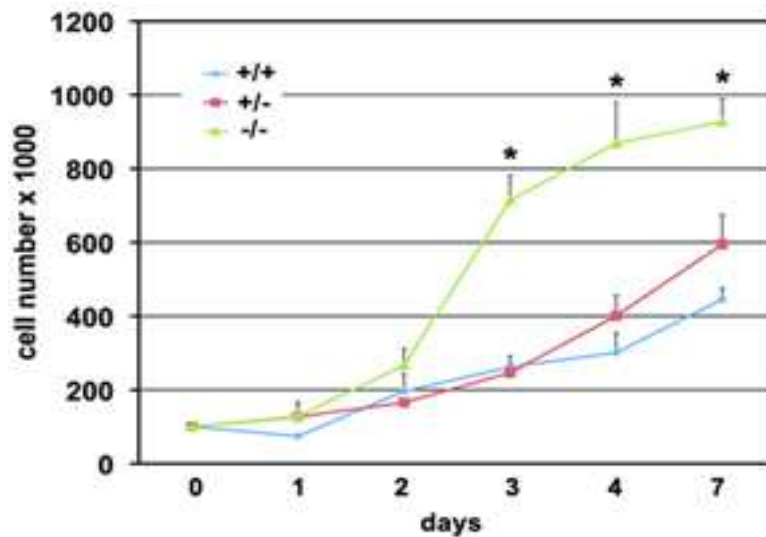


Figure 4: Fe65 suppression enhances proliferation of primary MEFs

Passage 2 MEFs, wt (+/+), Fe65^{+/-} or Fe65^{-/-}, from three distinct pools of at least three embryos each, were plated at 100 000 cells/60 mm dish at day 0, and counted at the indicated times. Error bars represent S.D.. The asterisks indicate significant differences with $p < 0.01$.

2.1 Fe65 knock down (KD) cells have the same phenotype of KO MEFs

To confirm the phenotype observed in Fe65 KO MEFs we analyzed the cell proliferation in other cellular systems in which Fe65 knockdown was obtained by RNA interference strategy. In NIH3T3 cells Fe65 expression was transiently suppressed by transfecting a siRNA targeting Fe65. A non silencing (ns) siRNA was transfected in control cells. As shown in figure 3A the western blot analysis with a specific Fe65 antibody, revealed that Fe65 protein level was reduced of about 80% compared to non silencing transfected cells. After 24 h these cells were plated as in figure 4 and counted every 12 hours for 3 days. As shown in the graph (Figure 5), Fe65 silencing in NIH3T3 cells resulted in a significant increase of the growth rate, similar to what observed in Fe65 KO MEFs.

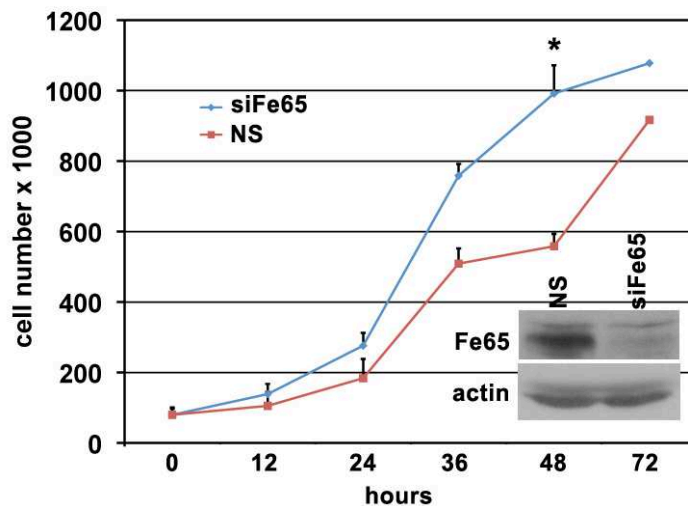
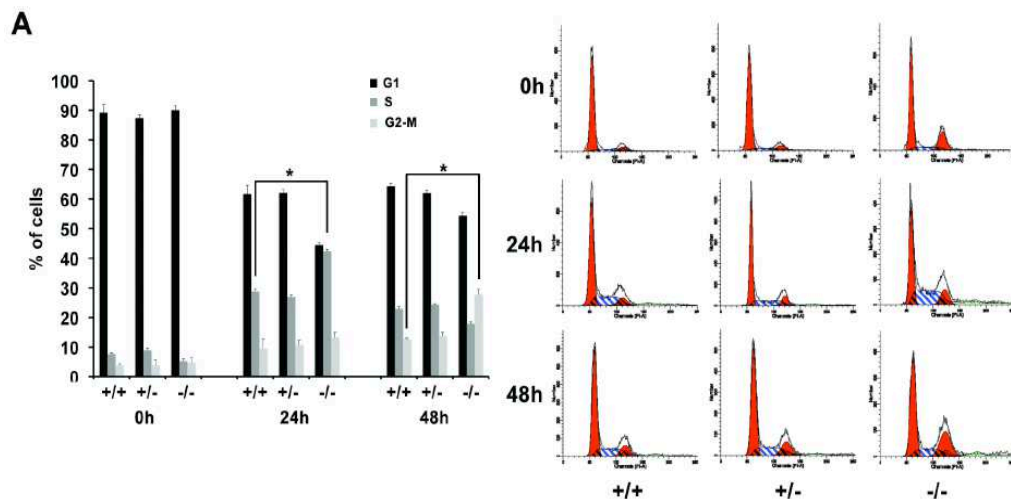


Figure 5: Suppression of Fe65 by RNA interference results in the same phenotype observed in Fe65 KO MEFs

NIH3T3 cells were transfected with with non-silencing (NS) or Fe65 targeting siRNAs. Western blot analysis demonstrated that the decrease of Fe65 levels due to RNAi was of about 80%, compared to cells transfected with non silencing (ns) siRNA. After 24h these cells were plated at 10^5 cells/60 mm dish at day 0 and counted every 12 hours for 3 days. Error bars represent S.D.. The asterisks indicate significant differences with $p < 0.01$.

2.2 Fe65 suppression affects the cell cycle control

To understand the mechanism of cell proliferation phenotype I examined the effects of Fe65 suppression on cell cycle progression using flow cytometry. This method allows to distinguish cells in different phases of the cell cycle. The fluorescence intensity of the stained cells at certain wavelengths will therefore correlate with the amount of DNA they contain. As the DNA content of cells duplicates during the S phase of the cell cycle, the relative amount of cells in the G0 phase and G1 phase (before S phase), in the S phase, and in the G2 phase and M phase (after S phase) can be determined, as the fluorescence of cells in the G2/M phase will be twice as high as that of cells in the G0/G1 phase. The analysis of the cell cycle progression upon serum stimulation showed that Fe65^{-/-} MEFs enter S-phase before wild-type and heterozygous cells, as demonstrated in figure 6, by FACS profiles of propidium iodide stained MEFs at various times after serum stimulation for 48 hours of serum starved cells. I observed an altered control of cell cycle in Fe65 KO cells also in exponentially growing cells. Indeed, Fe65^{-/-} cells showed an increased percentage of cells in G2-M phases compared to wt and heterozygous cells and a reduced number of cells in S phase. Furthermore, when Fe65^{-/-} cells were irradiated with 1 Gy of X rays they showed a defective arrest of the cell cycle, compared to wt cells that, on the contrary, responded to the damage with a G1 arrest (Figure 6B).



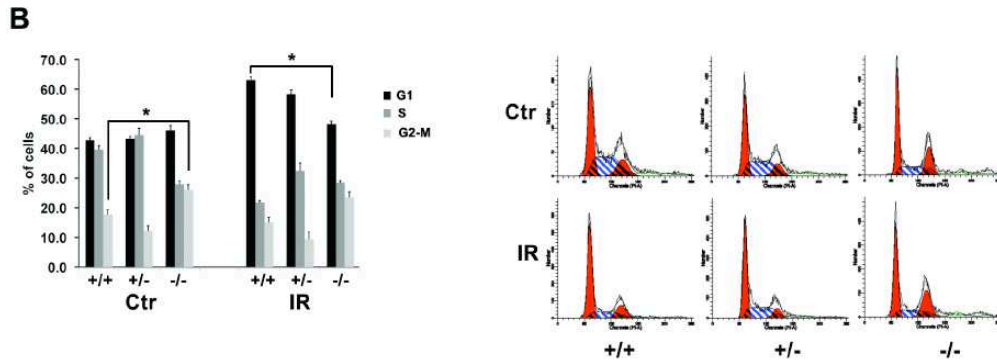


Figure 6: Altered cell cycle kinetics in Fe65^{-/-} MEFs.

A. Cell cycle re-entry after 72-hour serum starvation was analyzed by FACS profiling of propidium iodide (PI) stained cells. Histograms report the percentage of cells in G1, S and G2/M phases of the cell cycle at time 0, 24 and 48 hours after the exposure to 10% FBS. **B.** Exponentially growing cells at 70% confluence were exposed or not to 1 Gy of X rays (IR). 24 hours after the irradiation, the cells were stained with PI and analyzed by FACS as in panel A. Error bars represent S.D.. The asterisks indicate significant differences with $p < 0.01$.

It is well known that p21 induction, by p53, blocks cell cycle and increases the apoptosis. So, I investigated whether p21 is involved in defective arrest of cell cycle in Fe65^{-/-} MEFs. To this aim, MEFs were irradiated with a lethal dose of X-Rays and were harvested 16 hours after irradiation. As shown in figure 7, Fe65^{-/-} MEFs lack the induction of p21 following DNA damage.

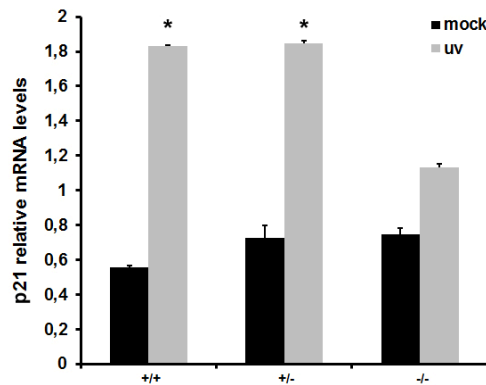
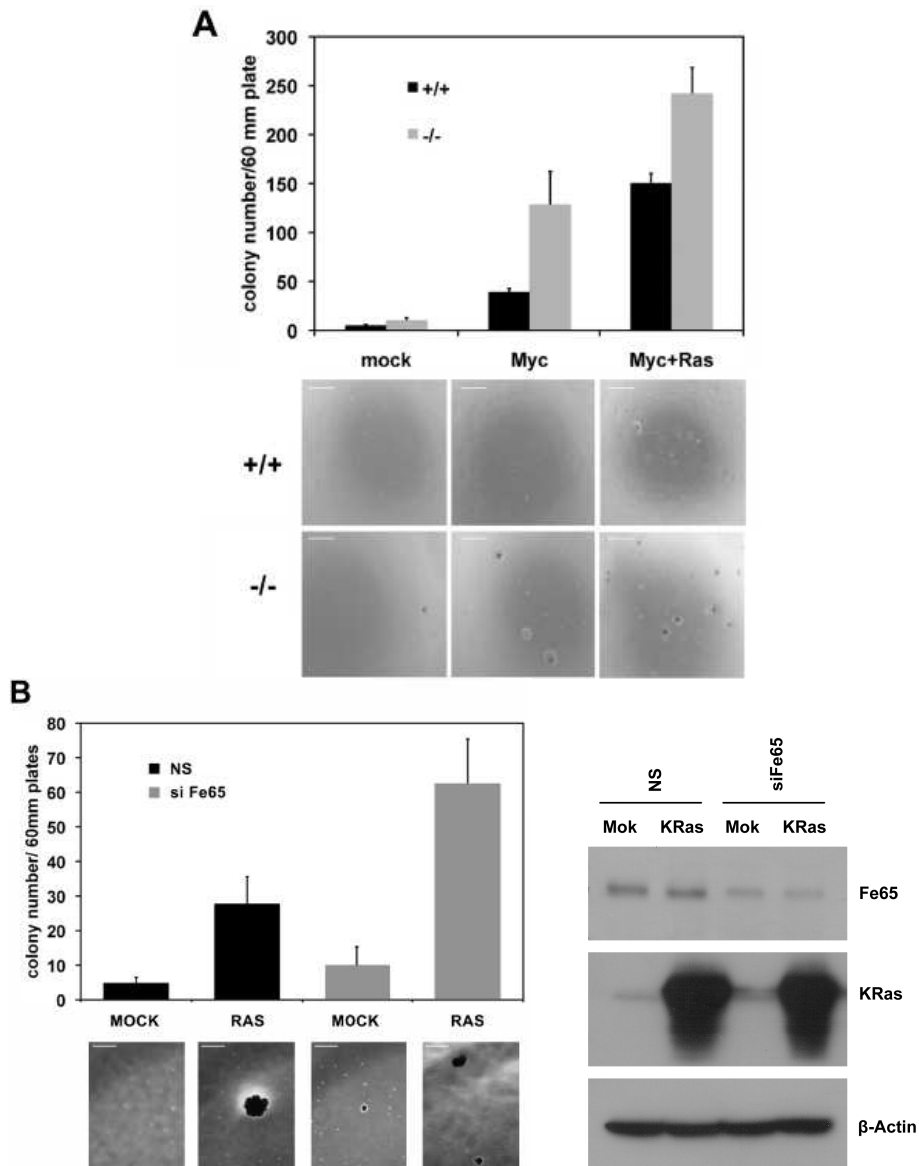


Figure 7: UV not induced p21 activation in Fe65^{-/-} MEFs

MEFs were irradiated with 30 J/sqm of UV rays and harvested 16 hours after irradiation. Expression of p21 in mRNA samples was analyzed by Q-PCR. Error bars represent S.D.. The asterisks indicate significant differences with $p < 0.01$.

3 Fe65 deficiency favors oncogenic transformation *in vitro*

The phenotypes of Fe65 suppression on the induction of apoptosis and on cell proliferation could obviously have relevant effects on cell transformation. Early passage primary fibroblasts are poorly susceptible to oncogenic transformation, so, I tested whether Fe65 KO has any effects on the ability of Myc and oncogenic H-RasV12 to transform MEFs. To this aim, I performed an anchorage-independent growth assay in soft agar. This assay is a common method to monitor anchorage-independent growth, which measures proliferation in a semisolid culture media after 3-4 weeks by manual counting of colonies. It is one of the hallmarks of cell transformation, because it is considered the most accurate and stringent *in vitro* assay for detecting malignant transformation of cells. MEFs Fe65 $+/+$ and Fe65 $-/-$ were infected with viral vectors driving the expression of Myc and/or RasV12. Then the cells were plated on soft agar. As shown in Figure 8A, Myc alone had very little effect on cell transformation in wild type MEFs. On the contrary, c-Myc was able to induce the growth of a significant number of colonies of Fe65 $-/-$ cells. Also the contemporary expression of both Myc and H-RasV12 induced a significant higher number of colonies in KO than in WT cells, thus indicating that the suppression of Fe65 sensitizes primary fibroblasts to transformation. Then, I examined whether Fe65 suppression by RNA interference may favor the appearance of the transformed phenotype induced by mutant Ras transfection also in NIH3T3. In this assay, NIH3T3 cells were transfected with K-Ras A59T or with an empty vector and the resulting colonies were counted 21 days after transfection. The results of figure 8B indicated that the silencing of Fe65 by RNAi significantly increased the number of the colonies and also their main size. Taken together these results indicate that Fe65 behaves in primary MEFs and in NIH3T3 cells as a tumor suppressor, as its downregulation favors the transformation induced by c-Myc and/or by mutant Ras.



three independent experiments. Error bars represent S.D.. Representative fields of the plates are shown (scale bar= 500 mm).

3.1 Fe65 expression levels are decreased in various human lymphoma and ovary cancers

The results obtained in Fe65^{-/-} MEFs and in NIH3T3 cells suggest the possibility that Fe65 may function as a tumor suppressor gene. So, I decide to first examine the expression of Fe65 in transformed cell culture. I found that in NIH3T3 cell line transformed *in vitro* by mutant K-Ras, the expression of Fe65 was down-regulated. As shown in figure 9A, the amount of Fe65 mRNA present in NIH3T3 transformed cells is significantly decreased compared to wt cells. This downregulation is paralleled by an almost complete disappearance of Fe65 protein in NIH3T3 K-Ras cells (Figure 9B), thus suggesting that the dramatic decrease of the protein could be due also to post-translation events.

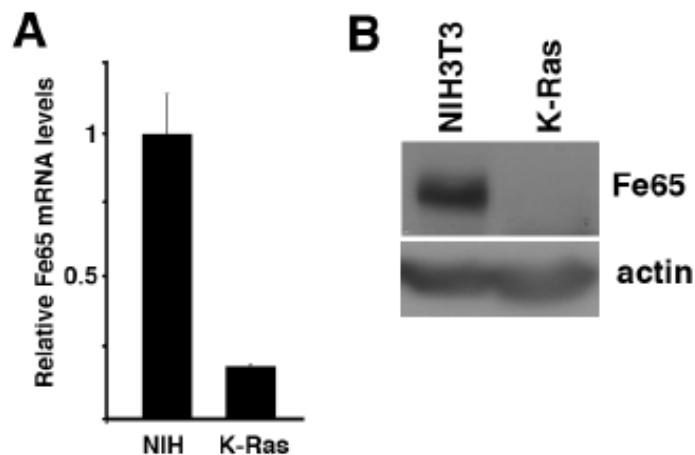


Figure 9: Fe65 in K-Ras transformed cells

A. Fe65 mRNA levels in normal and in a NIH3T3 cell line transformed with K-Ras. B. Fe65 protein levels in K-Ras transformed cells and in normal counterparts. Error bars represent S.D..

Then, I measured Fe65 expression in human lymphoma and ovary cancers by Q-PCR, and I observed low levels of Fe65 in many cases (Figure 10).

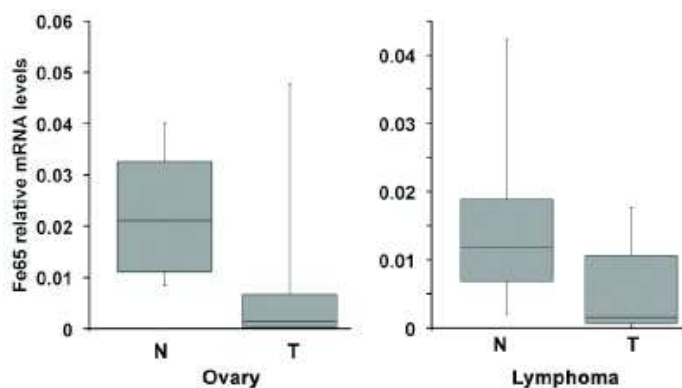


Figure 10: Fe65 mRNA levels in human tumors

Boxplot distribution of Fe65 mRNA levels in ovary (n. 25) cancers and lymphoma (n. 19). Corresponding normal tissue were: ovary (n. 6) and reactive lymph node (n. 9). Values of Fe65 mRNA are relative to GAPDH mRNA levels in the same samples. Real-time PCR were performed in triplicate for each samples.

Fe65 down-regulation in cancer cells could be due to gene deletion or rearrangements or promoter methylation. To this aim, I checked the presence of deletions in Fe65 gene in normal and ovary tumors samples by PCR (Figure 11A). Then, I assayed Fe65 promoter methylation in normal and cancer ovary (Figure 11B). None of such modifications were observed in several cases of ovary cancer where Fe65 mRNA was undetectable.

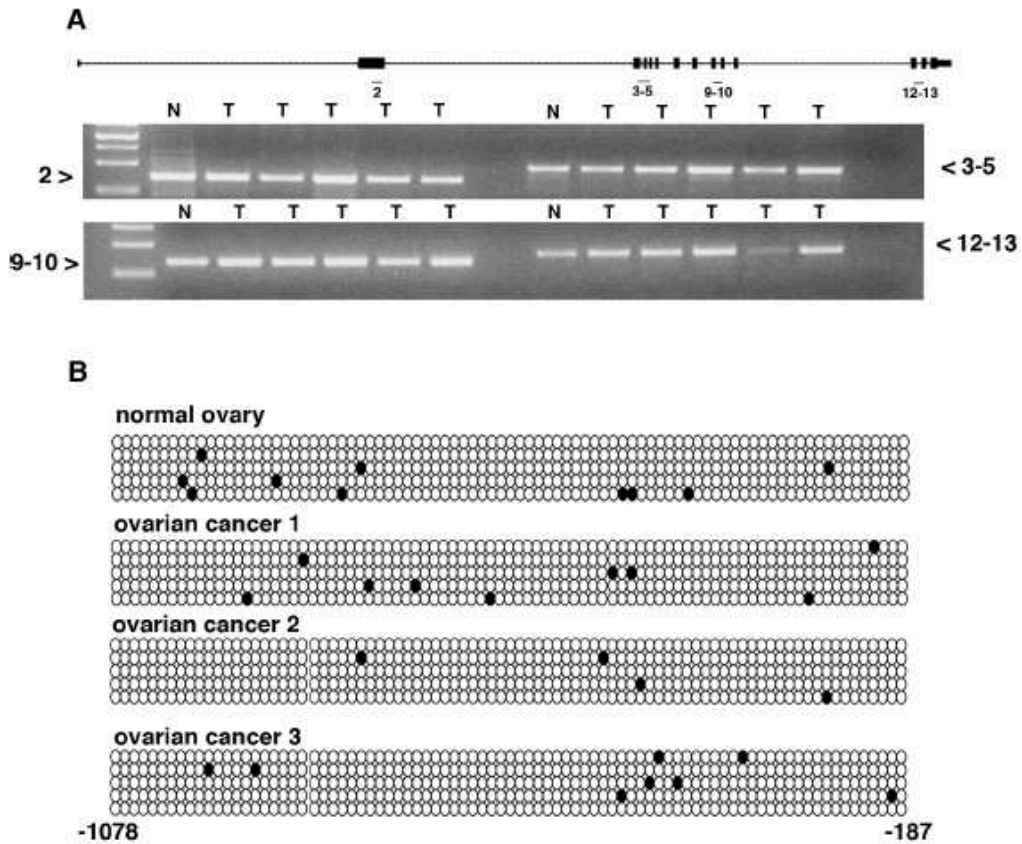


Figure 11: Fe65 suppression in lymphoma and ovary tumors could be due to gene deletion or promoter methylation

A. Genomic sequences of Fe65 gene are intact in human ovary cancers. Genomic DNA was amplified by using four oligonucleotides pairs to examine the integrity of exons 2, 3-5, 9, 10, 12-13. **B.** Bisulfite genomic sequencing of the promoter region of the human Fe65 gene from nt. 1122 to nt. -187. Open and closed circles indicate unmethylated and methylated CpG islands. One normal ovary and three ovary cancers were analyzed sequencing 5 independent clones.

4 The apoptotic response of the cells to genotoxic stress is altered in Fe65^{-/-} MEFs

To investigate the mechanisms underlying the effects of Fe65 suppression we analyzed the status of several pathways that play crucial roles in the apoptotic response to DNA damage and in the regulation of cell proliferation. All the experiments reported above were made in MEFs at passage 2 and that these

experiments were performed in at least two different pools of MEFs from three distinct embryos. In this way the possibility of an *in vitro* selection of mutant cells bearing additional genetic defects targeting tumor suppressor genes appears to be unlikely. The best-characterized pathway opposing to Myc-induced transformation depends on the activation of p53, which induces the apoptotic response by transcriptional activation of pro-apoptotic members of Bcl-2 family. To this aim, I irradiated Fe65 *+/+*, Fe65 *+/-* and Fe65 *-/-* MEFs with 30 J/sqm of UV rays, after 4 hours the cells were harvested and extracted the protein. Then, I analyzed the activation of p53 by Western Blot using an antibody against the serine 15 phosphorylated of p53. As shown in Figure 12A, p53 phosphorylation upon DNA damage is similar in all the three Fe65 genotypes examined. However, when I looked at the effectors downstream of p53, I observed that Fe65^{-/-} MEFs failed to accumulate BAX and PUMA mRNAs, upon DNA damage (Figure 12B, 12C).

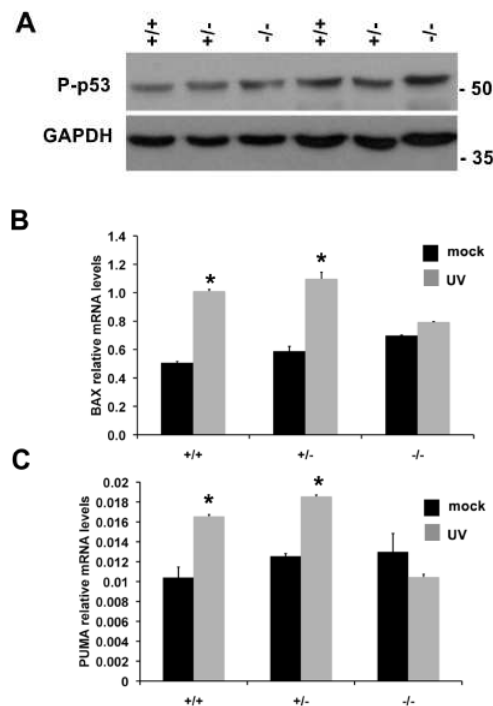


Figure 12: Pro-apoptotic pathway is altered in Fe65 *-/-* MEFs

A. Phospho-S15 p53 western blot analysis of MEF pools, from at least three independent embryos with the three genotypes, 4 hours after the exposure to 30 J/sqm of UV rays. **B** and **C.** Q-PCR analysis of BAX (B) and PUMA (C) mRNAs from untreated cells and UV-treated MEFs. mRNA samples for cDNA preparation were from cells harvested 16 hours after irradiation. Histograms represent the mean values of three independent experiments. Error bars represent S.D. Asterisks indicate significant differences with $p < 0.01$.

This observation is in agreement with the finding that Fe65^{-/-} MEFs fail to undergo apoptosis (Fig. 2 and 3) when exposed to genotoxic stress. The nuclear translocation of FOXO3A is necessary to the transcription of pro-apoptotic genes, this mechanism is under the control of AKT. Indeed, the pro-survival effects of this kinase also depend on the inhibition of FOXO3A induction. So we examined the AKT status in Fe65^{-/-} MEFs. To this purpose MEFs were irradiated with 5 Gy of X-Rays; 4 hours after irradiation the cells were harvested and protein extracts were prepared. Activated AKT was analyzed by Western Blot analysis. In these cells, I observed that basal levels of the phosphorylated form of this kinase are robustly increased when Fe65 is suppressed (Figure 13A). It is well known that PTEN inhibits the PI3P pathway that activates AKT. So, I investigated PTEN expression and I observed that the increase of AKT phosphorylation is accompanied by a slight decrease of the amount of PTEN in Fe65^{-/-} MEFs (Figure 13B), which was always observed in all the MEFs isolated from several different embryos.

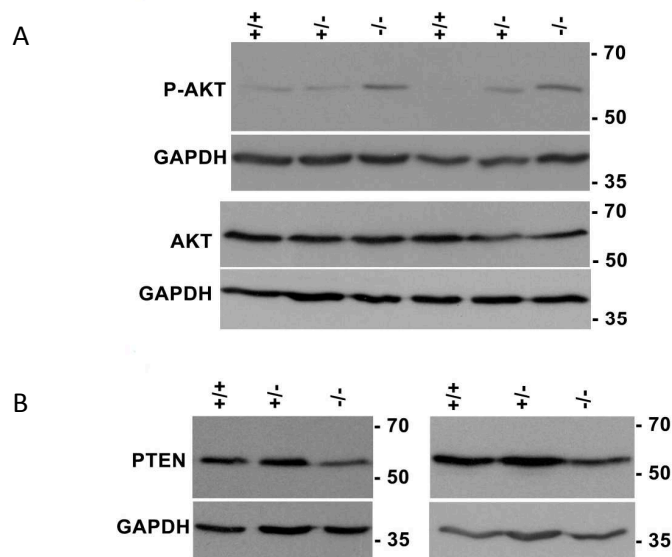


Figure 13: pro-survival pathways are altered in Fe65^{-/-} MEFs

MEFs were irradiated with 5 Gy of X-Rays and harvested after 4 hours. Western blot analysis of phospho-S473 AKT and total AKT (A) and of PTEN (B). Each lane contains the extracts from a MEF pool from three distinct embryos.

A possible explanation of the phenotype observed in Fe65^{-/-} MEFs could be based on the recent demonstration that the silencing of Fe65 results in the abolishment of the recruitment of JNK1 to Y142 phosphorylated H2A.X and that this event hampers the apoptotic response of the cells to DNA damage (Cook et al., 2009). Therefore, the resistance to apoptosis in Fe65^{-/-} MEFs

could be also due to the absence of Fe65 on the JNK/ γ -H2A.X interaction. So, I investigated whether, in Fe65^{-/-} MEFs exposed to IR, the recruitment of JNK1 to γ -H2A.X is affected. To this purpose, MEFs were irradiated, JNK1 and γ -H2A.X were co-immunoprecipitated and analyzed by Western Blot. As shown in Fig. 14A, JNK1 and γ -H2A.X co-immunoprecipitated in wild-type MEFs but not in Fe65^{-/-} MEFs. Furthermore, I checked the basal expression of activated JNK and I observed that the suppression of Fe65 was also associated with reduced basal levels of phosphorylated JNK (Figure 13B). Therefore, the resistance to apoptosis we observed in Fe65^{-/-} MEFs could be, at least in part, a consequence of the reduced recruitment/activation of JNK at DNA lesions occupied by γ -H2A.X.

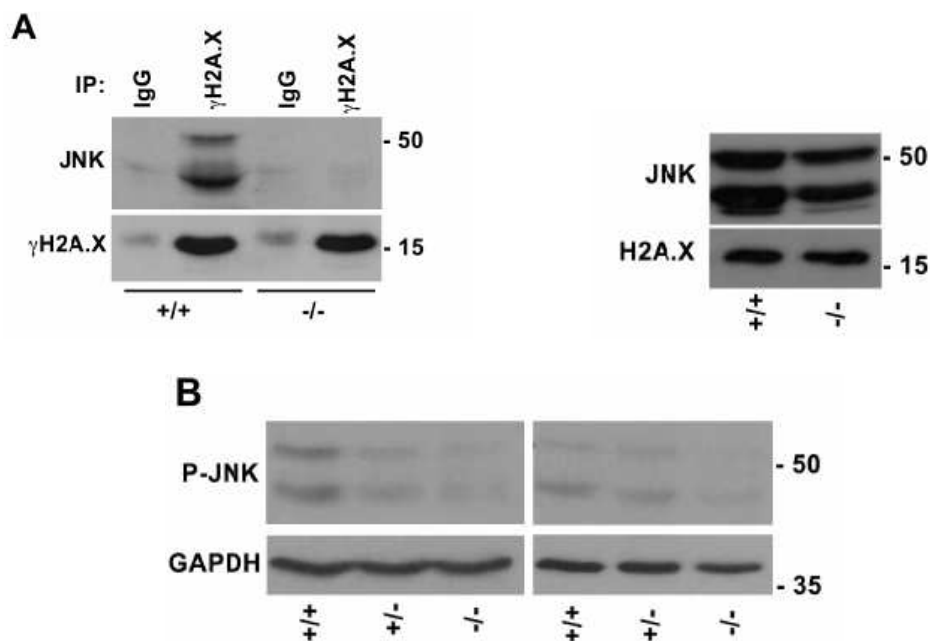


Figure 13: The absence of Fe65 prevents the recruitment of JNK to γ -H2A.X.

A. Nuclear extracts from irradiated (15 Gy of X-rays) wild-type or Fe65^{-/-} MEF pools were prepared 30' after irradiation and immunoprecipitated with phospho-S139 H2A.X antibody or control mouse IgG. Western blot analysis of co-immunoprecipitated proteins with JNK antibody. The latter was used to assess the levels of JNK in nuclear extracts (on the right); H2A.X was used as loading control. **B.** Western blot analysis of total extracts from distinct MEF pools with the phospho-(T183, Y185) JNK antibody; GAPDH was used as loading control.

5 Discussion

This study demonstrates that Fe65 suppression is associated with the inhibition of the apoptotic response of primary MEFs to IR and UV rays or to oncogenes. This phenotype is associated with an increased susceptibility of Fe65^{-/-} MEFs to oncogenes-induced transformation. Accordingly, we have found that human lymphoma and ovary tumors have reduced levels of Fe65. These data indicate that Fe65 has the characteristics of a tumor suppressor gene.

The phenotype of Fe65 KO cells and mice observed before my PhD project suggested us to explore the possible link between the function of this protein and the cellular machinery devoted to protect from and/or respond to DNA damages. Previous results suggested that Fe65 could have some nuclear functions, considering its presence in the nucleus and its interaction with several nuclear proteins. These results supported the hypothesis that Fe65 could be involved in the regulation of transcription, although most of them rely on the use of reporter gene assays. Fe65 appears to function as a key regulator of signals received and integrated at the membrane by APP holoprotein which modulates Fe65 nuclear localization and functions. Starting from the observation that the absence of Fe65 results *in vivo* and *in vitro* in high vulnerability to DNA damaging agents we tried to understand the molecular mechanism involving Fe65 in the DNA damage response.

Apoptosis, or programmed cell death, is a physiologic genetically encoded program that results in cell death. It plays an important role in the elimination of unwanted cells during development and also as a balancing factor in maintaining proliferate homeostasis.

The results reported here indicate that the inhibition of apoptosis observed in the Fe65^{-/-} MEFs can be due, at least in part, to the constitutive activation of AKT and, at the same time, to the decreased levels of active JNK. These regulatory enzymes influence survival/apoptosis of the cells through several mechanisms. Their action converges on FOXO, a transcription factor required for the transcription of p53 targets, like BAX and PUMA (You et al., 2006). Indeed, AKT phosphorylates FOXO thus inhibiting its nuclear translocation (Brunet et al., 2002), while JNK-dependent phosphorylation of FOXO prevents its phosphorylation by AKT (Essers et al., 2004). On this basis, the constitutive activation of AKT and the contemporary failure of JNK activation are coherent with our observation that, despite the normal phosphorylation of p53, BAX and PUMA are not induced as a consequence of DNA damage. In addition to the apoptotic defects, we also observed a defective cell cycle arrest when Fe65^{-/-} MEFs were exposed to IR. This finding is in agreement with the lack of induction of p21 following DNA damage. Considering that the complete activation of p53 also depends on its acetylation by Tip60 (Tang et al., 2006) we cannot exclude that the reduced recruitment of Tip60 at DNA lesions, observed as a consequence of Fe65 suppression (Stante et al., 2009), could also impair p53 acetylation and complete activation.

An important issue regards with the mechanistic relationship between Fe65 suppression and the observed phenotype. It was previously shown that Fe65 functions as an adaptor protein required for the recruitment of JNK at the DNA lesions labeled by the γ -H2A.X (Cook et al., 2009). This interaction is crucial for the induction of the apoptotic response downstream of an unrepaired DNA damage. I have demonstrated that the interaction of γ -H2A.X with JNK is abolished in Fe65^{-/-} MEFs, thus indicating that the altered apoptotic phenotype observed in these cells could depend on the failure of this mechanism. On the basis of available results, it is impossible to support a direct relationship between the lack of activation of nuclear JNK with the downregulation of PTEN and the constitutive activation of AKT. Of course, the latter could be due to mechanisms involving Fe65 but independent from JNK. Indeed, numerous results indicated that Fe65 could function as an adaptor protein with a relatively large array of possible interactors. Thus the absence, or reduced levels, of Fe65 could affect many different pathways.

The observation that the expression of Fe65 is reduced in lymphoma and ovary cancers opens the question of the mechanisms governing this downregulation. The results obtained in Fe65^{-/-} MEFs suggest that the suppression of Fe65 could favor the selection of cancer cells more resistant to apoptosis and with a more aggressive proliferative behavior. The mechanisms that causes Fe65 suppression *in vivo* appear to act on the transcription of the gene because I observed a decrease of Fe65 mRNA levels. I have explored the integrity of the gene and methylation *status* of the CpG island present in the Fe65 gene promoter in five cases of ovary cancer where Fe65 was downregulated, but no gross alterations of the gene or CpG hypermethylation were observed compared to normal tissues. Despite the small number of cases examined, this result suggested that CpG hypermethylation is not the major cause for the downregulation.

There are only few data on the regulation of the Fe65 gene. It has been previously observed that Pura and YY1 are the main transcription factors interacting with Fe65 promoter (Zambrano et al., 1997b). *In vitro* experiments indicated that both Pura and YY1 contribute to the activation of the transcription of the gene, through independent and non-cooperative mechanisms. Several results suggest the possibility that Pura downregulation is associated with malignancy and its enhanced expression results in cell cycle arrest and resistance to oncogenes-induced transformation (Lezon-Geyda et al., 2001) (Stacey et al., 1999) (Barr and Johnson, 2001). All the same, YY1 is overexpressed in many human tumors and controls, functioning as activator or repressor, a large array of genes, most of which associated with cancer (Gordon et al., 2006). Therefore, it is plausible that the regulation of Fe65 gene by Pura and YY1 could have a role in its suppression during tumor progression.

Conclusions

The DNA is continuously exposed to the action of endogenous or exogenous genotoxic agents. However, in cells, many proteins are deputies to the maintenance of the integrity of the genetic material, repairing injuries through specific mechanisms that differ depending on the type of damage that occurs and on the phase of the cell cycle. The activation of the cell response to DNA damage is a complex phenomenon that involves many factors. All the alterations of the proteins involved in different repair mechanisms cause the accumulation of mutations within the genome compromising cell survival and function.

In this study, starting from the observation that Fe65 suppression shows greater sensitivity to DNA damage, I demonstrated that the loss of Fe65 is associated to a lower efficiency in the activation of the DDR. In particular, I observed a strong decrease in apoptosis activation and an altered cell cycle that leads a neoplastic transformation. This phenotype could be due to an inadequate activation of JNK pathway and a constitutive activation of AKT that block the apoptotic response.

References

- Alessi, D.R., Andjelkovic, M., Caudwell, B., Cron, P., Morrice, N., Cohen, P., and Hemmings, B.A. (1996). Mechanism of activation of protein kinase B by insulin and IGF-1. *EMBO J* 15, 6541-6551.
- Ando, K., Iijima, K.I., Elliott, J.I., Kirino, Y., and Suzuki, T. (2001). Phosphorylation-dependent regulation of the interaction of amyloid precursor protein with Fe65 affects the production of beta-amyloid. *J Biol Chem* 276, 40353-40361.
- Baek, S.H., Ohgi, K.A., Rose, D.W., Koo, E.H., Glass, C.K., and Rosenfeld, M.G. (2002). Exchange of N-CoR corepressor and Tip60 coactivator complexes links gene expression by NF-kappaB and beta-amyloid precursor protein. *Cell* 110, 55-67.
- Barbato, C., Canu, N., Zambrano, N., Serafino, A., Minopoli, G., Ciotti, M.T., Amadoro, G., Russo, T., and Calissano, P. (2005). Interaction of Tau with Fe65 links tau to APP. *Neurobiol Dis* 18, 399-408.
- Barr, S.M., and Johnson, E.M. (2001). Ras-induced colony formation and anchorage-independent growth inhibited by elevated expression of Puralpha in NIH3T3 cells. *J Cell Biochem* 81, 621-638.
- Bergink, S., and Jentsch, S. (2009). Principles of ubiquitin and SUMO modifications in DNA repair. *Nature* 458, 461-467.
- Bertram, L., Lill, C.M., and Tanzi, R.E. (2010) The genetics of Alzheimer disease: back to the future. *Neuron* 68, 270-281.
- Biggs, W.H., 3rd, Meisenhelder, J., Hunter, T., Cavenee, W.K., and Arden, K.C. (1999). Protein kinase B/Akt-mediated phosphorylation promotes nuclear exclusion of the winged helix transcription factor FKHR1. *Proc Natl Acad Sci U S A* 96, 7421-7426.
- Bimonte, M., Gianni, D., Allegra, D., Russo, T., and Zambrano, N. (2004). Mutation of the feh-1 gene, the *Caenorhabditis elegans* orthologue of mammalian Fe65, decreases the expression of two acetylcholinesterase genes. *Eur J Neurosci* 20, 1483-1488.
- Bird, A.W., Yu, D.Y., Pray-Grant, M.G., Qiu, Q., Harmon, K.E., Megee, P.C., Grant, P.A., Smith, M.M., and Christman, M.F. (2002). Acetylation of histone H4 by Esa1 is required for DNA double-strand break repair. *Nature* 419, 411-415.
- Bononi, A., Agnoletto, C., De Marchi, E., Marchi, S., Patergnani, S., Bonora, M., Giorgi, C., Missiroli, S., Poletti, F., Rimessi, A., and Pinton, P. (2011) Protein kinases and phosphatases in the control of cell fate. *Enzyme Res* 2011, 329098.
- Bressler, S.L., Gray, M.D., Sopher, B.L., Hu, Q., Hearn, M.G., Pham, D.G., Dinulos, M.B., Fukuchi, K., Sisodia, S.S., Miller, M.A., *et al.* (1996). cDNA cloning and chromosome mapping of the human Fe65 gene: interaction of the conserved cytoplasmic domains of the human beta-amyloid precursor protein and its homologues with the mouse Fe65 protein. *Hum Mol Genet* 5, 1589-1598.

- Brunet, A., Kanai, F., Stehn, J., Xu, J., Sarbassova, D., Frangioni, J.V., Dalal, S.N., DeCaprio, J.A., Greenberg, M.E., and Yaffe, M.B. (2002). 14-3-3 transits to the nucleus and participates in dynamic nucleocytoplasmic transport. *J Cell Biol* 156, 817-828.
- Bruni, P., Minopoli, G., Brancaccio, T., Napolitano, M., Faraonio, R., Zambrano, N., Hansen, U., and Russo, T. (2002). Fe65, a ligand of the Alzheimer's beta-amyloid precursor protein, blocks cell cycle progression by down-regulating thymidylate synthase expression. *J Biol Chem* 277, 35481-35488.
- Cao, X., and Sudhof, T.C. (2001). A transcriptionally [correction of transcriptively] active complex of APP with Fe65 and histone acetyltransferase Tip60. *Science* 293, 115-120.
- Chalhoub, N., and Baker, S.J. (2009). PTEN and the PI3-kinase pathway in cancer. *Annu Rev Pathol* 4, 127-150.
- Ciccia, A., and Elledge, S.J. (2010) The DNA damage response: making it safe to play with knives. *Mol Cell* 40, 179-204.
- Cook, P.J., Ju, B.G., Telese, F., Wang, X., Glass, C.K., and Rosenfeld, M.G. (2009). Tyrosine dephosphorylation of H2AX modulates apoptosis and survival decisions. *Nature* 458, 591-596.
- Cui, R., Widlund, H.R., Feige, E., Lin, J.Y., Wilensky, D.L., Igras, V.E., D'Orazio, J., Fung, C.Y., Schanbacher, C.F., Granter, S.R., and Fisher, D.E. (2007). Central role of p53 in the suntan response and pathologic hyperpigmentation. *Cell* 128, 853-864.
- Ermeikova, K.S., Zambrano, N., Linn, H., Minopoli, G., Gertler, F., Russo, T., and Sudol, M. (1997). The WW domain of neural protein FE65 interacts with proline-rich motifs in Mena, the mammalian homolog of *Drosophila* enabled. *J Biol Chem* 272, 32869-32877.
- Esler, W.P., and Wolfe, M.S. (2001). A portrait of Alzheimer secretases--new features and familiar faces. *Science* 293, 1449-1454.
- Esposito, F., Ammendola, R., Duilio, A., Costanzo, F., Giordano, M., Zambrano, N., D'Agostino, P., Russo, T., and Cimino, F. (1990). Isolation of cDNA fragments hybridizing to rat brain-specific mRNAs. *Dev Neurosci* 12, 373-381.
- Essers, M.A., Weijzen, S., de Vries-Smits, A.M., Saarloos, I., de Ruyter, N.D., Bos, J.L., and Burgering, B.M. (2004). FOXO transcription factor activation by oxidative stress mediated by the small GTPase Ral and JNK. *EMBO J* 23, 4802-4812.
- Fiore, F., Zambrano, N., Minopoli, G., Donini, V., Duilio, A., and Russo, T. (1995). The regions of the Fe65 protein homologous to the phosphotyrosine interaction/phosphotyrosine binding domain of Shc bind the intracellular domain of the Alzheimer's amyloid precursor protein. *J Biol Chem* 270, 30853-30856.
- Forni, P.E., Fornaro, M., Guenette, S., and Wray, S., (2011) A role for FE65 in controlling GnRH-1 neurogenesis. *J Neurosci* 31, 480-491.

- Frech, M., Andjelkovic, M., Ingley, E., Reddy, K.K., Falck, J.R., and Hemmings, B.A. (1997). High affinity binding of inositol phosphates and phosphoinositides to the pleckstrin homology domain of RAC/protein kinase B and their influence on kinase activity. *J Biol Chem* 272, 8474-8481.
- Gardai, S.J., Hildeman, D.A., Frankel, S.K., Whitlock, B.B., Frasch, S.C., Borregaard, N., Marrack, P., Bratton, D.L., and Henson, P.M. (2004). Phosphorylation of Bax Ser184 by Akt regulates its activity and apoptosis in neutrophils. *J Biol Chem* 279, 21085-21095.
- Gasser, S., and Raulet, D.H. (2006). The DNA damage response arouses the immune system. *Cancer Res* 66, 3959-3962.
- Gordon, S., Akopyan, G., Garban, H., and Bonavida, B. (2006). Transcription factor YY1: structure, function, and therapeutic implications in cancer biology. *Oncogene* 25, 1125-1142.
- Gorrini, C., Squatrito, M., Luise, C., Syed, N., Perna, D., Wark, L., Martinato, F., Sardella, D., Verrecchia, A., Bennett, S., *et al.* (2007). Tip60 is a haplo-insufficient tumour suppressor required for an oncogene-induced DNA damage response. *Nature* 448, 1063-1067.
- Guenette, S., Chang, Y., Hiesberger, T., Richardson, J.A., Eckman, C.B., Eckman, E.A., Hammer, R.E., and Herz, J. (2006). Essential roles for the FE65 amyloid precursor protein-interacting proteins in brain development. *EMBO J* 25, 420-431.
- Haas-Kogan, D., Shalev, N., Wong, M., Mills, G., Yount, G., and Stokoe, D. (1998). Protein kinase B (PKB/Akt) activity is elevated in glioblastoma cells due to mutation of the tumor suppressor PTEN/MMAC. *Curr Biol* 8, 1195-1198.
- Harper, J.W., and Elledge, S.J. (2007). The DNA damage response: ten years after. *Mol Cell* 28, 739-745.
- Hass, M.R., and Yankner, B.A. (2005). A γ -secretase-independent mechanism of signal transduction by the amyloid precursor protein. *J Biol Chem* 280, 36895-36904.
- Hebert, S.S., Serneels, L., Tolia, A., Craessaerts, K., Derks, C., Filippov, M.A., Muller, U., and De Strooper, B. (2006). Regulated intramembrane proteolysis of amyloid precursor protein and regulation of expression of putative target genes. *EMBO Rep* 7, 739-745.
- Herms, J., Anliker, B., Heber, S., Ring, S., Fuhrmann, M., Kretschmar, H., Sisodia, S., and Muller, U. (2004). Cortical dysplasia resembling human type 2 lissencephaly in mice lacking all three APP family members. *EMBO J* 23, 4106-4115.
- Hoe, H.S., Magill, L.A., Guenette, S., Fu, Z., Vicini, S., and Rebeck, G.W. (2006). FE65 interaction with the ApoE receptor ApoEr2. *J Biol Chem* 281, 24521-24530.
- Jackson, S.P., and Bartek, J. (2009). The DNA-damage response in human biology and disease. *Nature* 461, 1071-1078.

- Jazirehi, A.R., Wenn, P.B., and Damavand, M. (2012) Therapeutic implications of targeting the PI3Kinase/AKT/mTOR signaling module in melanoma therapy. *Am J Cancer Res* 2, 178-191.
- Kajiwara, Y., Akram, A., Katsel, P., Haroutunian, V., Schmeidler, J., Beecham, G., Haines, J.L., Pericak-Vance, M.A., and Buxbaum, J.D. (2009). FE65 binds Teashirt, inhibiting expression of the primate-specific caspase-4. *PLoS One* 4, e5071.
- Kesavapany, S., Banner, S.J., Lau, K.F., Shaw, C.E., Miller, C.C., Cooper, J.D., and McLoughlin, D.M. (2002). Expression of the Fe65 adapter protein in adult and developing mouse brain. *Neuroscience* 115, 951-960.
- Kim, H.S., Kim, E.M., Lee, J.P., Park, C.H., Kim, S., Seo, J.H., Chang, K.A., Yu, E., Jeong, S.J., Chong, Y.H., and Suh, Y.H. (2003). C-terminal fragments of amyloid precursor protein exert neurotoxicity by inducing glycogen synthase kinase-3beta expression. *FASEB J* 17, 1951-1953.
- Kimberly, W.T., Zheng, J.B., Guenette, S.Y., and Selkoe, D.J. (2001). The intracellular domain of the beta-amyloid precursor protein is stabilized by Fe65 and translocates to the nucleus in a notch-like manner. *J Biol Chem* 276, 40288-40292.
- Kwiatkowski, A.V., Gertler, F.B., and Loureiro, J.J. (2003). Function and regulation of Ena/VASP proteins. *Trends Cell Biol* 13, 386-392.
- Lau, K.F., Chan, W.M., Perkinton, M.S., Tudor, E.L., Chang, R.C., Chan, H.Y., McLoughlin, D.M., and Miller, C.C. (2008). Dexas1 interacts with FE65 to regulate FE65-amyloid precursor protein-dependent transcription. *J Biol Chem* 283, 34728-34737.
- Levy-Lahad, E., Lahad, A., Wijsman, E.M., Bird, T.D., and Schellenberg, G.D. (1995). Apolipoprotein E genotypes and age of onset in early-onset familial Alzheimer's disease. *Ann Neurol* 38, 678-680.
- Lezon-Geyda, K., Najfeld, V., and Johnson, E.M. (2001). Deletions of PURA, at 5q31, and PURB, at 7p13, in myelodysplastic syndrome and progression to acute myelogenous leukemia. *Leukemia* 15, 954-962.
- Li, J., Yen, C., Liaw, D., Podsypanina, K., Bose, S., Wang, S.I., Puc, J., Miliareis, C., Rodgers, L., McCombie, R., *et al.* (1997). PTEN, a putative protein tyrosine phosphatase gene mutated in human brain, breast, and prostate cancer. *Science* 275, 1943-1947.
- Ma, Q.H., Futagawa, T., Yang, W.L., Jiang, X.D., Zeng, L., Takeda, Y., Xu, R.X., Bagnard, D., Schachner, M., Furley, A.J., *et al.* (2008). A TAG1-APP signalling pathway through Fe65 negatively modulates neurogenesis. *Nat Cell Biol* 10, 283-294.
- Manning, B.D., and Cantley, L.C. (2007). AKT/PKB signaling: navigating downstream. *Cell* 129, 1261-1274.
- Martin, L., Latypova, X., and Terro, F. (2011) Post-translational modifications of tau protein: implications for Alzheimer's disease. *Neurochem Int* 58, 458-471.

- Minopoli, G., de Candia, P., Bonetti, A., Faraonio, R., Zambrano, N., and Russo, T. (2001). The beta-amyloid precursor protein functions as a cytosolic anchoring site that prevents Fe65 nuclear translocation. *J Biol Chem* 276, 6545-6550.
- Minopoli, G., Gargiulo, A., Parisi, S., and Russo, T. (2012) Fe65 matters: new light on an old molecule. *IUBMB Life* 64, 936-942.
- Minopoli, G., Stante, M., Napolitano, F., Telese, F., Aloia, L., De Felice, M., Di Lauro, R., Pacelli, R., Brunetti, A., Zambrano, N., and Russo, T. (2007). Essential roles for Fe65, Alzheimer amyloid precursor-binding protein, in the cellular response to DNA damage. *J Biol Chem* 282, 831-835.
- Muller, T., Schrotter, A., Loosse, C., Pfeiffer, K., Theiss, C., Kauth, M., Meyer, H.E., and Marcus, K. (2012) A ternary complex consisting of AICD, FE65, and TIP60 down-regulates Stathmin1. *Biochim Biophys Acta* 1834, 387-394.
- Nicholson, K.M., and Anderson, N.G. (2002). The protein kinase B/Akt signalling pathway in human malignancy. *Cell Signal* 14, 381-395.
- Pardossi-Piquard, R., Petit, A., Kawarai, T., Sunyach, C., Alves da Costa, C., Vincent, B., Ring, S., D'Adamio, L., Shen, J., Muller, U., St George Hyslop, P., Checler, F., (2005). Presenilin-dependent transcriptional control of the Abeta-degrading enzyme neprilysin by intracellular domains of betaAPP and APLP. *Neuron* 46, 541-554.
- Perez, R.G., Soriano, S., Hayes, J.D., Ostaszewski, B., Xia, W., Selkoe, D.J., Chen, X., Stokin, G.B., and Koo, E.H. (1999). Mutagenesis identifies new signals for beta-amyloid precursor protein endocytosis, turnover, and the generation of secreted fragments, including Abeta42. *J Biol Chem* 274, 18851-18856.
- Perkinton, M.S., Standen, C.L., Lau, K.F., Kesavapany, S., Byers, H.L., Ward, M., McLoughlin, D.M., and Miller, C.C. (2004). The c-Abl tyrosine kinase phosphorylates the Fe65 adaptor protein to stimulate Fe65/amyloid precursor protein nuclear signaling. *J Biol Chem* 279, 22084-22091.
- Rena, G., Guo, S., Cichy, S.C., Unterman, T.G., and Cohen, P. (1999). Phosphorylation of the transcription factor forkhead family member FKHR by protein kinase B. *J Biol Chem* 274, 17179-17183.
- Robakis, N.K. (2011) Mechanisms of AD neurodegeneration may be independent of Abeta and its derivatives. *Neurobiol Aging* 32, 372-379.
- Rodriguez-Viciana, P., Warne, P.H., Dhand, R., Vanhaesebroeck, B., Gout, I., Fry, M.J., Waterfield, M.D., and Downward, J. (1994). Phosphatidylinositol-3-OH kinase as a direct target of Ras. *Nature* 370, 527-532.
- Rogaev, E.I., Sherrington, R., Rogaeva, E.A., Levesque, G., Ikeda, M., Liang, Y., Chi, H., Lin, C., Holman, K., Tsuda, T., and et al. (1995). Familial Alzheimer's disease in kindreds with missense mutations in a gene on

- chromosome 1 related to the Alzheimer's disease type 3 gene. *Nature* 376, 775-778.
- Sabo, S.L., Ikin, A.F., Buxbaum, J.D., and Greengard, P. (2001). The Alzheimer amyloid precursor protein (APP) and FE65, an APP-binding protein, regulate cell movement. *J Cell Biol* 153, 1403-1414.
- Sabo, S.L., Lanier, L.M., Ikin, A.F., Khorkova, O., Sahasrabudhe, S., Greengard, P., and Buxbaum, J.D. (1999). Regulation of beta-amyloid secretion by FE65, an amyloid protein precursor-binding protein. *J Biol Chem* 274, 7952-7957.
- Santiard-Baron, D., Langui, D., Delehedde, M., Delatour, B., Schombert, B., Touchet, N., Tremp, G., Paul, M.F., Blanchard, V., Sergeant, N., *et al.* (2005). Expression of human FE65 in amyloid precursor protein transgenic mice is associated with a reduction in beta-amyloid load. *J Neurochem* 93, 330-338.
- Sarbassov, D.D., Guertin, D.A., Ali, S.M., and Sabatini, D.M. (2005). Phosphorylation and regulation of Akt/PKB by the rictor-mTOR complex. *Science* 307, 1098-1101.
- Scott, P.H., Brunn, G.J., Kohn, A.D., Roth, R.A., and Lawrence, J.C., Jr. (1998). Evidence of insulin-stimulated phosphorylation and activation of the mammalian target of rapamycin mediated by a protein kinase B signaling pathway. *Proc Natl Acad Sci U S A* 95, 7772-7777.
- Selkoe, D., and Kopan, R. (2003). Notch and Presenilin: regulated intramembrane proteolysis links development and degeneration. *Annu Rev Neurosci* 26, 565-597.
- Simeone, A., Duilio, A., Fiore, F., Acampora, D., De Felice, C., Faraonio, R., Paolocci, F., Cimino, F., and Russo, T. (1994). Expression of the neuron-specific FE65 gene marks the development of embryo ganglionic derivatives. *Dev Neurosci* 16, 53-60.
- St George-Hyslop, P.H., Haines, J.L., Farrer, L.A., Polinsky, R., Van Broeckhoven, C., Goate, A., McLachlan, D.R., Orr, H., Bruni, A.C., Sorbi, S., *et al.* (1990). Genetic linkage studies suggest that Alzheimer's disease is not a single homogeneous disorder. *Nature* 347, 194-197.
- Stacey, D.W., Hitomi, M., Kanovsky, M., Gan, L., and Johnson, E.M. (1999). Cell cycle arrest and morphological alterations following microinjection of NIH3T3 cells with Pur alpha. *Oncogene* 18, 4254-4261.
- Stante, M., Minopoli, G., Passaro, F., Raia, M., Vecchio, L.D., and Russo, T. (2009). Fe65 is required for Tip60-directed histone H4 acetylation at DNA strand breaks. *Proc Natl Acad Sci U S A* 106, 5093-5098.
- Stephens, L., Anderson, K., Stokoe, D., Erdjument-Bromage, H., Painter, G.F., Holmes, A.B., Gaffney, P.R., Reese, C.B., McCormick, F., Tempst, P., *et al.* (1998). Protein kinase B kinases that mediate phosphatidylinositol 3,4,5-trisphosphate-dependent activation of protein kinase B. *Science* 279, 710-714.

- Tang, Y., Luo, J., Zhang, W., and Gu, W. (2006). Tip60-dependent acetylation of p53 modulates the decision between cell-cycle arrest and apoptosis. *Mol Cell* 24, 827-839.
- Taru, H., and Suzuki, T. (2004). Facilitation of stress-induced phosphorylation of beta-amyloid precursor protein family members by X11-like/Mint2 protein. *J Biol Chem* 279, 21628-21636.
- Telese, F., Bruni, P., Donizetti, A., Gianni, D., D'Ambrosio, C., Scaloni, A., Zambrano, N., Rosenfeld, M.G., and Russo, T. (2005). Transcription regulation by the adaptor protein Fe65 and the nucleosome assembly factor SET. *EMBO Rep* 6, 77-82.
- Trommsdorff, M., Borg, J.P., Margolis, B., and Herz, J. (1998). Interaction of cytosolic adaptor proteins with neuronal apolipoprotein E receptors and the amyloid precursor protein. *J Biol Chem* 273, 33556-33560.
- von Rotz, R.C., Kohli, B.M., Bosset, J., Meier, M., Suzuki, T., Nitsch, R.M., and Konietzko, U. (2004). The APP intracellular domain forms nuclear multiprotein complexes and regulates the transcription of its own precursor. *J Cell Sci* 117, 4435-4448.
- Waldron, E., Jaeger, S., and Pietrzik, C.U. (2006). Functional role of the low-density lipoprotein receptor-related protein in Alzheimer's disease. *Neurodegener Dis* 3, 233-238.
- Wang, B., Hu, Q., Hearn, M.G., Shimizu, K., Ware, C.B., Liggitt, D.H., Jin, L.W., Cool, B.H., Storm, D.R., and Martin, G.M. (2004). Isoform-specific knockout of FE65 leads to impaired learning and memory. *J Neurosci Res* 75, 12-24.
- Weston, C.R., and Davis, R.J. (2002). The JNK signal transduction pathway. *Curr Opin Genet Dev* 12, 14-21.
- Wolfe, M.S. (2006). Alzheimer protease hitches a ride. *Nat Med* 12, 1352-1354.
- Wood, J.G., Mirra, S.S., Pollock, N.J., and Binder, L.I. (1986). Neurofibrillary tangles of Alzheimer disease share antigenic determinants with the axonal microtubule-associated protein tau (tau). *Proc Natl Acad Sci U S A* 83, 4040-4043.
- Xie, Z., Dong, Y., Maeda, U., Xia, W., and Tanzi, R.E. (2007). RNA interference silencing of the adaptor molecules ShcC and Fe65 differentially affect amyloid precursor protein processing and A β generation. *J Biol Chem* 282, 4318-4325.
- You, H., Pellegrini, M., Tsuchihara, K., Yamamoto, K., Hacker, G., Erlacher, M., Villunger, A., and Mak, T.W. (2006). FOXO3a-dependent regulation of Puma in response to cytokine/growth factor withdrawal. *J Exp Med* 203, 1657-1663.
- Zambrano, N., Bimonte, M., Arbucci, S., Gianni, D., Russo, T., and Bazzicalupo, P. (2002). feh-1 and apl-1, the *Caenorhabditis elegans* orthologues of mammalian Fe65 and beta-amyloid precursor protein genes, are involved in the same pathway that controls nematode pharyngeal pumping. *J Cell Sci* 115, 1411-1422.

- Zambrano, N., Bruni, P., Minopoli, G., Mosca, R., Molino, D., Russo, C., Schettini, G., Sudol, M., and Russo, T. (2001). The beta-amyloid precursor protein APP is tyrosine-phosphorylated in cells expressing a constitutively active form of the Abl protooncogene. *J Biol Chem* 276, 19787-19792.
- Zambrano, N., Buxbaum, J.D., Minopoli, G., Fiore, F., De Candia, P., De Renzis, S., Faraonio, R., Sabo, S., Cheetham, J., Sudol, M., and Russo, T. (1997a). Interaction of the phosphotyrosine interaction/phosphotyrosine binding-related domains of Fe65 with wild-type and mutant Alzheimer's beta-amyloid precursor proteins. *J Biol Chem* 272, 6399-6405.
- Zambrano, N., De Renzis, S., Minopoli, G., Faraonio, R., Donini, V., Scaloni, A., Cimino, F., and Russo, T. (1997b). DNA-binding protein Pur alpha and transcription factor YY1 function as transcription activators of the neuron-specific FE65 gene promoter. *Biochem J* 328 (Pt 1), 293-300.
- Zambrano, N., Minopoli, G., de Candia, P., and Russo, T. (1998). The Fe65 adaptor protein interacts through its PID1 domain with the transcription factor CP2/LSF/LBP1. *J Biol Chem* 273, 20128-20133.
- Zhou, B.B., and Elledge, S.J. (2000). The DNA damage response: putting checkpoints in perspective. *Nature* 408, 433-439.

Tumorigenesis and Neoplastic Progression

Nutritional Limitation Sensitizes Mammalian Cells to GSK-3 β Inhibitors and Leads to Growth Impairment

Paola de Candia,* Giuseppina Minopoli,[†]
Viola Verga,* Anna Gargiulo,[†] Marco Vanoni,*
and Lilia Alberghina*

From the Department of Biotechnology and Biosciences,*
University of Milano-Bicocca, Milan; and CEINGE Centro
d'Ingegneria Genetica Biotecnologie Avanzate,[†] European School
of Molecular Medicine, and the Department of Biochemistry and
Medical Biotechnologies, University of Naples Federico II,
Naples, Italy

The serine/threonine kinase GSK-3 β was initially described as a key enzyme involved in glucose metabolism, but it is now known to regulate a wide range of biological processes, including proliferation and apoptosis. We previously reported a transformation-dependent cell death induced by glucose limitation in *K-ras*-transformed NIH3T3. To address the mechanism of this phenomenon, we analyzed GSK-3 β regulation in these cells in conditions of high versus low glucose availability. We found that glucose depletion caused a marked inhibition of GSK-3 β through posttranslational mechanisms and that this inhibition was much less pronounced in normal cells. Further inhibition of GSK-3 β with lithium chloride, combined with glucose shortage, caused specific activation of AMP-activated protein kinase and significant suppression of proliferation in transformed but not normal cells. The cooperative effect of lithium and low glucose availability on cell growth did not seem to depend exclusively on *ras* pathway activation because two human cell lines, A549 and MDA-MB-231, both harboring an activated *ras* gene, showed very different sensitivity to lithium. These findings thus provide a rationale to further analyze the biochemical bases for combined glucose deprivation and GSK-3 β inhibition as a new approach to control transformed cell growth. (Am J Pathol 2011, 178:1814–1823; DOI: 10.1016/j.ajpath.2010.12.047)

GSK-3 is a multifunctional serine/threonine kinase that plays a major role in Wnt and Hedgehog signaling pathways, the regulation of cell division cycle, cell fate and survival, stem cell renewal, apoptosis, neuronal cell

growth and differentiation, and circadian rhythm.¹ In mammals, two isoforms are encoded by distinct genes, GSK-3 α and GSK-3 β , that, despite a high degree of similarity, are not functionally redundant.² The protein function of GSK-3 β is much better investigated. Consistent with the observation that GSK-3 β is involved in many cellular pathways, its dysregulation has been implicated in various human diseases, such as bipolar mood disorder, neurodegenerative pathologic conditions, and diabetes.³

Regarding the role of GSK-3 β in cancer, conflicting results are found in the literature. Oncogenic transcription factors (eg, c-Jun and c-Myc) and proto-oncoproteins (ie, β -catenin) are putative GSK-3 β substrates for phosphorylation-dependent inactivation⁴; therefore, GSK-3 β could interfere with tumor development.⁵ However, although pharmacologic inhibition of GSK-3 would be expected to promote cancer, no direct *in vivo* evidence has indicated that such a phenomenon occurs on administration of GSK-3 antagonists. In fact, the risk of cancer development among psychiatric patients treated with lithium salts, long known as an inhibitor of GSK-3 β ,⁶ is significantly lower than that in the general population, suggesting that inhibition of GSK-3 β may have a generally protective effect toward carcinogenesis.⁷ Accordingly, recent studies show that GSK-3 β inhibitors lead to significant reduction in cell growth and proliferation of prostate,⁸ pancreatic,⁹ colorectal,¹⁰ ovarian,¹¹ medullary thyroid,¹² and pheochromocytoma¹³ cancer cell lines and that GSK-3 β activity is essential for maintenance of a subset of leukemias.¹⁴

The first role identified for GSK-3 β almost 30 years ago recognized it as a crucial factor in glucose metabolism, being the kinase that phosphorylates and inactivates glycogen synthase, the first enzyme in glycogen biosynthesis.¹⁵ It is well-known that even in the presence of oxygen, tumors consistently rely on glycolysis to generate a substantial fraction of total cellular ATP production. Furthermore, tumor cells maintain ATP production by in-

Supported by grants from FIRB-ItaBioNet to L.A.

P.d.C. and G.M. contributed equally to this work.

Accepted for publication December 14, 2010.

Current address of P.d.C., Fondazione Istituto Nazionale Genetica Molecolare (INGM), Milan, Italy.

Address reprint requests to Paola de Candia, Ph.D., INGM, Via F. Sforza, 32; 20122, Milan, Italy. E-mail: decandiapaola@ingm.it.

creasing glucose influx to fuel the energy requirements of unrestricted proliferation.¹⁶ The role of GSK-3 β in this phenotype is still unclear. Nonetheless, it is conceivable, although still not completely demonstrated, that GSK-3 β could be involved in glucose metabolism of tumor cells through its effect on glycogen metabolism.

To explore whether altered carbon metabolism of transformed cells involves GSK-3 β dysregulation, we used murine NIH3T3 cells, a largely studied immortalized cell line established as a model parental cell line for the study of cell transformation.¹⁷ Similar to most cancer cells, NIH3T3 cells transformed by an activated form of the *K-ras* oncogene exhibit a higher rate of glucose consumption associated with mitochondrial dysfunction.¹⁸ So, whereas normal NIH3T3 cells cope with glucose shortage by relying on oxidative metabolism and decelerating cell proliferation, *K-ras*-transformed cells are remarkably sensitive to glucose deprivation, losing their growth advantage and high survival rate.¹⁹

Analysis of GSK-3 β regulation in *K-ras*-transformed fibroblasts and their parental counterparts in conditions of high versus low glucose availability showed posttranslational inhibition of GSK-3 β in the latter condition. This pattern was uncoupled from regulation of glycogen synthase and β -catenin. After this observation, we exposed normal and transformed cells to glucose deprivation and GSK-3 β chemical inhibition and found that nutrient limitation sensitizes transformed cells, but not parental NIH3T3, to growth impairment by two different GSK-3 β inhibitors. Glucose limitation also rendered more effective the growth inhibition properties of lithium chloride (LiCl) in the human neoplastic MDA-MB-231 cells.

Materials and Methods

Cell Culture and Synchronization

Normal murine fibroblasts (obtained from the American Type Culture Collection, Manassas, VA) and a *K-ras*-transformed derived cell line (226.4.1),²⁰ A549 lung carcinoma, HeLa cells, and MDA-MB-231 breast cancer cells were grown in Dulbecco's modified Eagle's medium (Invitrogen, Carlsbad, CA) containing 10% newborn calf serum (or 10% fetal bovine serum for human cell lines), 2 mmol/L glutamine, 100 U/mL of penicillin, and 100 mg/mL of streptomycin (normal growth medium) at 37°C in a humidified atmosphere of 5% CO₂. To verify the cell response to glucose depletion, the cells were grown in medium without glucose and sodium pyruvate (Invitrogen) supplemented with the appropriate concentration of glucose (25 and 1 mmol/L). For cell growth assays, cells were plated in six-well plates (NIH3T3 and *K-ras*-transformed cells at 28,800 cells per well, A549 at 133,000 cells per well, HeLa at 77,000 cells per well, and MDA-MB-231 at 106,000 cells per well) and were allowed to attach overnight. The medium was changed with different concentrations of glucose in the presence of either carrier (or NaCl) or GSK-3 inhibitors (three wells were used for each condition). Cells were collected using trypsin-EDTA (Invitrogen) at different time points and were counted using a Bürker counting chamber.

Cell death was determined by trypan blue (Sigma-Aldrich, St. Louis, MO) dye exclusion assay. For synchronization in G2-M phase, cells were incubated for 16 hours with nocodazole, 100 ng/mL; then, synchronized cells were recovered by gentle shaking, released by the drug-induced block in fresh medium, and harvested after 4, 6, and 8 hours. For protein kinase B (PKB) inhibition, *K-ras*-transformed cells were plated in six-well plates at 28,800 cells per well, and the medium was changed as described. After 72 hours of growth, either wortmannin, 10 μ mol/L, or dimethyl sulfoxide alone was added to the medium for 30 minutes, and then cells were harvested for protein evaluation. For AMP-activated protein kinase (AMPK) activation, cell growth assay was performed, as described previously herein, in the presence of either carrier or 500 μ mol/L aminoimidazole carboxamide ribonucleotide (Sigma-Aldrich). For *K-ras* overexpression, 1×10^6 HeLa cells were transfected with 10 μ g of a porcine cytomegalovirus-transforming-*K-ras* expression vector as previously reported²¹ or with 10 μ g of a porcine cytomegalovirus empty vector using FuGENE (Roche Molecular Biochemicals, Mannheim, Germany) following the manufacturer's instructions. Twelve hours after transfection, cells were plated in six-well plates (77,000 cells per well) and were grown as described previously herein.

RNA Preparation and Real-Time PCR

Total RNA was extracted from NIH3T3 and *K-ras*-transformed cells using the SV Total RNA Isolation Kit (Promega, Madison, WI). First-strand cDNA was synthesized using a High Capacity cDNA Reverse Transcription Kit (Applied Biosystems, Foster City, CA). The first-strand cDNA was then used as a template for quantitative RT-PCR with the TaqMan Gene Expression Master Mix and the specific TaqMan Gene Expression Assays for the GSK3- β , c-src, and β -actin genes (Applied Biosystems). The cycling conditions were as follows: initial denaturation at 94°C for 2 minutes, followed by 40 cycles of denaturation at 94°C for 15 seconds and annealing/extension at 60°C for 1 minute. β -actin was used as normalizing internal control for gene expression analyses. Differences in gene expression were evaluated using a *t*-test.

Gel Electrophoresis and Immunoblotting

Cells were lysed in radioimmunoprecipitation assay buffer plus phosphatase and protease inhibitors. After incubation for 15 minutes on ice, the extracts were centrifuged at 13,200 rpm for 10 minutes. The protein concentration of supernatant was measured using the Bradford procedure (Bio-Rad Laboratories, Richmond, CA), using bovine serum albumin as a standard. Total and fractionated cellular extracts were subjected to electrophoresis in SDS-polyacrylamide gel and were transferred to a nitrocellulose membrane (Amersham, Otelfingen, Switzerland). Membranes were preincubated in Tris-buffered saline [20 mmol/L Tris-HCl (pH 7.5), 150 mmol/L NaCl]/-5% defatted milk powder for 1 hour at room temperature and then were incubated in Tris-buffered saline/-0.01% Tween 20/5% defatted milk powder containing the appropriate antibodies overnight at

4°C. The antibodies used were against GSK-3 β , phospho-GSK-3 β (Ser9), phospho-GSK-3 β (Tyr216), glycogen synthase, phospho-glycogen synthase (Ser641), phospho-AKT substrate, phospho-AMPK (Thr172), and AMPK α (Cell Signaling Technology, Beverly, MA); β -catenin (BD Transduction Laboratories, Heidelberg, Germany); N-terminal anti- β -catenin S/T-nonphosphorylated and pan *ras* (Upstate Biotechnology, Lake Placid, NY); and vinculin and actin (Sigma-Aldrich). After three washings (5 minutes each) in Tris-buffered saline/–0.05% Tween 20, the membranes were incubated with a peroxidase-coupled secondary antibody (Amersham) for 30 minutes at room temperature. After incubation, the membranes were washed three times in Tris-buffered saline/–0.05% Tween 20. The reaction was visualized using ECL (Amersham), followed by exposure to an X-ray film. Images were scanned at a minimum resolution of 300 dpi. Protein levels were quantified by densitometry of JPEG images using the NIH image-based software ImageJ.

BrdU Incorporation Assay

For the 5-bromo-2'-deoxyuridine (BrdU) incorporation assay, *K-ras*-transformed cells were grown in duplicate on polylysine-precoated glass coverslips in six-well plates and were treated as described previously herein. The cells were

then incubated with 10 μ mol/L 5-bromo-2'-deoxyuridine (Roche Molecular Biochemicals) for 5 hours. Cells on coverslips were fixed with paraformaldehyde (4% in PBS, pH 7.4), permeabilized with 0.5% Triton X-100 (Roche Diagnostics GmbH, Mannheim, Germany), and incubated in 0.5-N HCl for 30 minutes. Coverslips were washed three times with PBS in a 10-minute period and were incubated with a primary mouse anti-BrdU antibody (5-Bromo-2'-deoxyuridine Labeling and Detection Kit; Roche Molecular Biochemicals) following the instructions of the supplier. Then, the cells were stained with Alexa Fluor 546–conjugated secondary antibody (Molecular Probe, Invitrogen), with nuclear counterstaining with DAPI (Sigma-Aldrich), 1:1000. The coverslips were mounted in Mowiol (Calbiochem, San Diego, CA) onto a glass microscope slide, and fluorescence was examined using an Axiophot microscope (Zeiss Jena GmbH, Jena, Germany). The number of total and BrdU-positive cells in each condition were counted in 10 nonoverlapping fields per coverslip, and the quantification of BrdU-positive cells per total number of DAPI-positive nuclei was determined as a mean \pm SD percentage.

Flow Cytometric Analysis

The distribution of cells at specific cell cycle phases was evaluated by flow cytometry as previously described.²²

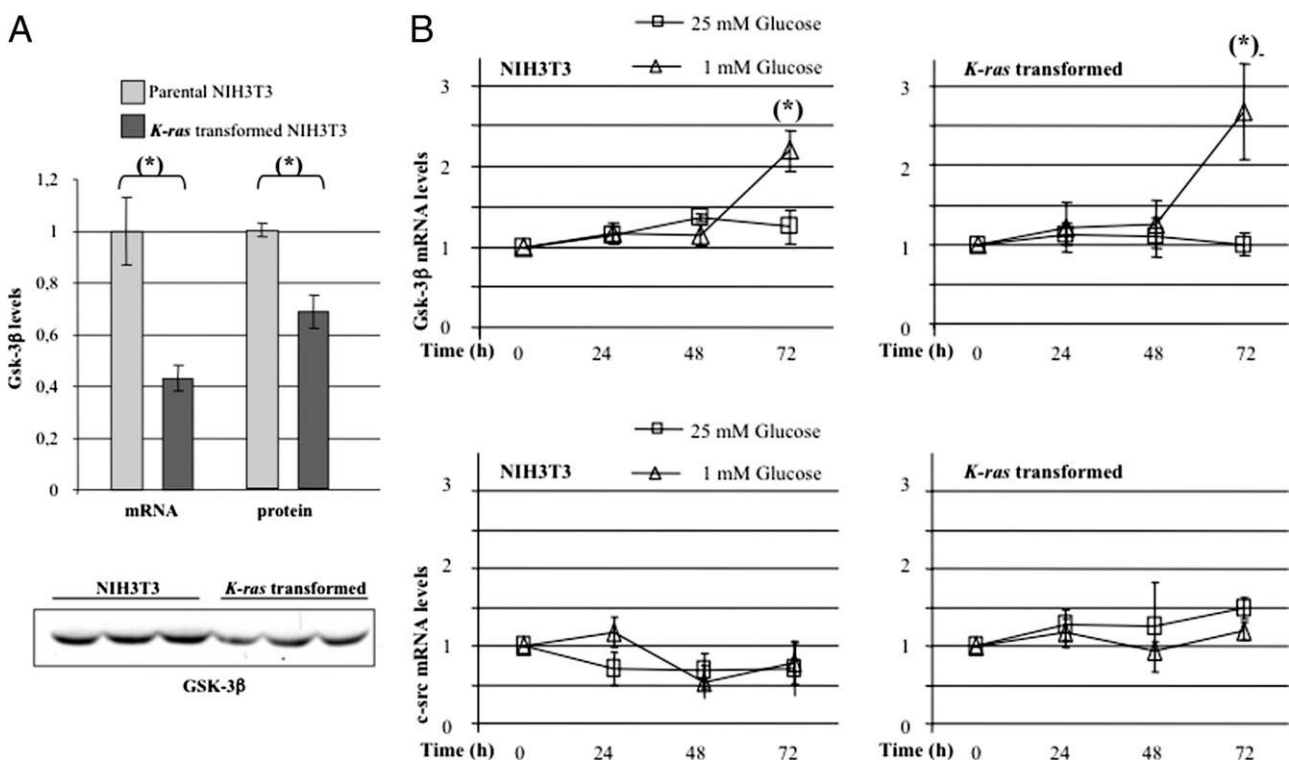


Figure 1. Parental and *K-ras*-transformed fibroblasts were plated at 3000 cells/cm² density. After 16 hours of growth, the medium was changed with a glucose concentration maintained at 25 mmol/L (A) and with a glucose concentration of either 25 or 1 mmol/L (B). Cells were harvested after 24 hours (A) or after 24, 48, and 72 hours (B). Total RNA was prepared and was subjected to real-time PCR with oligonucleotides specific to GSK-3 β (A) or to GSK-3 β and *c-src* genes (B), as indicated. Each sample was normalized by β -actin internal control. Results are the mean of biological triplicate determinations and were plotted considering the value obtained for parental samples mean (A) or time 0 (B) as equal to 1. For protein expression analysis, normal and transformed cells were plated and grown as described previously herein in 25 mmol/L glucose and were collected at 24 hours. Proteins (50 μ g) from total cellular extracts of biological triplicates were subjected to SDS–polyacrylamide gel electrophoresis, followed by Western blotting with an anti-GSK-3 β antibody. Relative quantitative values of protein levels after Western blot film acquisition were obtained by densitometric analysis using the ImageJ program and then were plotted considering the densitometric value obtained for the parental samples mean as equal to 1. Error bars represent SD. **P* < 0.05 for the *t*-test.

Briefly, cells were trypsinized, washed with PBS, and fixed in 75% ethanol at 4°C. Subsequently, samples were stained with propidium iodide (Sigma-Aldrich) and were analyzed using a fluorescence-activated cell sorter (FACS-Scan; BD Biosciences, Franklin Lakes, NJ), using Cell Quest software (BD Biosciences). Data analysis was performed using WinMDI software.

Results

GSK-3 β mRNA Is Induced by Glucose Limitation

Parental and *K-ras*-transformed fibroblasts were plated at 3000 cells/cm² density. After 16 hours of growth, the medium was changed with a glucose concentration maintained at 25 mmol/L. Twenty-four hours after medium change, in the condition of exponential growth, we harvested parental and transformed cells and prepared total RNA to evaluate the mRNA levels of GSK-3 β using real-time PCR. Transformed cells showed a lower mRNA level for GSK-3 β , and the protein level was also sensibly lower in transformed versus parental cells as assessed by Western blotting (Figure 1A).

Normal and transformed cells were then plated as described previously herein, and after 16 hours, the medium was changed (cells were also harvested at this time, referred to as time 0). Media were supplemented with either high (25 mmol/L) or low (1 mmol/L) glucose concentration. Cells were then harvested after 24, 48, and 72 hours of growth. All the experiments reported in this and the following paragraphs refer to the previously mentioned experimental setup, already used for several studies.^{18,19}

To evaluate the effect of glucose shortage on GSK-3 β regulation, we prepared RNA from normal and *K-ras*-transformed NIH3T3 cells grown in either high or low glucose availability. GSK-3 β mRNA levels were measured using real-time PCR. In normal and transformed cells, the level of mRNA for GSK-3 β was constant until 48 hours of growth and increased at 72 hours in low glucose, more substantially in transformed cells (Figure 1B, top). This time-dependent expression pattern was specific for GSK-3 β mRNA and was not a general response to glucose limitation because expression of an unrelated gene, *c-src*, remained constant over the timeframe of the experiment (Figure 1B, bottom).

Preferential GSK-3 β Inhibition in Transformed Cells Grown in Low Glucose

The GSK-3 β protein level remained fairly stable over time in normal and transformed cells, with no increase at late time points in low glucose (Figure 2A), suggesting a compensatory mechanism for the observed transcriptional activation. In *K-ras*-transformed cells, the level of GSK-3 β inhibitory phosphorylation at Ser9 was consistently higher in low compared with high glucose, with the largest difference at 72 hours. On the other hand, activating Tyr216 phosphorylation was slightly decreased in low versus high glucose at the same time point (Figure 2A). Through quantification of Western blotting by ImageJ, we showed an increase in the ratio between Ser9 phosphorylated and total protein over time specifically in low glucose and a 12-fold difference of this ratio in low versus high glucose at 72 hours (Figure 2B, top). In normal cells, on the other hand, Ser9 phosphorylation did

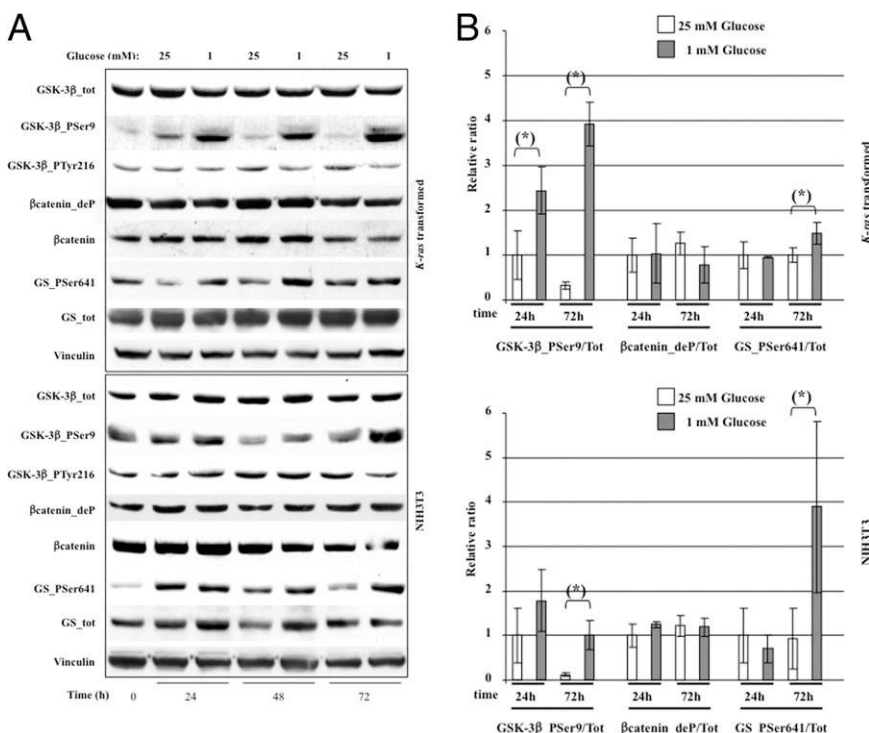


Figure 2. **A:** *K-ras*-transformed and parental fibroblasts were plated at 3000 cells/cm² density. After 16 hours of growth, the medium was changed with a glucose concentration of either 25 or 1 mmol/L, and cells were harvested at specific time points, as indicated. For protein expression analysis, proteins (50 μ g) from total cellular extracts of transformed or normal cells were subjected to SDS-polyacrylamide gel electrophoresis, followed by Western blotting with the indicated antibodies. One of at least three independent experiments is shown. Vinculin was used as a control of equal gel loading. **B:** Transformed (**top**) and parental (**bottom**) cells were plated, grown as described previously herein, and harvested 24 and 72 hours after medium change. Proteins from three independent cellular extracts were subjected to SDS-polyacrylamide gel electrophoresis, followed by Western blotting for the indicated proteins, and then their quantitative values were plotted considering the densitometric value obtained for the sample in 25 mmol/L glucose at 24 hours as equal to 1. Results are the mean of triplicate determinations. Error bars represent SD. **P* < 0.05 for the *t*-test.

not increase significantly or even decreased over time also in low glucose, and the difference between high and low glucose at 72 hours was less pronounced than in transformed cells (Figure 2B, bottom).

Given that GSK-3 is known to inhibit cell proliferation and glycogen accumulation mainly through phosphorylation of β -catenin and glycogen synthase, respectively, we analyzed the regulation of these targets in cells grown in either high or low glucose. Activation of β -catenin was evaluated by using an antibody specific for the active form of the protein, dephosphorylated on Ser37 or Thr41. As shown in Figure 2A, neither the phosphorylation pattern nor total protein accumulation seemed to be affected by glucose deprivation in normal and transformed cells. Quantification analysis performed on triplicates at 24 and 72 hours confirmed that the ratio between the activated and total forms of the protein was not modulated in the two cell lines (Figure 2B). We also evaluated β -catenin nuclear localization in transformed cells: at 24 and 72 hours, the total and active forms of β -catenin were mostly in the nuclear/insoluble fraction, and this pattern was likewise not affected by glucose availability (data not shown). In contrast to the observed GSK-3 β phosphorylation pattern, glycogen synthase seemed to be phosphorylated at a higher level after 72 hours of growth in low compared with high glucose in normal and transformed cells (Figure 2A). The quantitative analysis of the ratio between the phosphorylated and total forms of the protein confirmed that glycogen synthase phosphorylation was increased in low glucose- versus high glucose-grown cells, with the difference being larger in normal cells than in transformed cells (Figure 2B).

Glucose Limitation Sensitizes Transformed Cells to Growth Impairment by GSK-3 β Antagonists

The observation that GSK-3 β posttranslational inhibition increased in conditions of nutrient limitation prompted us to evaluate the effect of GSK-3 β inhibition on proliferation of normal and transformed NIH3T3 cells. To this end, we treated both cell lines grown in either high or low initial glucose with the GSK-3 β inhibitor LiCl, using NaCl as an isotonic control. During the experiment, *K-ras*-transformed cells grew significantly less in media supplemented with low as opposed to high initial glucose concentrations (Figure 3A, left), as previously reported.¹⁹ Cell growth was significantly further inhibited by the addition of LiCl (Figure 3A, left; $P < 0.05$).

Sb-216763, a cell-permeable maleimide compound that selectively inhibits GSK-3,²³ failed to inhibit proliferation of *K-ras*-transformed cells grown in media supplemented with a high initial glucose concentration (Figure 3A, right) when used at a concentration of 25 μ mol/L. On the other hand, this concentration was sufficient to effectively inhibit growth of transformed cells grown with low glucose availability (Figure 3A, right; $P < 0.05$). A higher concentration (50 μ mol/L) of the drug was necessary to observe an effect similar to that observed with lithium (data not shown). These data thus suggest that *K-ras*-transformed NIH3T3 fibroblasts are exquisitely sensitive to GSK-3 β inhibition when grown under con-

ditions of glucose limitation. Normal NIH3T3 cells grew similarly in media supplemented with different glucose concentrations (Figure 3B), and LiCl had little, if any, inhibitory effect (Figure 3B, left). Similar to LiCl, Sb-216763 did not affect the growth of parental cells (Figure 3B, right).

K-ras-transformed cells could not sustain their growth through the citric acid cycle because cells did not restore a normal growth rate when medium was supplemented with sodium pyruvate (Figure 4A). This result is in keeping with previous studies showing that *K-ras*-transformed cells have defective mitochondria¹⁹ and, more specifically, that the reduction in respiration observed is due to a decrease in complex I activity.²⁴

In Transformed Cells, Glucose Limitation Activates AMPK Only When GSK-3 β Is Pharmacologically Inhibited

To ascertain whether the PI3K/PKB pathway was responsible of the increased Ser9 phosphorylation of GSK-3 β in the condition of glucose shortage, transformed cells were grown in either high or low glucose, and 72 hours after medium change, cells were treated with wortmannin, a specific inhibitor of PI3K. The subsequent inhibited activity of PKB on wortmannin exposure was evaluated by Western blotting using an antibody that recognizes the phospho-(Ser/Thr) PKB substrate motif (RXXS/T). This control showed similar suppression of the phosphorylation level for different PKB substrates (Figure 4B). On the other hand, whereas wortmannin treatment dramatically inhibited GSK-3 β phos-

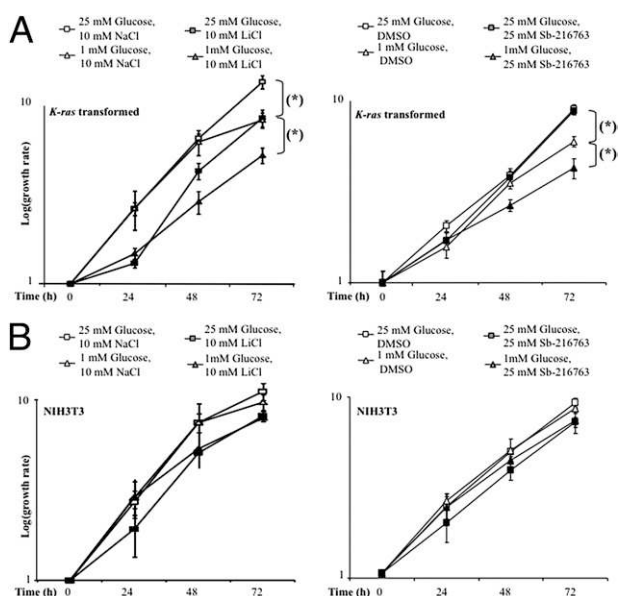


Figure 3. *K-ras*-transformed (A) and parental (B) fibroblasts were plated at 3000 cells/cm² density in six-well plates. After 16 hours of growth, the medium was changed with those shown. Cells were collected by trypsinization at the indicated times and were counted using a Bürker counting chamber. The fold increase in cell number was plotted considering the cell number at time 0 as equal to 1. The experiment reported is representative of three different ones. Results are the mean of triplicate determinations in a single experiment. Error bars represent SD. DMSO, dimethyl sulfoxide. * $P < 0.05$ for the *t*-test.

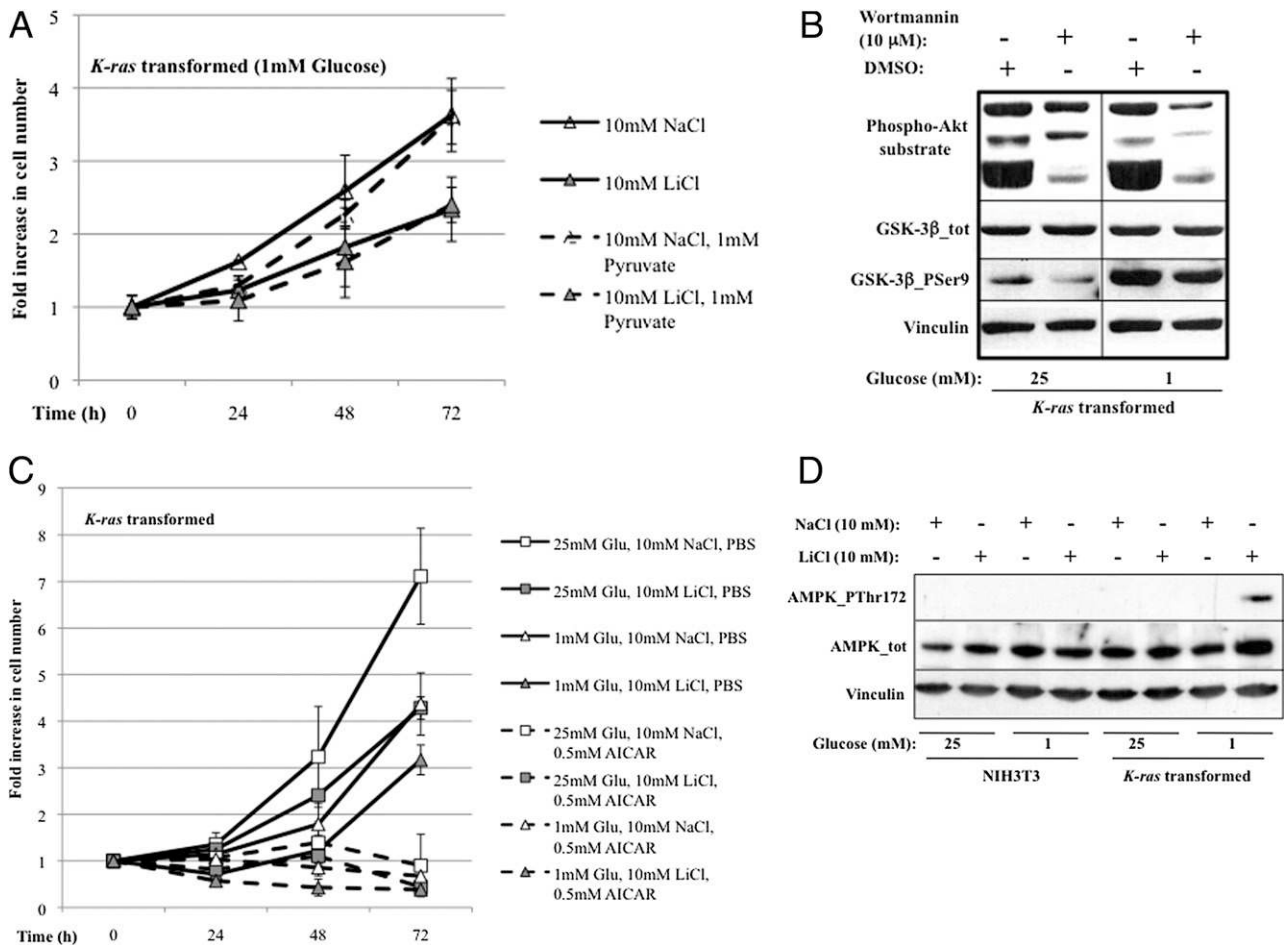


Figure 4. **A:** *K-ras*-transformed cells were plated as described previously herein, and at the time of medium change, to the above media were added either sodium pyruvate or its vehicle, as indicated. Cells were collected by trypsinization at the indicated times and were counted using a Bürker counting chamber. The fold increase in cell number was plotted considering cell number at time 0 as equal to 1. Results are the mean of triplicate determinations in a single experiment. Error bars represent SD. **B:** *K-ras*-transformed cells were plated at 3000 cells/cm² density. After 16 hours of growth, the medium was changed with a glucose concentration of either 25 or 1 mmol/L. At 72 hours of growth, cells were treated with wortmannin, 10 μmol/L [or with dimethyl sulfoxide (DMSO) alone], for 30 minutes and then were harvested. For protein expression analysis, proteins (50 μg) from total cellular extracts were subjected to SDS-polyacrylamide gel electrophoresis, followed by Western blotting with the indicated antibodies. **C:** *K-ras*-transformed cells were plated as described previously herein, and at the time of medium change, to the above media were added either aminoimidazole carboxamide ribonucleotide (AICAR) or PBS alone, as indicated. Cells were collected by trypsinization at the indicated times and were counted using a Bürker counting chamber. The fold increase in cell number was plotted considering cell number at time 0 as equal to 1. Results are the mean of triplicate determinations in a single experiment. **D:** *K-ras*-transformed and parental fibroblasts were grown in either 25 or 1 mmol/L glucose plus 10 mmol/L NaCl or LiCl, as indicated. Cells were harvested after 72 hours of growth, and for protein expression analysis, proteins (50 μg) from total cellular extracts were subjected to SDS-polyacrylamide gel electrophoresis, followed by Western blotting with the indicated antibodies. Error bars represent SD.

phorylation in high glucose, it only marginally decreased it in low glucose (Figure 4B), suggesting that in the condition of nutrient depletion, kinases other than PKB are responsible for the observed Ser9 phosphorylation.

Normal cells are known to have a lower rate of nutrient consumption than transformed cells and not to consume the glucose completely during the exponential phase of growth in conditions of glucose shortage.¹⁹ Consequently, we observed that normal cells did not activate AMPK after 72 hours of growth in 1 mmol/L glucose, as assessed by the lack of activating phosphorylation on AMPK Thr172 (Figure 4D). On the other hand, transformed cells do consume glucose very rapidly.¹⁹ We confirmed this by observing complete consumption of glucose already at 48 hours of growth in 1 mmol/L glucose (data not shown). Unexpectedly, though, glucose depletion was unable to activate AMPK, not even at 72 hours, and only when glucose shortage was combined with GSK-3β inhibition, phospho-AMPK was clearly detected by Western blotting (Figure 4D). In

transformed cells, AMPK activation was a strong signal of cell growth inhibition; in fact, treatment with a specific AMPK-activating drug, aminoimidazole carboxamide ribonucleotide, caused complete suppression of proliferation, independent of glucose availability (Figure 4C).

Glucose Limitation Dramatically Enhances the Inhibition of Cell Proliferation Due to GSK-3β Inactivating Drugs

Reduced cell growth of *K-ras*-transformed cells in low glucose has been shown to be partly due to increased apoptosis.¹⁹ To ascertain whether the reduced growth in the presence of GSK-3 inhibitors was due to an effect on cell death and/or cell proliferation, the overall cell viability of *K-ras*-transformed cells and their ability to enter S phase were monitored. To evaluate the level of cell death, we harvested adherent and floating cells and ran a trypan

blue exclusion assay. The percentage of trypan blue positive over total cell number was comparable for different treatments at 24 and 48 hours (Figure 5A, top). At 72 hours, however, the amount of dead cells increased specifically when cells were glucose depleted, thereby confirming previous findings.¹⁹ Even at this time point, no relevant differences between cells treated with lithium and the control were observed, and the same observation was made with Sb-216763 (data not shown).

Therefore, to analyze whether cell proliferation was, indeed, responsible for the apparent inhibition of cell growth, the percentage of cells in S phase was measured by analyzing BrdU incorporation in DNA. We incubated cells for 5 hours with BrdU before each time point (ie, at 24 and 48 hours). At 24 hours, the level of BrdU incorporation was comparable in high glucose, high glucose plus lithium, or low glucose, whereas it was already sig-

nificantly lower in cells growing in low glucose plus lithium (Figure 5A, center). At 48 hours, the inhibition of GSK-3 β caused a moderate decrease in the percentage of BrdU-positive cells, but the effect was dramatically more pronounced when lithium was used in combination with low glucose (Figure 5A, center; $P < 0.05$). Similar patterns were obtained with Sb-216763 (data not shown). Taken together, these results indicate that GSK-3 β inhibition brought about by either LiCl or Sb-216763 in glucose-depleted transformed cells is due to reduced proliferation, with no substantial effect on cell death.

LiCl Delays the Cell Cycle of Transformed Cells by Impairing Exit from M Phase

To further analyze the role of GSK-3 β in cell proliferation, we evaluated cell cycle distribution by propidium iodide

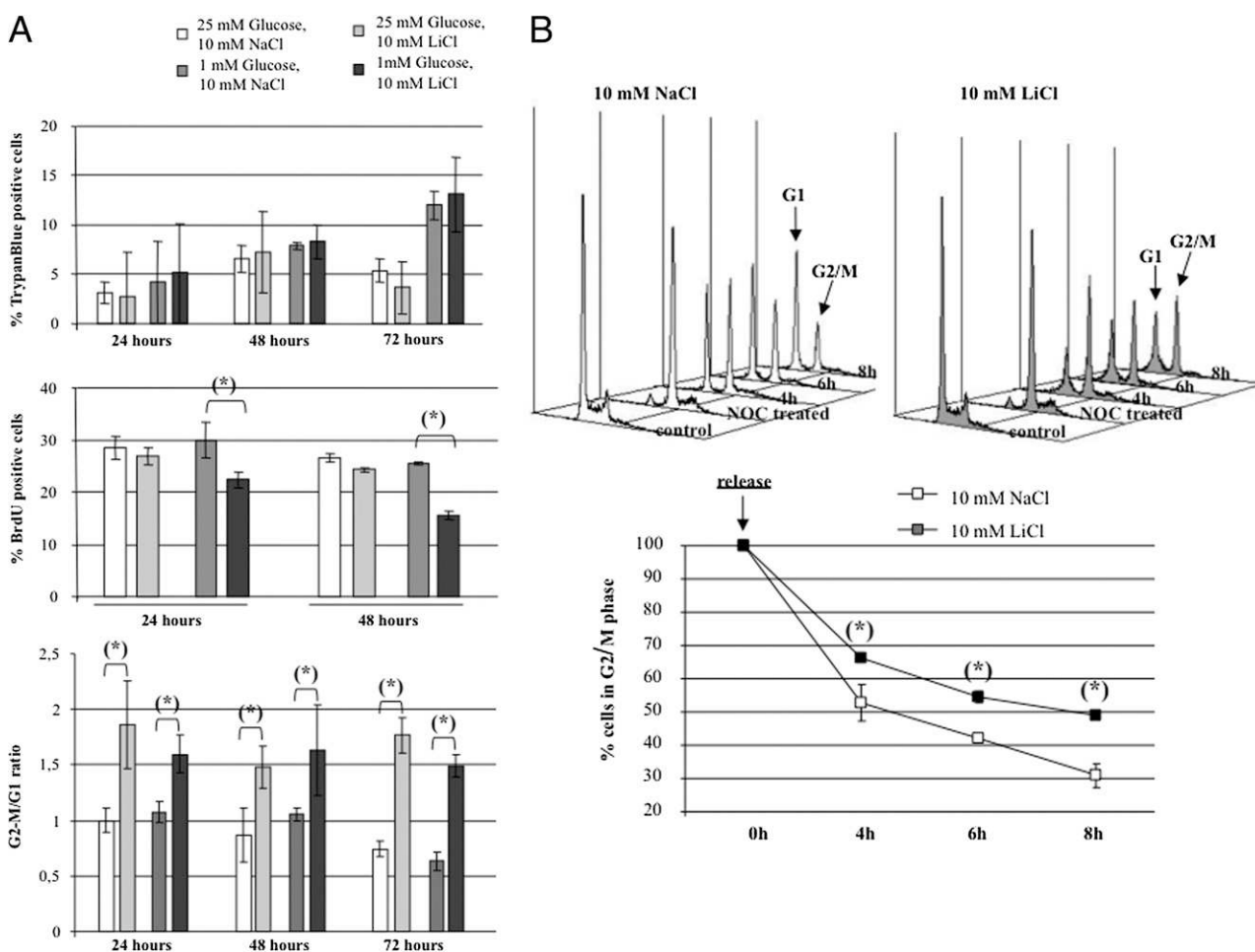


Figure 5. A, top: *K-ras*-transformed fibroblasts were plated at 3000 cells/cm² density and were grown on polylysine-precoated glass coverslips. After 16 hours of growth, the medium was changed with those shown. Adherent and floating cells were collected at the indicated time points, and dead cells were evaluated using a trypan blue exclusion assay. Percentage of trypan blue-positive over total cells was plotted as a mean value of biological triplicates. **A, center:** Transformed cells were plated at 3000 cells/cm² density in six-well plates. They were treated as described previously herein and then were pulsed 5 hours with BrdU before harvesting at the indicated time points. The cells were analyzed by fluorescence microscopy using an anti-BrdU-specific antibody. The numbers of total and BrdU-positive cells in each condition were counted in 10 nonoverlapping fields per coverslip, and the quantification of BrdU-positive cells per total numbers of DAPI-positive nuclei was determined as a mean percentage taking into account two independent experiments. **A, bottom:** Transformed cells were plated at 3000 cells/cm² density in 145-mm plates. They were treated as described previously herein and then were collected at the indicated time points after medium change, stained with propidium iodide, and analyzed using a fluorescence-activated cell sorter. The ratio G2-M/G1 was plotted considering the ratio of cells growing in high glucose at 24 hours as equal to 1. Error bars represent SD. * $P < 0.05$ for the *t*-test. **B:** Transformed cells were plated as described previously herein and were grown in 25 mmol/L glucose for 48 hours. Cells were then treated with nocodazole (NOC), 100 ng/mL, for 16 hours; synchronized cells were released and harvested at the indicated time points. They were then stained with propidium iodide and were analyzed using a fluorescence-activated cell sorter. The experiment reported is representative of three different ones. Results are the mean of triplicate determinations in a single experiment. Error bars represent SD. * $P < 0.05$ for the *t*-test.

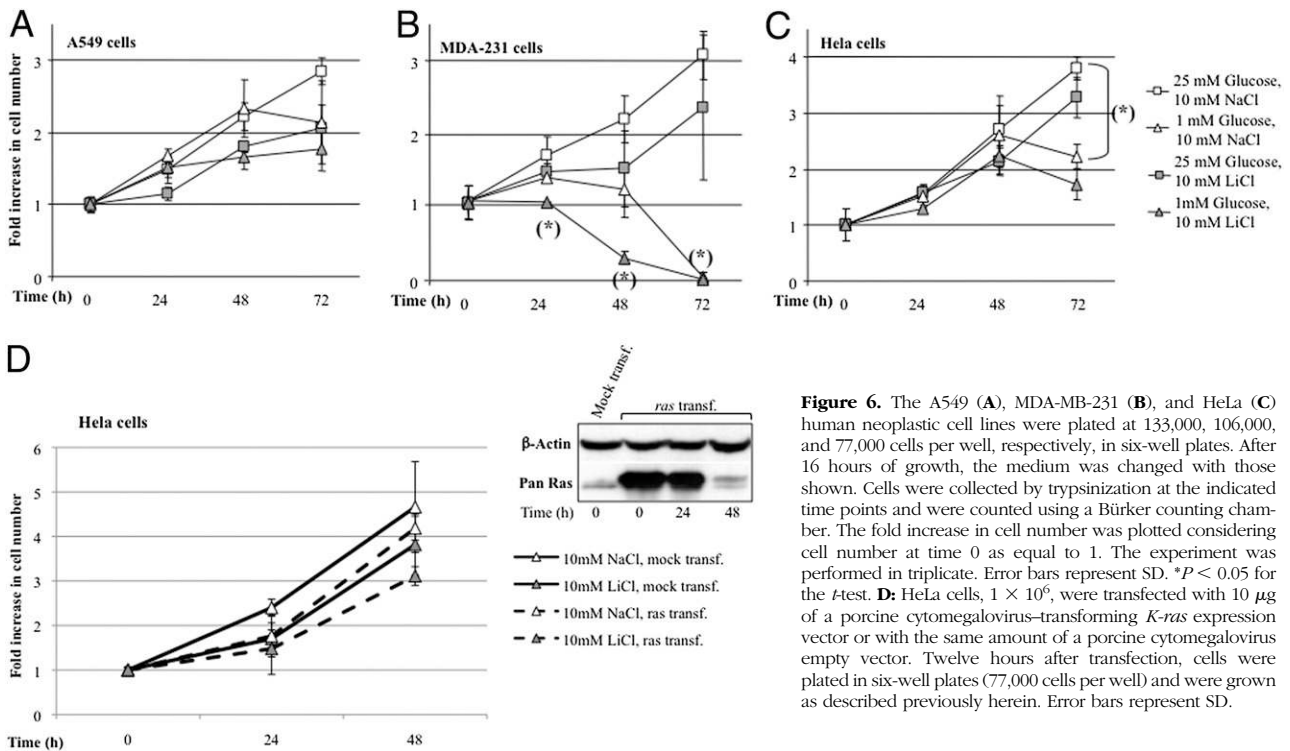


Figure 6. The A549 (A), MDA-MB-231 (B), and HeLa (C) human neoplastic cell lines were plated at 133,000, 106,000, and 77,000 cells per well, respectively, in six-well plates. After 16 hours of growth, the medium was changed with those shown. Cells were collected by trypsinization at the indicated time points and were counted using a Bürker counting chamber. The fold increase in cell number was plotted considering cell number at time 0 as equal to 1. The experiment was performed in triplicate. Error bars represent SD. **P* < 0.05 for the *t*-test. **D:** HeLa cells, 1×10^6 , were transfected with $10 \mu\text{g}$ of a porcine cytomegalovirus-transforming *K-ras* expression vector or with the same amount of a porcine cytomegalovirus empty vector. Twelve hours after transfection, cells were plated in six-well plates (77,000 cells per well) and were grown as described previously herein. Error bars represent SD.

incorporation and cytofluorimetric analysis. The ratio of cells in G2-M over cells in G1 increased significantly in lithium-treated cells compared with the isotonic control at all time points and independent of glucose concentration, suggesting a discrete accumulation of these cells in G2-M phase of the cell cycle (Figure 5A, bottom). To study the possible effect of GSK-3 β inhibition on exit from mitosis, cells grown in high glucose were blocked in M phase by 16 hours of treatment with nocodazole, a microtubule destabilizer known to induce a mitotic checkpoint arrest. To determine the drug-induced accumulation of cells in mitosis, control- and nocodazole-treated cells were stained with propidium iodide, showing the efficacy of the block with greater than 95% of cells with a 4-N DNA content (Figure 5B). Blocked cells were harvested by gentle shaking and were released from the block with high glucose medium in the presence of either LiCl or the isotonic control. Although 50% of control-treated cells had completed M phase and entered G1 phase approximately 4 hours after the release, lithium-treated cells took approximately 8 hours to reach the same percentage of cells with a 2-N DNA content, indicating that GSK-3 β inhibition causes a dramatic delay in exit from mitosis in this setting (Figure 5B).

Human Neoplastic Cell Lines Show Different Responses to LiCl

To evaluate whether the cooperative effect in growth inhibition observed in *K-ras*-transformed NIH3T3 was specific to murine fibroblasts, we analyzed the behavior of two human cell lines, lung carcinoma A549 and breast cancer MDA-MB-231, both harboring an activated *ras* pathway. Their growth was sensitive to glucose concen-

tration (Figure 6, A and B), although to a different extent. MDA-MB-231 cells had similar GSK-3 β protein levels (data not shown), but they were much more sensitive to glucose deprivation: in 1 mmol/L glucose, they grew poorly in the first 24 hours, and a dramatic reduction in cell number was apparent at 72 hours (Figure 6B). Strikingly, LiCl completely blocked cell growth of glucose-depleted cells as early as 24 hours after addition, and severe cell loss started at 48 hours (Figure 6B; *P* < 0.05). HeLa cells were also sensitive to glucose depletion, although to a lesser extent, whereas the cooperative effect of glucose shortage and GSK-3 inhibition on cell growth was almost undetectable (Figure 6C). They did not acquire sensitivity when transfected with an activated transforming *K-ras* gene,²¹ suggesting that *ras* activation is not the only factor determining the cellular sensitivity of transfected cells to glucose deprivation plus GSK-3 β inhibition (Figure 6D). The experiment could not go beyond 42 hours of growth, when the exogenous *K-ras* expression had disappeared (Figure 6D, inset).

Discussion

The serine/threonine kinase GSK-3 β has been carefully described as being inhibited by insulin signaling in conditions of high nutrient availability; consequently, it is expected to be active under conditions of low glucose. The work presented herein goes against this dogma, showing that murine fibroblasts, in fact, repress GSK-3 β action through Ser9 phosphorylation in conditions of glucose shortage. This phenomenon is much more important in *K-ras*-transformed cells than in their normal counterparts. By using a PI3K inhibitor, we analyzed the role of

the pathway in these cells and found that PKB is only marginally responsible for the signal at Ser9 in low glucose, suggesting that other pathways are, indeed, involved in this regulation.

Starting from this unexpected observation, the major result presented in this work is the first demonstration that glucose limitation sensitizes *K-ras*-transformed fibroblasts to pharmacologic growth inhibition by two GSK-3 β antagonists, LiCl and Sb-216763. The two molecules inhibit GSK-3 β through different mechanisms: lithium directly inhibits GSK-3 β by competing with magnesium but not with substrate or ATP,²⁵ whereas Sb-216763 inhibits GSK-3 β in an ATP-competitive manner.²³ Results obtained with Sb-216763 are particularly striking because when given at 25 μ mol/L, this inhibitor is completely ineffective on transformed cells grown in the presence of high glucose, whereas it significantly impairs growth when given to cells in low-glucose media.

During the experiments reported herein, GSK-3 β -negative regulation by glucose availability was uncoupled from β -catenin accumulation, phosphorylation, and intracellular localization. This behavior is consistent with studies showing that the correlation between GSK-3 β and β -catenin could be looser than initially thought, with no β -catenin accumulation being found in tissues of GSK-3 β knockout mice.²⁶ Furthermore, an extensive study of colon cancer cell lines and tumor samples revealed that the expression level or activity of GSK-3 β does not correlate with β -catenin activation.¹⁰ We showed that only when treated with LiCl could transformed cells activate AMPK in low glucose: this result is highly significant because it shows that these cells cannot sense nutrient deprivation through the AMPK pathway unless GSK-3 β is completely blocked, and it is also in keeping with the cross talk between AMPK and GSK-3 β reported in rat isolated muscle.²⁷

Different effects of GSK-3 antagonists on the cell cycle have been reported. These effects include induction of G1 arrest,¹⁴ impaired spindle dynamics, delay in chromosome alignment, and mitotic entry-exit and cell cycle arrest at G2-M.^{28,29} In keeping with the latter studies, propidium iodide-stained *K-ras*-transformed cells showed a significant increase in the percentage of G2-M phase subpopulations in cells treated with LiCl due to a specific delay in exit from mitosis. Interestingly, AMPK has been implicated in cell division in distant cellular contexts,³⁰ so we are interested in analyzing the role that the AMPK pathway exerts in mitotic defects shown by LiCl-treated transformed cells.

Moreover, it has been described that regulation of reactive oxygen species (ROS) concentrations has a definite role on the rate of cell cycle progression³¹ and that ROS production could be crucial for mitotic events in tumor cells, with reduced levels of ROS delaying spindle assembly and exit from mitosis.³² In the present transformed cells, lithium treatment caused a specific decrease in ROS levels, evaluated by 2,7-dichlorofluorescein diacetate assay, and this effect was augmented in low glucose (data not shown), suggesting that GSK-3 β pharmacologic inhibition could delay exit from mitosis, at least in part, by impairing the production of intracellular ROS.

We observed a dramatic effect of low glucose on LiCl sensitivity not only of murine *K-ras*-transformed fibroblasts but also of MDA-MB-231 cells. These cells, derived from human breast carcinoma, grew very poorly in low glucose and could not grow at all when also treated with lithium. MDA-MB-231 cells have an activated *ras* gene, similar to our NIH3T3 fibroblasts, and a further mutation in the *rafB* gene, encoding a kinase in the same pathway (<http://www.sanger.ac.uk/perl/genetics/CGP/cosmic?action=sample&id=905960>, last accessed February 2011). Growth of A549 cells, also harboring a *ras* activating mutation,³³ was not dramatically inhibited in conditions of low glucose and LiCl, and HeLa cells transfected with an activated *ras* allele did not acquire any further sensitivity to the treatment, suggesting that *ras* pathway deregulation is not the only factor determining cancer cell sensitivity to the cooperation effect between nutrient limitation and GSK-3 β pharmacologic inhibition.

The interrelationship between drug treatment and nutritional stress is not limited to GSK-3 β inhibition. Starvation-dependent differential stress resistance has been reported to protect normal cells, but not transformed cells, against chemotherapy,³⁴ suggesting that modulation of the nutritional status of cancer cells may be a valuable tool in cancer therapy of possibly wide applicability. The ability of cells to respond to nutritional stress seems, thus, to be an important property to score in genotype-phenotype correlation studies that, as has been pointed out recently,³⁵ must be placed in context to give prognostic and therapeutic value to the large number of personal genome sequences that are expected to be obtained in the next few years.

Acknowledgments

We thank Tommaso Russo for precious advice, Addolorata Maria Luce Coluccia for sharing reagents, and Roberta Visconti for stimulating discussions.

References

1. Kockeritz L, Doble B, Patel S, Woodgett JR: Glycogen synthase kinase-3: an overview of an over-achieving protein kinase. *Curr Drug Targets* 2006, 11:1377-1388
2. Rayasam GV, Tulasi VK, Sodhi R, Davis JA, Ray A: Glycogen synthase kinase 3: more than a namesake. *Br J Pharmacol* 2009, 156: 885-898
3. Martinez A: Preclinical efficacy on GSK-3 inhibitors: towards a future generation of powerful drugs. *Med Res Rev* 2008, 28:773-796
4. Manoukian AS, Woodgett JR: Role of glycogen synthase kinase-3 in cancer: regulation by Wnts and other signaling pathways. *Adv Cancer Res* 2002, 84:203-229
5. Polakis P: The oncogenic activation of beta-catenin. *Curr Opin Genet Dev* 1999, 9:15-21
6. Stambolic V, Ruel L, Woodgett JR: Lithium inhibits glycogen synthase kinase-3 activity and mimics wingless signalling in intact cells. *Curr Biol* 1996, 6:1664-1668
7. Cohen Y, Chetrit A, Cohen Y, Sirota P, Modan B: Cancer morbidity in psychiatric patients: influence of lithium carbonate treatment. *Med Oncol* 1998, 15:32-36
8. Mazor M, Kawano Y, Zhu H, Waxman J, Kypta RM: Inhibition of glycogen synthase kinase-3 represses androgen receptor activity and prostate cancer cell growth. *Oncogene* 2004, 23:7882-7892

9. Ougolkov AV, Fernandez-Zapico ME, Savoy DN, Urrutia RA, Billadeau DD: Glycogen synthase kinase-3 β participates in nuclear factor κ B-mediated gene transcription and cell survival in pancreatic cancer cells. *Cancer Res* 2005, 65:2076–2081
10. Shakoori A, Ougolkov A, Yu ZW, Zhang B, Modarressi MH, Billadeau DD, Mai M, Takahashi Y, Minamoto, T. Deregulated GSK3 β activity in colorectal cancer: its association with tumor cell survival and proliferation. *Biochem Biophys Res Commun* 2005, 334:1365–1373
11. Cao Q, Lu X, Feng YJ: Glycogen synthase kinase-3 β positively regulates the proliferation of human ovarian cancer cells. *Cell Res* 2006, 16:671–677
12. Kunnimalaiyaan M, Vaccaro AM, Ndiaye MA, Chen H: Inactivation of glycogen synthase kinase-3 β , a downstream target of the raf-1 pathway, is associated with growth suppression in medullary thyroid cancer cells. *Mol Cancer Ther* 2007, 6:1151–1158
13. Kappes A, Vaccaro A, Kunnimalaiyaan M, Chen H: Lithium ions: a novel treatment for pheochromocytomas and paragangliomas. *Surgery* 2007, 141:161–165
14. Wang Z, Smith KS, Murphy M, Piloto O, Somerville TC, Cleary ML: Glycogen synthase kinase 3 in MLL leukaemia maintenance and targeted therapy. *Nature* 2008, 455:1205–1209
15. Rylatt DB, Aitken A, Bilham T, Condon GD, Embi N, Cohen P: Glycogen synthase from rabbit skeletal muscle: amino acid sequence at the sites phosphorylated by glycogen synthase kinase-3, and extension of the N-terminal sequence containing the site phosphorylated by phosphorylase kinase. *Eur J Biochem* 1980, 107:529–537
16. Gatenby RA, Gawlinski ET: The glycolytic phenotype in carcinogenesis and tumor invasion: insights through mathematical models. *Cancer Res* 2003, 63(14):3847–3854
17. Kahn S, Yamamoto F, Almuquera C, Winter E, Forrester K, Jordano J, Perucho M: The c-K-ras gene and human cancer (review). *Anticancer Res* 1987, 7:639–652
18. Chiaradonna F, Gaglio D, Vanoni M, Alberghina L: Expression of transforming K-Ras oncogene affects mitochondrial function and morphology in mouse fibroblasts. *Biochem Biophys Acta* 2006, 1757:1338–1356
19. Chiaradonna F, Sacco E, Manzoni R, Giorgio M, Vanoni M, Alberghina L: Ras-dependent carbon metabolism and transformation in mouse fibroblasts. *Oncogene* 2006, 25:5391–5404
20. Pulciani S, Santos E, Long LK, Sorrentino V, Barbacid M: Ras gene amplification and malignant transformation. *Mol Cell Biol* 1985, 5:2836–2841
21. Baker SJ, Markowitz S, Fearon ER, Willson JK, Vogelstein B: Suppression of human colorectal carcinoma cell growth by wild-type p53. *Science* 1990, 249:912–915
22. Gaglio D, Soldati C, Vanoni M, Alberghina L, Chiaradonna F: Glutamine deprivation induces abortive s-phase rescued by deoxyribonucleotides in k-ras transformed fibroblasts. *PLoS One* 2009, 4:e4715
23. Coghlan MP, Culbert AA, Cross DA, Corcoran SL, Yates JW, Pearce NJ, Rausch OL, Murphy GJ, Carter PS, Roxbee Cox L, Mills D, Brown MJ, Haigh D, Ward RW, Smith DG, Murray KJ, Reith AD, Holder JC: Selective small molecule inhibitors of glycogen synthase kinase-3 modulate glycogen metabolism and gene transcription. *Chem Biol* 2000, 7:793–803
24. Baracca A, Chiaradonna F, Sgarbi G, Solaini G, Alberghina L, Lenaz G: Mitochondrial Complex I decrease is responsible for bioenergetic dysfunction in K-ras transformed cells. *Biochim Biophys Acta* 2010, 1797:314–323
25. Ryves WJ, Harwood AJ: Lithium inhibits glycogen synthase kinase-3 by competition for magnesium. *Biochem Biophys Res Commun* 2001, 280:720–725
26. Hoefflich KP, Luo J, Rubie EA, Tsao MS, Jin O, Woodgett JR: Requirement for glycogen synthase kinase-3 β in cell survival and NF- κ B activation. *Nature* 2000, 406:86–90
27. Fediuc S, Gaidhu MP, Ceddia RB: Inhibition of insulin-stimulated glycogen synthesis by 5-aminoimidazole-4-carboxamide-1-beta-d-ribofuranoside-induced adenosine 5'-monophosphate-activated protein kinase activation: interactions with Akt, glycogen synthase kinase 3- α /beta, and glycogen synthase in isolated rat soleus muscle. *Endocrinology* 2006, 147:5170–5177
28. Wakefield JG, Stephens DJ, Tavaré JM: A role for glycogen synthase kinase-3 in mitotic spindle dynamics and chromosome alignment. *J Cell Sci* 2003, 116(Pt 4):637–646
29. Tighe A, Ray-Sinha A, Staples OD, Taylor SS: GSK-3 inhibitors induce chromosome instability. *BMC Cell Biol.* 2007, 8:34
30. Williams T, Brenman JE: LKB1 and AMPK in cell polarity and division. *Trends Cell Biol* 2008, 18:193–198
31. Sarsour EH, Kumar MG, Chaudhuri L, Kalen AL, Goswami PC: Redox control of the cell cycle in health and disease. *Antioxid Redox Signal* 2009, 11:2985–3011
32. Visconti R, Grieco D: New insights on oxidative stress in cancer. *Curr Opin Drug Discov Devel* 2009, 12:240–245
33. Barbie DA, Tamayo P, Boehm JS, Kim SY, Moody SE, Dunn IF, Schinzel AC, Sandy P, Meylan E, Scholl C, Fröhling S, Chan EM, Sos ML, Michel K, Mermel C, Silver SJ, Weir BA, Reiling JH, Sheng Q, Gupta PB, Wadlow RC, Le H, Hoersch S, Wittner BS, Ramaswamy S, Livingston DM, Sabatini DM, Meyerson M, Thomas RK, Lander ES, Mesirov JP, Root DE, Gilliland DG, Jacks T, Hahn WC: Systematic RNA interference reveals that oncogenic KRAS-driven cancers require TBK1. *Nature* 2009, 462:108–112
34. Raffaghello L, Lee C, Safdie FM, Wei M, Madia F, Bianchi G, Longo VD: Starvation-dependent differential stress resistance protects normal but not cancer cells against high-dose chemotherapy. *Proc Natl Acad Sci U S A* 2008, 105:8215–8220
35. Snyder M, Weissman S, Gerstein M: Personal phenotypes to go with personal genomes. *Mol Syst Biol* 2009, 5:273

Critical Review

Fe65 Matters: New Light on an Old Molecule

Giuseppina Minopoli^{1,2}, Anna Gargiulo², Silvia Parisi^{1,2}, and Tommaso Russo^{1,2}

¹Dipartimento di Biochimica e Biotecnologie Mediche, Università di Napoli Federico II, Napoli, Italy

²CEINGE Biotecnologie Avanzate, Napoli, Italy

Summary

The discovery that the main constituents of amyloid deposits, characteristic of Alzheimer neuropathology, derive from the proteolytic processing of the membrane precursor amyloid precursor protein (APP) is one of the milestones of the research history of this disease. Despite years of intense studies, the functions of APP and of its amyloidogenic processing are still under debate. One focus of these studies was the complex network of protein–protein interactions centered at the cytosolic domain of APP, which suggests the involvement of APP in a lively signaling pathway. Fe65 was the first protein to be demonstrated to interact with the APP cytodomain. Starting from this observation, a large body of data has been gathered, indicating that Fe65 is an adaptor protein, which binds numerous proteins, further than APP. Among these proteins, the crosstalk with Mena, mDab, and Abl suggested the involvement of the Fe65–APP complex in the regulation of cell motility, with a relevant role in differentiation and development. Other partners, like the histone acetyltransferase Tip60, indicated the possibility that the nuclear fraction of Fe65 could be involved in gene regulation and/or DNA repair. © 2012 IUBMB

IUBMB *Life*, 00: 000–000, 2012

Keywords neurodegenerative disorders; transcription; DNA damage; cytoskeleton; adaptor proteins.

INTRODUCTION

Alzheimer's disease (AD) is a neurodegenerative disorder that represents the most common form of dementia. The amyloid precursor protein (APP) has been in the limelight of the research on AD pathogenesis for more than 20 years. Many research groups focused their activity on this molecule, because its proteolytic processing by β - and γ -secretases gives rise to the β -amyloid peptides ($A\beta$). The latter are the main constitu-

ents of the senile plaques, which for many years were believed to be the pathologic trigger of AD. A large body of literature suggests that soluble oligomers of $A\beta$, in particular those involving $A\beta_{42}$, interfere with synaptic plasticity and/or with memory functions (1). Although several reports questioned the relevance of $A\beta$ in AD pathogenesis (2), the involvement of APP and its processing is undisputed, being supported by solid genetic data, indicating that the rare forms of familial AD are caused by mutations of the *APP* gene or of the *presenilin* genes, which encode the catalytic activity of γ -secretase (3). Experimental evidence supports the possibility that APP and/or γ -secretase dysfunction could lead to neurodegeneration (2). Obviously, the understanding of the functions of APP and of its processing is crucial to explore loss of function hypotheses in the pathogenesis of AD.

In 1995, we observed that the NPXY motif present in the small cytodomain of APP interacts with a PTB/PI domain of a protein of unknown function, named Fe65 (4, 5). This finding was followed by several new observations indicating that, further than with Fe65, the same region of APP can also interact with other proteins such as X11, JIP1, mDab, Numb, Shc, and Grb2 (6). Many of these partners have the characteristics of adaptor proteins, thus suggesting the existence of complex molecular machineries that are centered at the APP cytodomain. These findings opened a new promising scenario to understand the functions and the regulation of APP and of its processing, which could contribute to further understand the molecular basis of AD. Several review articles describe the main results on this topic. This review will focus only on one aspect of the entire story that aimed at addressing the function of Fe65.

THE ADAPTOR PROTEIN Fe65

Fe65 belongs to a protein family, evolutionarily conserved from worms to humans, which in mammals includes two more paralogs, Fe65L1 (7) and Fe65L2 (8), which share striking amino acid and domain homology to Fe65. All Fe65 proteins have an identical multimodular structure with three different

Received 10 September 2012; accepted 12 September 2012

Address correspondence to: Tommaso Russo, Dipartimento di Biochimica e Biotecnologie Mediche, Università di Napoli Federico II, Napoli, Italy. E-mail: tommaso.russo@unina.it

protein–protein interaction domains, a WW domain and two consecutive PTB domains (9).

During the past years, screenings for Fe65 binding partners led to the identification of many proteins. APP was the first binding partner of Fe65 that has been identified, and this interaction is highly conserved as all Fe65s examined so far are able to bind through their C-terminal PTB domain (PTB2) to the NPTY-containing region of all APP and APP-like proteins. Phosphorylation of Thr-668 of APP has been shown to impair Fe65 binding, suggesting a possible “molecular switch” mechanism to regulate the Fe65–APP interaction (10). Recently, another ligand of Fe65 PTB2 domain, the small G-protein *Dexras1*, has been shown to bind Fe65, in a noncompetitive way with APP, and this binding is reduced by the phosphorylation of Y547 within the Fe65 PTB2 (11). Differently, the N-terminal PTB domain of Fe65 (PTB1) binds several proteins, such as the transcription factor CP2/LSF/LBP1 (12), the histone acetyltransferase Tip60 (13), and the lipoprotein receptors (14). Furthermore, this PTB1 domain of Fe65 binds the N-terminal domain of Tau protein and their interaction is regulated by Tau phosphorylation (15). The WW domain of FE65 binds the proline-containing motif of Mena, the mammalian homolog of *enabled*, which is involved in the control of cell motility through regulation of the actin cytoskeleton (16). Another ligand of the WW domain is the c-Abl tyrosine kinase, which phosphorylates APP on Tyr-682 (17, 18) and Fe65 on Tyr-547, within the PTB2 domain (19). The member of INHAT complex SET/TAF1- β binds to a region of Fe65 overlapping the WW domain (20). Fe65 simultaneously recruits SET and Teashirt3, which in turn binds to histone deacetylases (21).

Fe65 interactions could be regulated by conformational changes and/or post-translational modifications. In 2004, Cao and Südhof (22) proposed a model in which Fe65 is inhibited by an intramolecular interaction of the WW domain with the PTB domains that can keep Fe65 in a “closed” inactive state. Data from structural studies showed that this intramolecular interaction is weak and easy to be opened by the binding of WW domain or PTB domains to their high-affinity ligands (23). Therefore, the binding of PTB2 to APP could induce the structural change that opens Fe65, thus allowing to unmask the PTB1 and WW domains that become available for their binding partners.

THE PHENOTYPE OF *Fe65* NULL ANIMALS

The study of the alterations observed in KO mice is the ideal shortcut to get information about the function of a protein. Unfortunately, the *Fe65* null mice have no obvious phenotypes, perhaps because the two *Fe65* paralogs, *Fe65L1* and *L2*, having similar structure and a great sequence similarity, could be able to substitute, at least in part, for Fe65. Therefore, the first data on the effects of *Fe65* gene ablation came from *Caenorhabditis elegans*, in which only one orthologous gene (*feh-1*) is present. The *feh-1* null worms either arrest during the early steps of

embryo development or, if this block is escaped, they arrest at the larval stage L1. In these arrested larvae, the functional defect consists of impaired feeding ability due to increased rate of pharyngeal contraction (24, 25), a phenotype similar to that caused by the suppression of the nematode ortholog of *APP*. To get an evident phenotype in mammals, two genes, *Fe65* and *Fe65L1*, should be ablated. These mice show cortical dysplasia (26), also in this case similar to that observed in the triple KO of the *APP* family members, *APP*, *APLP1*, and *APLP2* (27).

Although apparently normal, the *Fe65* null mice have some subtle defects. Indeed, they show learning and memory impairment and defective early-phase LTP at the Shaffer collateral-CA1 synapses (28). Moreover, *Fe65* null mice show enhanced neurogenesis (29), similar to that observed in *APP*^{-/-} mice, as well as a slight increase of GnRH-1 neurons during development (30). In another set of experiments, it was demonstrated that *Fe65* null mice are more sensitive to DNA-damaging agents, as etoposide and ionizing radiations (31).

The molecular bases of these defects are still not definitively addressed and various possible explanations have been proposed.

FE65 AS A REGULATOR OF APP PROTEOLYTIC PROCESSING

The discovery of Fe65 and of the other partners of APP cytodomain raised the possibility that these proteins could be involved in the proteolytic processing of APP and in the generation of $A\beta$, therefore perhaps relevant for AD pathology. APP is a type I membrane protein with a large extracellular/intraluminal (EC/IL) domain, a single transmembrane tract, and a short cytosolic domain. APP EC/IL domain can be cleaved by two enzymes, α -secretase or β -secretase, acting at two different sites near the EC/IL layer of the membrane. These cleavages result in the shedding of the APP N-terminal domain in the EC or IL environment (sAPP). The resulting transmembrane stubs, called C83 or C99, respectively, are then cleaved by γ -secretase giving rise to the P3 fragment or to the $A\beta$ peptides of various lengths, mostly of 40 or 42 residues (1). The cleavage catalyzed by the γ -secretase also causes the formation of a C-terminal fragment, released in the cytosol, called APP intracellular domain (AICD).

The regulation of APP processing is of obvious interest, because APP fragments, including $A\beta$, could have important functional and/or pathological roles. It is clearly established that APP processing depends on the trafficking of the molecule among various intracellular compartments. In particular, mutation of the internalization signal YENPTY of the cytodomain of APP blocks endocytic trafficking and decreases $A\beta$ production (32). Considering that this motif is the binding site of Fe65, it can be hypothesized that the binding of Fe65 to APP influences the endocytosis and in turn the processing. Experimental evidence did not help to definitively address this point. Indeed, there are reports indicating that $A\beta$ production is increased by

Fe65 overexpression (33) and reduced by Fe65 knockdown (34), whereas other studies reported that FE65 increased sAPP α and decreased A β production (10). Apparently, the results obtained in animal models are similarly conflicting: APP knock-in mice carrying the Y682G mutation, which abolishes the binding of Fe65, showed decreased levels of A β and a massive increase in soluble APP α (35). However, the brain of transgenic mice overexpressing Fe65 contains reduced deposits of A β (36). Furthermore, mutations of T688 in the APP cytodomain, whose phosphorylation prevents Fe65 binding, does not affect the physiological processing of APP in knock-in animals (35). Lastly, in the *Fe65/Fe65L1* double KO (DKO) mice, no difference was observed in sAPP between wild type (wt) and DKO mice, whereas a slight decrease of A β 42 was present only in DKO male mice (26). The reasons for these apparently conflicting results are not clear. The complexity of the protein–protein interaction network centered at the YENPTY motif of the cytodomain of APP renders the phenomenon very difficult to dissect with loss or gain of function experiments. Furthermore, the proteolytic processing is also under the control of other likely unrelated events such as cell-type-specific intracellular trafficking and regulation of secretases.

Fe65, CYTOSKELETON REMODELING, AND CELL MOVEMENT

Having the characteristics of an adaptor protein, Fe65 was expected to interact with other proteins, further than APP. Mena was the first protein identified to interact with the WW domain of Fe65 (16). Mena belongs to a small family of proteins involved in the control of cell movement and morphology and in chemotactic responses (37). It was demonstrated that Fe65 and APP are present in dynamic adhesion complexes present on the surface of the cells and that their overexpression causes the acceleration of cell migration (38). Therefore, it can be speculated that an APP/Fe65/Mena complex is involved in the regulation of cell movement. This hypothesis is supported by further observations indicating that Fe65 and APP are also present in growth cones and synapses, mostly at the level of actin-rich lamellipodia (39). The neuropathological phenotype of the *Fe65/Fe65L1* (26) DKO mice and those of the triple KO of *APP/APLP1/APLP2* (27) or *Mena/VASP/EVL* (36) could be interpreted as defects of cell movement, thus confirming the possible role of Fe65 in this function. The *Drosophila* orthologs of the mammalian *Mena* and *mDab1* genes are genetic modulators of the phenotype observed in flies null for the Abl tyrosine kinase. Therefore, the observations that *mDab1* and Mena, directly or indirectly through Fe65, interact with APP reinforce the possibility that all these proteins are involved in a single pathway. Furthermore, we found that Fe65, through its WW domain, binds *in vitro* and *in vivo* the active form of Abl. The latter, recruited by Fe65 close to APP, phosphorylates a tyrosine residue of its cytodomain and then binds to this phospho-APP (17).

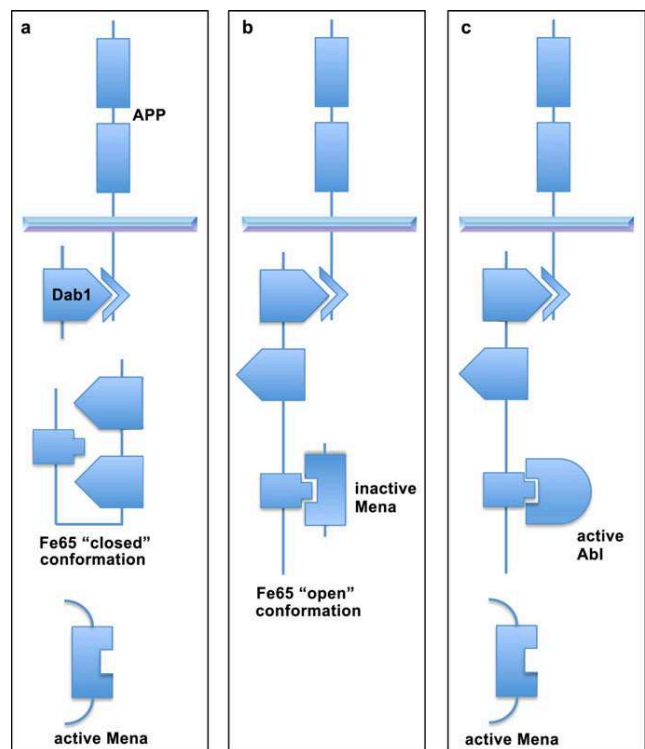


Figure 1. Possible competition among members of the APP-centered machinery. Mena belongs to the Ena/VASP family of regulators of actin dynamics and cell movement. Genetic experiments in *Drosophila* and many results obtained in mammalian cells support the possibility that the tyrosine kinase Abl and the Dab1 protein, the mammalian ortholog of *Drosophila* disabled, antagonize the effects of Mena on actin cytoskeleton and cell movements. The figure shows three possible scenarios of the competition among these molecules for the binding to the APP cytodomain. In panel a, Dab1 is associated with APP, thus Fe65 is in the “close” conformation and unable to interact with Mena. In panel b, Fe65 has displaced Dab1, acquired the active conformation, and thus can bind to Mena. In panel c, activated Abl competes with Mena for the binding to the WW domain of Fe65, thus Mena is displaced. Based on the phenotypes observed by manipulating the amounts of Abl, Dab, and Ena, it can be speculated that the interaction with Fe65 inhibits Mena activity and, in turn, Dab and active Abl, which prevent Mena–Fe65 interaction, favor the activity of Mena. [Color figure can be viewed in the online issue, which is available at wileyonlinelibrary.com.]

One important point that requires to be addressed is the role of the competition among the various players of this machinery, as Mena and Abl are expected to compete for the binding to the WW of Fe65, which in turn should compete with *mDab1* and Abl for the interaction with APP. Figure 1 shows only some of the possible complexes that can be formed by the above-mentioned proteins. Among the various hypothetical models that can be assembled, one of particular interest is based on the

competition between Dab1 and Fe65 for the binding to APP cytodomain. When Dab1 occupies the APP site, Fe65 is in the “closed” conformation (see above) that is unable to interact with Mena, being the WW domain masked. In these conditions, Mena is available to regulate cytoskeleton. Conversely, when Fe65 displaces Dab1 and binds to APP cytodomain, its WW domain is available for the binding to Mena, which in turn will be sequestered in an inactive form or in an irrelevant compartment. This scenario could be further modified by the activation of Abl, which competes with Mena for the binding to the WW of Fe65, thus liberating Mena in its active form and/or toward its relevant compartment. Obviously, the model could be further modulated by the involvement of other ligands of APP and Fe65.

NUCLEAR Fe65 AND THE REGULATION OF GENE TRANSCRIPTION

The possible nuclear functions of Fe65 are no less intriguing than those described in the previous paragraphs. The starting point in this case was the observation that Fe65 is also present in the nucleus and that its interaction with APP regulates its nuclear translocation (40). Other results indicated that further transcription factors or cofactors could be recruited at gene promoters associated with Fe65. This is the case, among the others, of: (i) late SV40 factor (LSF), whose interaction with the PTB1 domain of Fe65 affects the regulation of the thymidylate synthase gene (41); (ii) estrogen receptor α , through which estrogen appears to modulate the activity of Fe65-containing complex (42); (iii) SET, a component of the inhibitor of histone acetyltransferases (20); and (iv) Teashirt, which, together with SET, regulates the caspase 4 gene (21).

Another important study reported that nuclear Fe65 interacts with the histone acetyltransferases Tip60 and that the Fe65–Tip60 complex is able to activate the transcription from synthetic gene promoters (13). A very interesting point that emerged from this work is that the cytosolic fragment of APP, AICD, may take part in this machinery by forming a heterotrimeric complex with Fe65 and Tip60. The obvious relevance of this finding is that it suggested the possible similarity between the APP-centered complex and Notch. Indeed, Notch is a membrane-tethered transcription factor that, as a consequence of a proteolytic processing catalyzed by γ -secretase, liberates the Notch cytosolic domain (NICD). The latter goes into the nucleus, where in association with other proteins regulates the transcription of key developmental and differentiation genes (43). Therefore, AICD could function like NICD, together with Fe65, Tip60, and other proteins. Many research groups tried to address the AICD-dependent regulation of transcription; however, the results obtained so far still leave numerous doubts. Several genes have been suggested to be direct targets of AICD–Fe65, like APP itself, BACE, Tip60, KAIL, LRP, nephrilysin, and Stathmin1 (44–47); however, a systematic analysis of the Fe65-binding sites in the mammalian genome is still not

available. However, conflicting results are instead available on the role of the APP processing in gene regulation. Indeed, genetic and/or pharmacological suppression of γ -secretase gave very different results or was not effective on the regulation of the above-mentioned genes (48, 49). Therefore, the demonstration that AICD, through its interaction with Fe65, regulates gene expression is still lacking.

Fe65 IN THE CELLULAR RESPONSE TO DNA DAMAGE

The presence of Fe65 in the nucleus, associated with Tip60, does not imply its involvement exclusively in gene regulation. Indeed, Tip60 has a key role in the response to DNA damage, with the dual role of histone and ataxia telangiectasia mutated (ATM) acetyltransferase (50). The study of the phenotype of Fe65 null mice led to the observation that these mice are more sensitive to DNA-damaging agents (31). Low doses of etoposide or H₂O₂, which have only marginal effects on wt mouse embryo fibroblasts (MEFs), induced high levels of DNA damage and accumulation of γ -H2AX in Fe65 KO mouse embryo fibroblasts (MEFs). Irradiated mice showed a similar accumulation of γ -H2AX. Genotoxic stress induced by sorbitol causes the nuclear translocation of Fe65 in an APP-dependent manner (51). In this experimental system, Fe65 nuclear translocation precedes γ -H2AX accumulation, and the latter is decreased in the absence of Fe65. Therefore, it seems that nuclear Fe65 plays a key role in the response of the cell to DNA damage. Furthermore, the results available so far suggest that nuclear Fe65 should be in a specific conformation, which could depend on its interaction with APP (induction of open conformation; see ref. 22). Another possibility is that the activation of Fe65 also depends on post-translational modification on DNA damage. This possibility is supported by the observation that the electrophoretic migration of nuclear Fe65 is modified, likely due to phosphorylation, within few minutes from DNA damage (31).

The molecular mechanisms underlying the function of Fe65 in the nucleus of cells exposed to DNA-damaging agents are still not completely understood. A first set of experiments demonstrated that the Fe65 knockdown hampers the recruitment of Tip60 at DNA strand breaks and in turn the acetylation of histone H4 (52). This event could explain the defects in the DNA damage response and in the DNA repair observed as a consequence of Fe65 suppression. One possibility is that active Fe65 functions as a scaffold protein that interacts with chromatin, thus favoring the recruitment of soluble Tip60. In addition, nuclear Fe65 stabilizes p53 (53), and this could be a further mechanism through which Fe65 contributes to the response of the cells to DNA damage.

In this case, the crosstalk between Fe65 and APP/AICD also remains to be addressed. The first issue is concerned with the possible regulation of Fe65 nuclear translocation on DNA damage. One interesting possibility is that Fe65, bound to APP cytodomain and thus in its “open” active conformation, is released from APP as a consequence of APP phosphorylation at Thr668, possibly catalyzed by c-Jun N-terminal kinase JNK

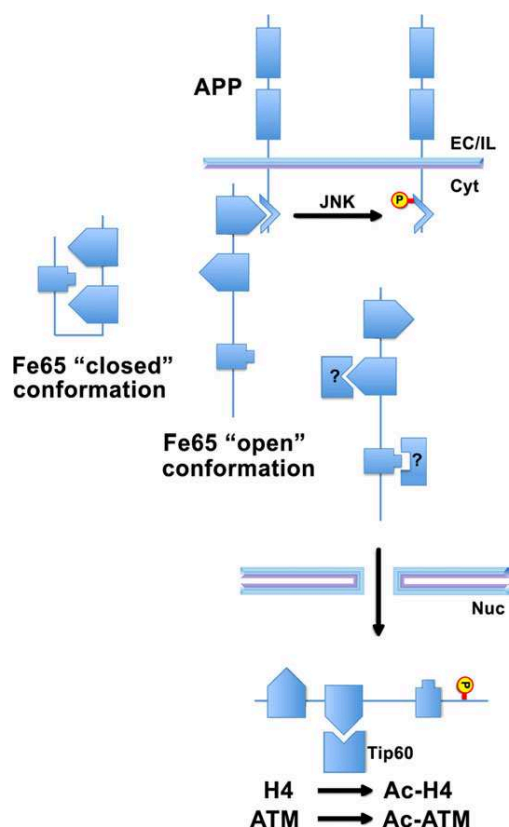


Figure 2. The Fe65–Tip60 complex in the DNA repair mechanisms. Following the induction of DNA double-strand breaks, Tip60 catalyzes the acetylation of histone H4 and of ATM. This event is the consequence of the recruitment of the enzyme at DNA lesions. It was demonstrated that Fe65 suppression inhibits Tip60 recruitment at DNA breaks and H4 acetylation. A similar phenotype was observed with the suppression of APP/APLP2. Based on this observation, it can be hypothesized that Fe65 interacts with APP (or APLP2) to acquire its “open” conformation, and then APP phosphorylation by stress kinases results in the liberation of Fe65 from the APP anchor followed by translocation into the nucleus, where Fe65 is required for the function of Tip60. Other partners of Fe65 and its post-translational modifications could be required for the proper function of the machinery. [Color figure can be viewed in the online issue, which is available at wileyonlinelibrary.com.]

(54). Nuclear Fe65 is then rapidly modified, likely phosphorylated, and it is necessary for Tip60 recruitment at the DNA breaks (see Fig. 2). Of course, Fe65 suppression leads to reduced phosphorylation of H2AX and decreased efficiency of DNA repair (52). The crucial involvement of APP in this machinery is supported by the observation that APP/APLP2 knock-down has the same effects observed with Fe65 suppression, that is, reduced recruitment of Tip60 at DNA breaks and reduced histone H4 acetylation (52). Considering that AICD seems not to be necessary in this machinery, the most likely explanation

for the role of APP in the mechanism is that the interaction of Fe65 with APP is necessary to allow Fe65 to acquire the proper conformation.

CONCLUSIONS

Despite the large literature on the function of Fe65 and on the consequences of its interaction with APP, many questions are still waiting for a definitive answer. Similarly, the possibility that Fe65 dysfunction could have any role in AD is far to be addressed. The information accumulated up to now is surprising, because Fe65 seems to be involved in several different functions. The number of proteins that appear to have more than one function is growing; however, in many cases, this multiplicity of functions is probably due to the incomplete understanding of the protein. This is obviously the case of Fe65. Robust data indicate that Fe65 is an adaptor protein with a wide choice of possible interactors. It shuttles between two intracellular compartments: in the cytosol, it could be involved with APP, Mena, mDab1, and Abl in the regulation of cell movement; and in the nucleus, in connection with transcription factors and/or histone-modifying enzymes, it could play a role in the response to DNA damage and/or in transcription regulation. In both cases, the proteolytic processing of APP and/or its post-translational modifications could be affected by Fe65 and regulate Fe65 intracellular trafficking. A speculation that deserves to be explored in detail is that Fe65 and its partners are part of a molecular machinery working during development and differentiation and are involved in a concerted cellular response to stress conditions.

ACKNOWLEDGEMENTS

The work performed in the authors' laboratory was supported by the Associazione Italiana Ricerca sul Cancro, Italy (AIRC) and the Italian Ministry of University and Research (PON1_02782).

REFERENCES

- Benilova, I., Karran, E., and De Strooper, B. (2012) The toxic A β oligomer and Alzheimer's disease: an emperor in need of clothes. *Nat. Neurosci.* **15**, 349–357.
- Robakis, N. K. (2010) Mechanisms of AD neurodegeneration may be independent of A β and its derivatives. *Neurobiol. Aging* **32**, 372–379.
- Bertram, R., Lill, C. M., and Tanzi, R. E. (2010) The genetics of Alzheimer disease: back to the future. *Neuron* **68**, 270–281.
- Fiore, F., Zambrano, N., Minopoli, G., Donini, V., Duilio, A., et al. (1995) The regions of the Fe65 protein homologous to the phosphotyrosine interaction/phosphotyrosine binding domain of Shc bind the intracellular domain of the Alzheimer's amyloid precursor protein. *J. Biol. Chem.* **270**, 30853–30856.
- Simeone, A., Duilio, A., Fiore, F., Acampora, D., De Felice, C., et al. (1994) Expression of the neuron-specific FE65 gene marks the development of embryo ganglionic derivatives. *Dev. Neurosci.* **16**, 53–60.
- Russo, T., Faraonio, R., Minopoli, G., De Candia, P., De Renzis, S., et al. (1998) Fe65 and the protein network centered around the cytosolic domain of the Alzheimer's β -amyloid precursor protein. *FEBS Lett.* **434**, 1–7.

7. Guénette, S. Y., Chen, J., Jondro, P. D., and Tanzi, R. E. (1996) Association of a novel human FE65-like protein with the cytoplasmic domain of the β -amyloid precursor protein. *Proc. Natl. Acad. Sci. USA* **93**, 10832–10837.
8. Duilio, A., Faraonio, R., Minopoli, G., Zambrano, N., and Russo, T. (1998) FE65L2: a new member of the Fe65 protein family interacting with the intracellular domain of the Alzheimer's β -amyloid precursor protein. *Biochem. J.* **330**, 513–519.
9. Zambrano, N., Buxbaum, J. D., Minopoli, G., Fiore, F., De Candia, P., et al. (1997) Interaction of the phosphotyrosine interaction/phosphotyrosine binding-related domains of Fe65 with wild-type and mutant Alzheimer's β -amyloid precursor proteins. *J. Biol. Chem.* **272**, 6399–6405.
10. Ando, K., Iijima, K. I., Elliott, J. I., Kirino, Y., and Suzuki, T. (2001) Phosphorylation-dependent regulation of the interaction of amyloid precursor protein with Fe65 affects the production of β -amyloid. *J. Biol. Chem.* **276**, 40353–40361.
11. Lau, K. F., Chan, W. M., Perkinson, M. S., Tudor, E. L., Chang, R. C., et al. (2008) Dexas1 interacts with FE65 to regulate FE65-amyloid precursor protein-dependent transcription. *J. Biol. Chem.* **283**, 34728–34737.
12. Zambrano, N., Minopoli, G., de Candia, P., and Russo, T. (1998) The Fe65 adaptor protein interacts through its PID1 domain with the transcription factor CP2/LSF/LBP1. *J. Biol. Chem.* **273**, 20128–20133.
13. Cao, X. and Südhof, T. C. (2001) A transcriptionally [correction of transcriptionally] active complex of APP with Fe65 and histone acetyltransferase Tip60. *Science* **293**, 115–120.
14. Waldron, E., Jaeger, S., and Pietrzik, C. U. (2006) Functional role of the low-density lipoprotein receptor-related protein in Alzheimer's disease. *Neurodegener. Dis.* **3**, 233–238.
15. Barbato, C., Canu, N., Zambrano, N., Serafino, A., Minopoli, G., et al. (2005) Interaction of Tau with Fe65 links tau to APP. *Neurobiol. Dis.* **18**, 399–408.
16. Ermekova, K. S., Zambrano, N., Linn, H., Minopoli, G., Gertler, F., et al. (1997) The WW domain of neural protein FE65 interacts with proline-rich motifs in Mena, the mammalian homolog of *Drosophila* enabled. *J. Biol. Chem.* **272**, 32869–32877.
17. Zambrano, N., Bruni, P., Minopoli, G., Mosca, R., Molino, D., et al. (2001) The β -amyloid precursor protein APP is tyrosine-phosphorylated in cells expressing a constitutively active form of the Abl protooncogene. *J. Biol. Chem.* **276**, 19787–19792.
18. Tarr, P. E., Contursi, C., Roncarati, R., Noviello, C., Ghersi, E., et al. (2002) Evidence for a role of the nerve growth factor receptor TrkA in tyrosine phosphorylation and processing of β -APP. *Biochem. Biophys. Res. Commun.* **295**, 324–329.
19. Perkinson, M. S., Standen, C. L., Lau, K. F., Kesavapany, S., Byers, H. L., et al. (2004) The c-Abl tyrosine kinase phosphorylates the Fe65 adaptor protein to stimulate Fe65/amyloid precursor protein nuclear signaling. *J. Biol. Chem.* **279**, 22084–22091.
20. Telese, F., Bruni, P., Donizetti, A., Gianni, D., D'Ambrosio, C., et al. (2005) Transcription regulation by the adaptor protein Fe65 and the nucleosome assembly factor SET. *EMBO Rep.* **6**, 77–82.
21. Kajiwara, Y., Akram, A., Katsel, P., Haroutunian, V., Schmeidler, J., et al. (2009) FE65 binds Teashirt, inhibiting expression of the primate-specific caspase-4. *PLoS One* **4**, e5071.
22. Cao, X. and Südhof, T. C. (2004) Dissection of amyloid- β precursor protein-dependent transcriptional transactivation. *J. Biol. Chem.* **279**, 24601–24611.
23. Radzimanowski, J., Ravaut, S., Schlesinger, S., Koch, J., Beyreuther, K., et al. (2008) Crystal structure of the human Fe65-PTB1 domain. *J. Biol. Chem.* **283**, 23113–23120.
24. Zambrano, N., Bimonte, M., Arbucci, S., Gianni, D., Russo, T., et al. (2002) feh-1 and apl-1, the *Caenorhabditis elegans* orthologues of mammalian Fe65 and β -amyloid precursor protein genes, are involved in the same pathway that controls nematode pharyngeal pumping. *J. Cell Sci.* **115**, 1411–1422.
25. Bimonte, M., Gianni, D., Allegra, D., Russo, T., and Zambrano, N. (2004) Mutation of the feh-1 gene, the *Caenorhabditis elegans* orthologue of mammalian Fe65, decreases the expression of two acetylcholinesterase genes. *Eur. J. Neurosci.* **20**, 1483–1488.
26. Guénette, S., Chang, Y., Hiesberger, T., Richardson, J. A., Eckman, C. B., et al. (2006) Essential roles for the FE65 amyloid precursor protein-interacting proteins in brain development. *EMBO J.* **25**, 420–431.
27. Herms, J., Anliker, B., Heber, S., Ring, S., Fuhrmann, M., et al. (2004) Cortical dysplasia resembling human type 2 lissencephaly in mice lacking all three APP family members. *EMBO J.* **23**, 4106–4115.
28. Wang, B., Hu, Q., Hearn, M. G., Shimizu, K., Ware, C. B., et al. (2004) Isoform-specific knockout of FE65 leads to impaired learning and memory. *J. Neurosci. Res.* **75**, 12–24.
29. Ma, Q. H., Futagawa, T., Yang, W. L., Jiang, X. D., Zeng, L., et al. (2008) A TAG1-APP signalling pathway through Fe65 negatively modulates neurogenesis. *Nat. Cell Biol.* **10**, 283–294.
30. Forni, P. E., Fomaro, M., Guénette, S., and Wray, S. (2011) A role for FE65 in controlling GnRH-1 neurogenesis. *J. Neurosci.* **31**, 480–491.
31. Minopoli, G., Stante, M., Napolitano, F., Telese, F., Aloia, L., et al. (2007) Essential roles for Fe65, Alzheimer amyloid precursor-binding protein, in the cellular response to DNA damage. *J. Biol. Chem.* **282**, 831–835.
32. Perez, R. G., Soriano, S., Hayes, J. D., Ostaszewski, B., Xia, W., et al. (1999) Mutagenesis identifies new signals for β -amyloid precursor protein endocytosis, turnover, and the generation of secreted fragments, including A β 42. *J. Biol. Chem.* **274**, 18851–18856.
33. Sabo, S. L., Lanier, L. M., Ikin, A. F., Khorkova, O., Sahasrabudhe, S., et al. (1999) Regulation of β -amyloid secretion by FE65, an amyloid protein precursor-binding protein. *J. Biol. Chem.* **274**, 7952–7957.
34. Xie, Z., Dong, Y., Maeda, U., Xia, W., and Tanzi, R. E. (2007) RNA interference silencing of the adaptor molecules ShcC and Fe65 differentially affect amyloid precursor protein processing and A β generation. *J. Biol. Chem.* **282**, 4318–4325.
35. Barbagallo, A. P., Weldon, R., Tamayev, R., Zhou, D., Giliberto, L., et al. (2010) Tyr(682) in the intracellular domain of APP regulates amyloidogenic APP processing in vivo. *PLoS One* **5**, e15503.
36. Santiard-Baron, D., Langui, D., Delehedde, M., Delatour, B., Schombert, B., et al. (2005) Expression of human FE65 in amyloid precursor protein transgenic mice is associated with a reduction in β -amyloid load. *J. Neurochem.* **93**, 330–338.
37. Kwiatkowski, A. V., Gertler, F. B., and Loureiro, J. J. (2003) Function and regulation of Ena/VASP proteins. *Trends Cell Biol.* **13**, 386–392.
38. Sabo, S. L., Ikin, A. F., Buxbaum, J. D., and Greengard, P. (2001) The Alzheimer amyloid precursor protein (APP) and FE65, an APP-binding protein, regulate cell movement. *J. Cell Biol.* **153**, 1403–1414.
39. Sabo, S. L., Ikin, A. F., Buxbaum, J. D., and Greengard, P. (2003) The amyloid precursor protein and its regulatory protein, FE65, in growth cones and synapses in vitro and in vivo. *J. Neurosci.* **23**, 5407–5415.
40. Minopoli, G., de Candia, P., Bonetti, A., Faraonio, R., Zambrano, N., et al. (2001) The β -amyloid precursor protein functions as a cytosolic anchoring site that prevents Fe65 nuclear translocation. *J. Biol. Chem.* **276**, 6545–6550.
41. Bruni, P., Minopoli, G., Brancaccio, T., Napolitano, M., Faraonio, R., et al. (2002) Fe65, a ligand of the Alzheimer's β -amyloid precursor protein, blocks cell cycle progression by down-regulating thymidylate synthase expression. *J. Biol. Chem.* **277**, 35481–35488.
42. Bao, J., Cao, C., Zhang, X., Jiang, F., Nicosia, S. V., et al. (2007) Suppression of β -amyloid precursor protein signaling into the nucleus by estrogens mediated through complex formation between the estrogen receptor and Fe65. *Mol. Cell Biol.* **27**, 1321–1333.
43. Andersson, E. R., Sandberg, R., and Lendahl, U. (2011) Notch signaling: simplicity in design, versatility in function. *Development* **138**, 3593–3612.
44. von Rotz, R. C., Kohli, B. M., Bosset, J., Meier, M., Suzuki, T., et al. (2004) The APP intracellular domain forms nuclear multiprotein

- complexes and regulates the transcription of its own precursor. *J. Cell Sci.* **117**, 4435–4448.
45. Baek, S. H., Ohgi, K. A., Rose, D. W., Koo, E. H., Glass, C. K., et al. (2002) Exchange of N-CoR corepressor and Tip60 coactivator complexes links gene expression by NF- κ B and β -amyloid precursor protein. *Cell* **110**, 55–67.
46. Pardossi-Piquard, R., Petit, A., Kawarai, T., Sunyach, C., Alves da Costa, C., et al. (2005) Presenilin-dependent transcriptional control of the A β -degrading enzyme neprilysin by intracellular domains of β -APP and APLP. *Neuron* **46**, 541–554.
47. Müller, T., Schrötter, A., Loosse, C., Pfeiffer, K., Theiss, C., et al. A ternary complex consisting of AICD, FE65, and TIP60 down-regulates Stathmin1. *Biochim. Biophys. Acta*, in press.
48. Hass, M. R. and Yankner, B. A. (2005) A γ -secretase-independent mechanism of signal transduction by the amyloid precursor protein. *J. Biol. Chem.* **280**, 36895–36904.
49. Hébert, S. S., Serneels, L., Tolia, A., Craessaerts, K., Derks, C., et al. (2006) Regulated intramembrane proteolysis of amyloid precursor protein and regulation of expression of putative target genes. *EMBO Rep.* **7**, 739–745.
50. Sun, Y., Jiang, X., and Price, B. D. (2010) Tip60: connecting chromatin to DNA damage signaling. *Cell Cycle* **9**, 930–936.
51. Nakaya, T., Kawai, T., and Suzuki, T. (2008) Regulation of FE65 nuclear translocation and function by amyloid β -protein precursor in osmotically stressed cells. *J. Biol. Chem.* **283**, 19119–19131.
52. Stante, M., Minopoli, G., Passaro, F., Raia, M., Vecchio, L. D., et al. (2009) Fe65 is required for Tip60-directed histone H4 acetylation at DNA strand breaks. *Proc. Natl. Acad. Sci. USA* **106**, 5093–5098.
53. Nakaya, T., Kawai, T., and Suzuki, T. (2009) Metabolic stabilization of p53 by FE65 in the nuclear matrix of osmotically stressed cells. *FEBS J.* **276**, 6364–6374.
54. Taru, H. and Suzuki, T. (2004) Facilitation of stress-induced phosphorylation of β -amyloid precursor protein family members by X11-like/Mint2 protein. *J. Biol. Chem.* **279**, 21628–21636.